THE SUPRACHIASMATIC NUCLEUS OF THE DOMESTIC CHICKEN, *Gallus domesticus*

A Dissertation

by

ELIZABETH LAYNE CANTWELL

Submitted to the Office of Graduate Studies of
Texas A&M University
in partial fulfillment of the requirements for the degree of

DOCTOR OF PHILOSOPHY

December 2005

Major Subject: Zoology

THE SUPRACHIASMATIC NUCLEUS OF THE DOMESTIC CHICKEN, *Gallus domesticus*

A Dissertation

by

ELIZABETH LAYNE CANTWELL

Submitted to the Office of Graduate Studies of
Texas A&M University
in partial fulfillment of the requirements for the degree of

DOCTOR OF PHILOSOPHY

Approved by:

Chair of Committee,	Vincent M. Cassone
Committee Members,	David J. Earnest
	Susan S. Golden
	Mark J. Zoran
Head of Department,	Vincent M. Cassone

December 2005

Major Subject: Zoology

ABSTRACT

The Suprachiasmatic Nucleus of the Domestic Chicken,

Gallus domesticus. (December 2005)

Elizabeth Layne Cantwell, B.A., University of Virginia

Chair of Advisory Committee: Dr. Vincent M. Cassone

The avian circadian system is composed of multiple inputs, oscillators and outputs. Among its oscillators is a hypothalamic structure presumed to be homologous to the primary circadian pacemaker in mammals, the suprachiasmatic nucleus (SCN). The SCN in avian species is poorly defined: two structures in the hypothalamus, the medial SCN (mSCN) and visual SCN (vSCN), have been referred to in the literature as the SCN. The present studies were designed to answer one central question: where is the avian homolog to the mammalian SCN? Uptake of 2-[^{14}C]-deoxyglucose (2DG), an indicator of glucose metabolism, fluctuates in the mSCN and vSCN in both a daily and circadian manner. These data indicate a possible role in the circadian system for both the vSCN and the mSCN. Additionally, several visual structures display daily fluctuations of 2DG uptake, two of which exhibit circadian variations, supporting previous studies indicting circadian regulation of the visual system. Efferents and afferents of the mSCN and vSCN were identified and compared to those of rodents. While the mSCN bears a stronger resemblance to the rodent SCN in its efferent connections than the vSCN, afferents of both are comparable. The total number of mSCN and vSCN neuronal connections far exceeds that of the rodent SCN. A subset of

these connections is strikingly similar to those of the rodent SCN, while others are found to connect these two nuclei to the visual system. These data further support the involvement of both the mSCN and vSCN in the circadian and visual systems. Suprachiasmatic organization was addressed using classical techniques. Though loosely similar in location to the mammalian SCN, the mSCN is cyto- and chemoarchitecturally different, while the vSCN bears more similarity to the mammalian SCN in this regard. A unique astrocytic bridge exists between the mSCN and vSCN, suggesting a role for astrocytes in the circadian system. Finally, the vSCN efferent to the medial nucleus of Edinger-Westphal was verified using a technique that may advance future studies of avian of circadian organization. The current data and the available literature were considered in the development of a working model of the avian SCN.

ACKNOWLEDGMENTS

I would first like to thank my advisor, Vinnie “Soul Crusher” Cassone, for sticking with me throughout my graduate career and for having “Git ’r done” at the top of the list. You helped me see the forest, encouraged me to think more critically, and motivated me when I needed it. I feel more prepared to move forward in my career than I ever thought possible, due in large part to your efforts. Knowing that I’ve made you proud means more to me than I think you’ll ever know.

I would also like to thank my committee members, Dave Earnest and Susan Golden, and Mark Zoran, who were always great sources of wisdom and encouragement. I must also thank Dave, for his gift of Cholera toxin in the eleventh hour, and Mark, for helping me with iontophoretic injections and for dreaming with me about some experiments I hope to accomplish in the future. Thanks also to Tom Champney, a founding member of my committee, for his advice and support early in my graduate career.

I have been lucky to have many supportive friends and labmates throughout my graduate career. I’d especially like to thank Arjun Natesan, Michael Gonzales, Jayna Ditty, Jen McGoogan and Kathryn Craven for their many pep talks. Heather Fugger was a great source of support throughout the writing process—sharing an office with you kept me sane. Jiffin Paulose helped me polish my defense and listened to it more times than any good person should have to. Paul Bartell really came through for me at crunch time and helped me strengthen my writing. The members of the Manson lab, my second home, have been a constant source of comic relief, particularly Arjan Bormans, who

took me to the emergency room occasionally. I'd like to thank Jen Peters, my lunch buddy, for our many deep conversations and commiserations. I'd like to thank Jen and Kevin Leiner for their friendship and for dancing with me to "You are my sunshine". Finally, I'd like to thank Shelby, Bobber, Gretchen and Roscoe for their healing powers.

I'd like to thank my husband, Brian Cantwell, for his love and support. You've done more than your fair share for quite some time now, while keeping me going. There are truly no words that adequately describe how much you've helped me or how much you mean to me.

Finally, I'd like to thank my mother. You always encouraged me in my aspirations and prodded me along when I was feeling like I might not be able to achieve them. You wouldn't let me beat myself up when I was feeling low. I'd have never gotten through this without your love, guidance and support, which have been constant throughout my entire life. You're my given, and I love you very much.

TABLE OF CONTENTS

CHAPTER Page

LIST OF FIGURES

FIGURE Page

LIST OF TABLES

NOMENCLATURE

3V	third ventricle
5HT	serotonin
AA	anterior archopallium
AL	ansa lenticularis
AM	hypothalamic anterior nucleus
AO	accessory optic pathway
AP	pretectal area
APH	parahippocampal area
Aq	cerebral aqueduct
AVP	arginine vasopressin (avian homolog, arginine vasotocin)
AVT	ventral tegmental area
Cb	cerebellum
CH	corticohabenular tract
CHCS	corticohabenular and corticoseptal tract
CO	optic chiasm
CP	posterior commissure
CT	tectal commissure
DIP	posterior dorsointermediate nucleus
DLAl	lateral anterior dorsolateral nucleus
DLAlr	rostrolateral dorsolateral nucleus
DLAm	medial anterior dorsolateral nucleus

DLAmc	magnocellular anterior dorsolateral nucleus
DLP	posterior dorsolateral nucleus
DMA	anterior thalamic dorsomedial nucleus
DMN	hypothalamic dorsomedial nucleus
DMP	posterior thalamic dorsomedial nucleus
DSD	dorsal supraoptic decussation
DSV	ventral supraoptic decussation
E	entopallium
EPR	encephalic photoreceptors
EW	nucleus of Edinger-Westphal
GABA	γ-aminobutyric acid
GAD	glutamic acid decarboxylase
GCt	midbrain central gray
GFA	glial fibrillary acidic protein
GHT	geniculohypothalamic tract
GLd	dorsolateral geniculate nucleus
GLv	ventrolateral geniculate nucleus
GnRH	gonadotropin releasing hormone
GRP	gastrin releasing peptide
GT	tectal gray
ICT	intercalated nucleus
IH	hypothalamic inferior nucleus

IN	infundibular nucleus
ICo	intercollicular nucleus
IO	isthmo-optic nucleus
HA	hyperpallium, apical part
Hb	habenula
HL	lateral habenular nucleus
HM	medial habenular nucleus
Hp	hippocampus
HTh	hypothalamus
LA	lateral anterior nucleus
LHy	lateral hypothalamic area
LMmc	mesencephalic lentiform nucleus, magnocellular part
LMpc	mesencephalic lentiform nucleus, parvocellular part
LoC	locus coeruleus
LSO	lateral septal organ
ME	median eminence
ML	lateral mamillary nucleus
MLd	dorsolateral mesencephalic nucleus
MM	medial mamillary nucleus
MPO	magnocellular preoptic nucleus
mSCN	medial suprachiasmatic nucleus
nBor	nucleus of the basal optic root

nBST	bed nucleus of the stria terminalis
nBSTL	lateral nBST
nBSTM	medial nBST
nCPa	bed nucleus of the pallial commissure
NE	norepinephrine
NPY	neuropeptide Y
nRot	nucleus rotundus
nTSM	nucleus of the septo-mesencephalic tract
OM	occipito-mesencephalic tract
OT	oxytocin (avian homolog, mesotocin)
OV	nucleus ovoidalis
Pap	papillioform nucleus
Pin	pineal gland
PMI	internal paramedian nucleus
POA	preoptic area
POD	dorsolateral preoptic nucleus
POM	medial preoptic nucleus
POP	preoptic periventricular nucleus
PPC	principal precommissural nucleus
PPT	pedunculopontine tegmental nucleus
pRot	perirotundal area
PST	pretecto-subpretectal tract

PT	pretectal nucleus
PVN	hypothalamic paraventricular nucleus
PVO	paraventricular organ
PVT	thalamic paraventricular nucleus
RHT	retinohypothalamic tract
Ru	red nucleus
SAC	central album layer of optic tectum
SCE	external cellular layer
SCN	suprachiasmatic nucleus
SCv	ventral nucleus subcoeruleus
SGC	central gray layer of optic tectum
SGFS	superficial gray and fiber layer of optic tectum
SGP	periventricular gray layer of optic tectum
SHL	lateral subhabenular nucleus
SHM	medial subhabenular nucleus
SL	lateral septal nucleus
SM	medial septal nucleus
SMe	stria medularis
SO	optic layer of optic tectum
SOv	ventral supraoptic nucleus
SP	subpretectal nucleus
SS	somatostatin

SSO	subseptal organ
SubP	substance P
T	nucleus triangularis
TeF	tectofugal visual pathway
Teg	tegmentum
TeO	optic tectum
TH	tyrosine hydroxylase
THth	tuberal hypothalamus
ThF	thalamofugal visual pathway
TIO	isthmo-optic tract
Tn	nucleus taeniae
TnBor	tract of the nucleus of the basal optic root
TrO	optic tract
TSM	septo-mesencephalic tract
VIP	vasoactive intestinal polypeptide
VLPO	ventrolateral preoptic nucleus
VLT	thalamic ventrolateral nucleus
VMN	ventromedial nucleus
vSCN	visual suprachiasmatic nucleus
VT	tectal ventricle

CHAPTER I

INTRODUCTION

FORMAL PROPERTIES OF CIRCADIAN RHYTHMS

Adaptation is necessary for all organisms to survive in their environmental conditions. Not only must an organism adapt to a climate, but also to the daily changes that occur as a result of Earth's rotation around the Sun, the Moon's rotation around the Earth and the Earth's rotation on its axis. This dynamic system creates changes in magnetic field and temperature and produces lunar and solar cycles. Thus, an organism is best adapted to its environment if it is able to anticipate the changes that take place over a day, a month, a season and a year. The biological clock evolved as a timing mechanism found in nearly every species studied, from single-celled prokaryotes to humans. The biological clock is a complex mechanism that allows organisms to predict events of varying cycle length, from annual to ultradian. The length of time that it takes to complete one cycle of a rhythm is called the period. Of specific interest in this document is the circadian system, so named because a circadian rhythm has a period of about 24 hours (Pittendrigh, 1960).

In order to be considered circadian, a rhythm must fulfill three requirements. First, a circadian rhythm must be endogenous, which means it must persist in constant conditions, devoid of timing cues, and the periodicity of the rhythm must be stable and approximately 24 hours. The most common constant conditions paradigm is constant

---

This dissertation follows the style of the Journal of Comparative Neurology.

darkness (DD; Pittendrigh, 1960). The endogenous period is specific to both the species and individual organism being studied and is known as the free running period (Menaker, 1982).

Second, the rhythm must be entrainable: the clock must be able to coordinate its activity with external time cues, called Zeitgebers. The most prominent Zeitgeber among vertebrate species is light, which is typically present in a cyclical manner due to the rotation of the Earth on its axis (Menaker and Tosini, 1995) When an organism lives in a cyclical paradigm, hours are measured in Zeitgeber time (ZT). For example, if an organism is kept in a light:dark (LD) cycle in which the lights are on for 12 hours and off for 12 hours (LD 12:12), ZT0 is dawn and ZT12 is dusk. In constant conditions, an organism begins to free run and the hours are now measured in circadian time (CT), in which subjective dawn is CT0 and subjective dusk is CT12. Circadian time is assessed by observing the temporal distribution of an organism's behavior. Any light paradigm involving light and dark is called a T cycle. Animals are able to entrain to T cycles in which the period differs from 24 hours; however, each species is limited in the T cycle periodicities to which it may entrain by upper and lower limits (Aschoff, 1981).

Third, a circadian rhythm must be temperature compensated. Most biochemical reactions are directly affected by changes in temperature and have a Q_{10} of 2 to 3. This means that for every ten-degree change in temperature, the reaction speed changes proportionally 2- to 3-fold. The circadian clock has a Q_{10} of 0.9 to 1.2, meaning that, although temperature is a zeitgeber in many organisms, the period of the clock stays relatively stable (Pittendrigh, 1960).

THE VERTEBRATE CIRCADIAN SYSTEM

The vertebrate circadian system is composed of multiple inputs, oscillators and outputs. Input pathways collect timing cues in the form of zeitgebers. This information is conveyed to the oscillators, which then drive rhythms through output pathways. The three major structures involved in the vertebrate circadian system are the retinae, the pineal gland and the suprachiasmatic nucleus (SCN) of the hypothalamus. Despite these common structures, circadian organization displays different levels of complexity between and within taxa (Menaker and Tosini, 1995).

Mammals, and rodents in particular, have the most studied vertebrate circadian system. In the rodent system, the retinae, which contain photoreceptors, collect light information as part of the primary input pathway. Enucleation results in animals that free run, even in an LD cycle (Korf et al., 2003). The pineal gland produces the indoleamine hormone melatonin, and its synthesis is an output that is driven by the clock (Cassone and Natesan, 1997). Pinealectomy has limited effects on rhythmicity: the locomotor activity rhythms of pinealectomized rats are disrupted in constant light conditions. These rhythms are gradually restored when the animals are placed into constant darkness, indicating that pineal melatonin may modulate the affects of light on the rat SCN (Cassone, 1992). The SCN itself, a pair of cell groupings apposed to the third ventricle and just dorsal to the optic chiasm in the anterior hypothalamus, is the primary pacemaker of the circadian system in mammals (Moore, 1979). Early in the literature, the SCN was divided into ventrolateral and dorsomedial regions (Moore, 1979) based on studies in rodents. The ventrolateral region is now designated the

"core", while the dorsomedial region is called the "shell" and these subdivisions are defined by retinal input and chemoarchitecture (cf. Moore et al., 2002). Lesion of the SCN produces arrhythmic locomotor behavior in every mammal studied (Klein and Moore, 1979; Moore and Eichler, 1972; Moore and Klein, 1974; Stephan and Zucker, 1972). Transplant of SCN tissue into the third ventricle restores behavioral rhythmicity (Lehman et al., 1987). When SCN transplants are harvested from hamsters with a genetic mutation that alters their free running period, the rhythms restored by the transplant have the period of the donor animal, and not the host (Ralph et al., 1990), suggesting that circadian rhythms are autonomously generated in the cells of the SCN.

THE AVIAN CIRCADIAN SYSTEM

The avian circadian system is more complex than the mammalian circadian system due to the presence of multiple oscillators. The current model describing the interaction of these oscillators states that there are multiple components in the avian circadian system (Cassone and Menaker, 1984). These components contain multiple oscillators that have variable, endogenously generated oscillations and are mutually coupled such that their oscillations are synchronized. If these pacemakers become uncoupled, disrupting their interaction, their rhythmicity becomes uncoordinated and eventually damps out. This model has been referred to as the internal resonance model (Gwinner, 1989) and the neuroendocrine loop model, which identifies the three components to this system: the pineal gland, the retinae and the SCN (Cassone and Menaker, 1984).

The pineal gland was the first avian oscillator discovered and, as in mammals, produces melatonin rhythmically. Further, the pineal gland contains photoreceptors, allowing it to respond to light in the absence of other circadian components until its rhythms damp out. Melatonin and the enzymes involved in its biosynthesis are the most useful outputs available to analyze the pacemaker activity of the pineal gland (Deguchi, 1979; Kasal et al., 1979). Pineal N-acetyl-transferase (NAT), the rate-limiting enzyme of melatonin biosynthesis, is expressed rhythmically *in vivo* in the house sparrow, *Passer domesticus,* and the chicken, *Gallus domesticus* (Takahashi and Menaker, 1979). Further, NAT activity is rhythmic in *in vitro* preparations of the pineal gland (Binkley et al., 1978). Cultured pineals from multiple avian species rhythmically produce melatonin in DD (cf. Natesan et al., 2002) and chick pineals in organ culture entrain to light cycles and phase shift in response to light pulses (Zatz et al., 1988). Dispersed pineal cultures are temperature compensated and entrain to temperature cycles (Barrett and Takahashi, 1995). Further, orthologs of mammalian clock genes have been identified in the avian pineal gland. In Japanese quail, *Coturnix coturnix,* mRNA of the period genes *per2* and *per3* is rhythmically expressed, while that of *clock* is constitutively available (Yoshimura et al., 2000). In the chick pineal, microarray study showed rhythmic expression of many gene transcripts, including those from the genes involved in melatonin biosynthesis and clock genes. Among the rhythmically expressed clock genes identified was *clock*, which is different from the situation in quail (Bailey et al., 2003, 2004).

As a component of the circadian system, the pineal gland oscillator has varying importance in different avian species. In house sparrows, pinealectomy abolishes locomotor activity (Ebihara and Kawamura, 1981; Gaston, 1971; Gaston and Menaker, 1968) and body temperature rhythms (Binkley et al., 1971), which damp gradually to arrhythmicity. Pineal transplant into the anterior chamber of the eye restores this rhythmicity (Zimmerman and Menaker, 1979). Exogenous melatonin rhythmically administered in drinking water also restores rhythmicity to pinealectomized sparrows (Lu and Cassone, 1993b). In European starlings, *Sturnus vulgarus*, however, the pineal gland is not as important, as pinealectomy results in disrupted, but rhythmic, perch-hopping activity in DD. In some birds, that rhythm is recovered after a transient episode of arrhythmicity (Gwinner, 1978). Further, this rhythm may be entrained by periodic injections of exogenous melatonin (Gwinner and Benzinger, 1978). In pigeons, pinealectomy also has little effect on locomotor activity rhythms in LD or constant light (LL), although it leads to decreased stability of this rhythm (Ebihara et al., 1984; Chabot and Menaker, 1992b). PINX also has no effect on feeding activity rhythms in pigeons (Chabot and Menaker, 1992b). Both locomotor activity and feeding activity rhythms may be entrained by rhythmically infused melatonin (Chabot and Menaker, 1992a). Pinealectomy has no effect on locomotor activity rhythms in either the Japanese quail (Underwood and Siopes, 1984) or the chicken (Nyce and Binkley, 1977). These studies not only reveal the varied importance of the pineal gland in avian circadian organization, but they indicate the presence of at least one more oscillator. The damping of sparrow rhythms to arrhythmicity after pinealectomy suggests that other circadian oscillators

have been decoupled and cannot maintain a synchronous rhythm. Were the pineal gland the only oscillator, rhythms would cease abruptly upon its removal. In species where pinealectomy had little or no effect, the remaining components of the circadian system remain tightly coupled and are capable of producing rhythms. Overall, these data indicate the existence of at least one more oscillator, thereby supporting the neuroendocrine loop model.

It was because of conclusions such as these that the oscillator in the avian retina was discovered. Like the pineal gland, the retina oscillator rhythmically drives the synthesis of melatonin in the chick (Binkley et al., 1979; Hamm and Menaker, 1980; Pang et al., 1983; Reppert and Sagar, 1983; Skene et al., 1991), Japanese quail (Pang et al., 1983; Skene et al., 1991; Underwood and Siopes, 1984) and the pigeon (Adachi et al., 1995; Pang et al., 1983). In the Japanese quail, exposure of each eye to a different light cycle, 180 degrees out of phase, results in ocular melatonin rhythms that are 180 degrees out of phase with each other (Steele et al., 2003), suggesting that each retina oscillates autonomously. Also in the quail retina, *per2* and *per3* mRNAs are rhythmically expressed, while *clock* is constitutively high (Yoshimura et al., 2000), as was found in the pineal gland. In the chick, the putative photoreceptive pigment mRNAs for RGR opsin and peropsin are rhythmically expressed, as is *clock*, again differing from data obtained in quail (Bailey and Cassone, 2004). Enucleation of house sparrows (Menaker, 1968) and most pigeons (Ebihara et al., 1984) fails to abolish either daily or circadian rhythms of locomotor activity, indicating that oscillators in the retinae do not affect overt circadian rhythmicity in those species. Conversely, enucleation

results in a damping to arrhythmicity of activity rhythms in the Japanese quail (Underwood and Siopes, 1984), suggesting a more substantial role for the retinae in this species.

Performed separately, pinealectomy and enucleation have little effect on pigeon locomotor activity rhythms. However, when PINX and EX are performed as a paired surgery, both locomotor activity and body temperature rhythms damp gradually to arrhythmicity after transfer from LD to constant conditions (Ebihara et al., 1984). The gradual damping that takes place after prolonged housing in constant conditions indicates the presence of a third oscillator. It has long been hypothesized that this third oscillator is located in the hypothalamus and is homologous to the mammalian SCN. Supporting this hypothesis, anterior hypothalamic lesions result in loss of locomotor activity rhythms in house sparrows (Takahashi and Menaker., 1982), Japanese quail (Simpson and Follett, 1981) and Java Sparrows, *Padda oryzivora* (Ebihara and Kawamura, 1981). The reported lesions comprised a large portion of the anterior hypothalamus, and two nuclei within the lesioned area have been identified in the literature as the avian homolog to the mammalian SCN. The first putative homolog to the mammalian SCN has been labeled the periventricular preoptic nucleus (PPN; van Tienhoven and Jühász, 1962; Cassone and Moore, 1987; revised nomenclature, POP; Kuenzel and Masson, 1988), the SCN (Hartwig, 1974, Kuenzel and van Tienhoven, 1982; Brandstatter et al., 2001), the medial hypothalamic nucleus (MHN; Norgren and Silver, 1989), the medial hypothalamic retinorecipient nucleus (MHRN; Shimizu et al., 1994) and the medial SCN (mSCN; Kuenzel and Masson, 1988; Yoshimura et al., 2001).

It will henceforth be referred to as the mSCN. The other putative homolog has been referred to in the literature as the SCN (Gamlin et al, 1982; Cooper et al., 1983), the lateral hypothalamic retinorecipient nucleus (LHRN) (Norgren and Silver, 1989; Shimizu et al., 1994) and the visual SCN (vSCN) (Cassone and Moore, 1987). The term vSCN will be used hereafter.

THE PUTATIVE AVIAN SUPRACHIASMATIC NUCLEUS

Based on cytoarchitectural evidence in early studies, the mSCN was identified as the SCN homolog (Crosby and Showers, 1969; Kuenzel and van Tienhoven, 1982; van Tienhoven and Juhasz, 1962). Some studies claim to have identified RHT terminals in the mSCN in house sparrows (Hartwig, 1974), Java sparrows (Ebihara and Kawamura, 1981) and Japanese quail (Oliver et al., 1978), although it is generally accepted that this input is weak and highly questionable, with the exception of a strong Cholera toxin b-subunit (CTB) signal in pigeons (Shimizu et al., 1994). The vSCN seems to be the primary, if not only, retinorecipient hypothalamic nucleus in the ringdove, *Streptopelia risoria* (Cooper et al., 1983; Norgren and Silver, 1989), house sparrow (Cassone and Moore, 1987), pigeon (Meier, 1973; Shimizu et al., 1994), duck (Bons, 1976) and chicken (Shimizu et al., 1984).

Chemoarchitectural studies have provided another means of comparison between these two structures and the mammalian SCN, which has a well-documented, heterogeneous antigen distribution. In rodents, cells immunoreactive for vasoactive intestinal polypeptide (VIP) are found in the core, while arginine vasopressin (AVP;

avian homolog, arginine vasotocin) immunoreactive cells are found in the shell (Moore et al., 2002). In the house sparrow, AVP immunoreactive cells are found ventral to the vSCN, while VIP positive cells are found at the medial border of the vSCN (Cassone and Moore, 1987). Other antigens found in the mammalian SCN include gastrin releasing peptide (GRP), glutamic acid decarboxylase, neuropeptide Y, neurotensin, serotonin, somatostatin and substance P (Moore et al., 2002), all of which are found in the vSCN of the house sparrow (Cassone and Moore, 1987). While the chemoarchitecture of the vSCN is similar to that of the eutherian mammalian SCN, it is not identical; therefore, it was proposed by Cassone and Moore (1987) that the vSCN is the retinorecipient portion of a suprachiasmatic complex in which one or more other structures may be involved.

Lesioning studies are another classical approach employed in the identification of circadian components. Ebihara et al. (1987) found that lesions of the pigeon mSCN do not abolish free running rhythms in all birds in constant dim light (dimLL), although, in some birds, temporal arrhythmicity occurs. vSCN lesions fail to abolish free running rhythms. In Japanese quail, discrete lesions of the mSCN result in normal activity in LD, but disrupted or abolished rhythms of locomotor activity in dimLL. Pinealectomy and enucleation of mSCN lesioned quail results in birds that are completely arrhythmic in all circumstances (Menaker and Underwood, 1976). In chicks, precise lesions to the vSCN disrupt the rhythm of norepinephrine turnover in the pineal gland. This does not occur with lesions of the mSCN (Cassone et al., 1990).

Analysis of clock gene expression has also been employed in the study of the avian SCN. Several of these genes have been identified in the mSCN but not the vSCN in Japanese quail (Yoshimura et al. 2001; Yasuo et al., 2003). In the house sparrow, *per2* expression is rhythmic in both the mSCN and the vSCN such that it is highest during the mid-day (Brandstatter et al., 2001), which is similar to the phasing seen in the mouse SCN (Tei et al. 1997). The house sparrow vSCN also rhythmically expresses *per2* mRNA, although the phase is slightly delayed compared to the mSCN (Abraham et al., 2002). Both the mSCN and vSCN express mRNA of the cryptochrome gene *cry2* (Bailey et al., 2002). In comparison, many genes in the mammalian SCN are also expressed rhythmically *in vivo* and *in vitro* (Yamazaki et al., 2000; Hastings and Herzog, 2004). Numerous clock genes have been found within the SCN that interact to drive rhythmic mRNA and protein expression with a period of about 24 hours. This oscillation impinges upon output pathways that produce overt circadian rhythms (Dunlap, 1999).

A variety of other studies have reported results indicating that the vSCN is a circadian structure. House sparrows show rhythmic uptake of 2-deoxy[^{14}C]glucose (2DG) metabolism *in vivo* in the vSCN and not the mSCN (Cassone, 1988). This rhythm of 2DG uptake in the vSCN may be entrained by a 12:12 cycle of melatonin treated water:untreated water in which vSCN activity is high during the subjective day and low during the subjective night. This is not found to be the case in the mSCN (Lu and Cassone, 1993b). Further, the radiolabeled melatonin agonist IMEL binds to the vSCN, but not the mSCN, of chickens (Brooks and Cassone, 1992). In Japanese quail,

the vSCN has rhythmic electrical activity *in vitro* (Juss et al., 1994). Similarly, the mammalian SCN displays rhythms of neuronal firing *in vivo* and *in vitro* (Inouye and Kawamura, 1979; Green and Gillette, 1982; Groos and Hendriks, 1982; Shibata et al, 1982). Finally, *c-fos*, an immediate early gene that may be induced in the mammalian SCN by 1-hour pulses of light, may also be induced in the vSCN, but not in the mSCN, of quail and starlings (King and Follett, 1997). The data available regarding the avian SCN is not sufficient to designate homology to either the mSCN or the vSCN.

VISUAL SYSTEM PATHWAYS

Studies have suggested that the circadian system is involved in regulation of the visual system (McGoogan and Cassone, 1999; Wu et al., 2000). The avian visual system is, as it is in mammals, comprised of four integrated pathways (Cassone and Moore, 1987; Nalbach et al., 1993), each of which bind the melatonin agonist 2-[^{125}I]-iodomelatonin (IMEL) at every level of sensory integration (Cassone et al., 1995). The circadian/hypothalamic pathway consists of the retinohypothalamic tract and its terminus, the vSCN (Cassone and Moore, 1987). The tectofugal pathway, the avian homolog of the colliculoextrastriate pathway, which is involved in gross visual detection, consists of the optic tectum, nucleus rotundus and ectostriatum (Engelage and Bischoff, 1993). The thalamofugal pathway is involved in binocular and fine vision and is homologous to the geniculostriate pathway. This pathway comprises the principal optic nucleus and visual Wülst (Güntürkün et al., 1993). Finally, the accessory optic pathway, which controls eye movement, consists of the nucleus of the basal optic root

and associated structures, the oculomotor nucleus and the cerebellum. The nucleus of Edinger-Westphal is also associated with the accessory optic pathway (Nalbach et al., 1993; Wallman and Letelier, 1993), since it regulates ocular physiology autonomically (Gamlin et al., 1982; Fitzgerald et al., 1990; Reiner et al., 1990).

OBJECTIVES AND SIGNIFICANCE

The fundamental question of this dissertation is, where is the avian homologue to the mammalian SCN? The model animal of the work described was performed in the chicken, *Gallus domesticus*. First, 2-deoxy[14C]glucose (2DG) uptake was studied to determine what structures in the hypothalamus are rhythmic, and whether they are affected by melatonin. This approach was taken because the SCN of mammals is rhythmic in many of its physiological properties, including glucose utilization *in vivo* and *in vitro* (Schwartz and Gainer, 1977; Schwartz et al., 1980; Newman et al., 1992).

Next, tract tracing techniques were used to determine the path of the RHT as well as the efferent and afferent connections of the mSCN and vSCN in order to determine whether one or both have connectivity similar to mammals. The mammalian SCN receives a number of afferents from cerebral structures, which send their termini to either the core or the shell of the SCN. There are three major inputs to the core. The first, and most well studied, is the retina, which sends its afferents via the retinohypothalamic tract (RHT; Moore, 1973; Moore and Lenn, 1972; Moore et al., 1971). Second, the intergeniculate leaflet and the pretectal area, which receive primary visual input, send a projection called the geniculohypothalamic tract (GHT) to the SCN

(Card and Moore, 1982, 1989; Moore et al., 1984; Harrington et al., 1985; Moore and Speh, 1993; Moore and Card, 1994). Third, serotonergic input arises from the midbrain raphe (Moore et al., 1978; Pickard, 1982; Moga and Moore, 1997). There are many nuclei that project almost exclusively to the shell of the mammalian SCN, including at least nine different nuclei in the adjacent hypothalamic area and the limbic system, which includes the lateral septal nucleus, the ventral subiculum and the infralimbic cortex (cf. Moga and Moore, 1997). Three regions send inputs to both the core and the shell of the mammalian SCN, including the thalamic paraventricular nucleus (PVT), the tuberomammillary nucleus and the subparaventricular zone (SPVZ). The SPVZ is ventral to the hypothalamic paraventricular nucleus (PVN), and appears to be part of a network of local circuits that includes the SCN (van den Pol, 1980; Watts, 1991).

Efferent fibers to many structures arise in the rodent SCN; however, the subdivision of these efferents between the core and the shell has not been detailed in publication (Watts and Swanson, 1987; Watts, 1991). Among these efferents are the intergeniculate leaflet, the preoptic area, SPVZ, PVT, and PVN. Interestingly, injections that encroach on the peri-SCN area and SPVZ send a larger contingent of fibers to these efferents than does the SCN itself. Other SCN fibers terminate in the lateral septal nucleus, the ventromedial and dorsomedial hypothalamic nuclei, the retrochiasmatic area, the posterior hypothalamus, the parataenial nucleus and the periaqueductal gray. The specific purpose of each connection is not known; however, it is abundantly clear that the SCN, the peri-nuclear area surrounding it and SPVZ are highly interconnected with a variety of structures, forming a complex network of interactions (cf. Watts, 1991).

Finally, retinal input to the mSCN and vSCN were reexamined using a second tract tracing method and the antigen distribution of the chick suprachiasmatic area was studied in order to draw anatomical comparisons between the chick, the house sparrow, described above, and mammals. In rodents, the core is retinorecipient, receiving light information transmitted by the RHT, as described previously. Antigen distribution is well characterized in the rodent SCN. The core contains neurons positive for vasoactive intestinal polypeptide, gastrin releasing peptide, substance P and neurotensin. The shell reacts positively with antibodies against vasopressin, enkephalin and somatostatin. Calretinin is found in both the core and the shell (Moore et al., 2002). Different from the situation in rodents, retinal input to the marsupial SCN terminates in the dorsomedial aspect, which is immunoreactive for both AVP and VIP immunoreactivity (Cassone et al., 1988b). Thus, specific details of immunohistochemical distributions in the SCN are phylogenetically labile even among mammals. The information obtained in the current studies, in concert with previously reported data, has led to the development of a working model of an avian suprachiasmatic complex, in which both the mSCN and vSCN are involved.

CHAPTER II

DAILY AND CIRCADIAN FLUCTUATION IN 2-DEOXY[^{14}C]-GLUCOSE UPTAKE IN CIRCADIAN AND VISUAL SYSTEM STRUCTURES OF THE CHICK BRAIN: EFFECTS OF EXOGENOUS MELATONIN*

INTRODUCTION

The circadian system has evolved to accurately time behavioral, physiological and metabolic outputs, aiding in the survival of organisms ranging from bacteria to vertebrates (Pittendrigh, 1993; Menaker and Tosini, 1995). In vertebrates, this system is composed of multiple photoreceptors, central oscillators and outputs. In birds, the photoreceptors are present in the retinae, the pineal gland and in the brain itself. Central oscillators in vertebrates are located in three structures—the pineal gland, the retinae and hypothalamic suprachiasmatic nuclei (SCN) (Menaker and Tosini, 1995). A number of measurable outputs have been identified in a variety of avian species, including locomotor activity, body temperature, feeding activity and plasma melatonin levels.

Birds have a particularly complex circadian system. The pineal gland synthesizes and secretes the hormone melatonin during the night both *in vivo* and *in vitro* in all species studied (Cassone, 1990; Klein et al., 1997). It is likely that the pineal affects overt rhythmicity in many species through the effects of melatonin (Klein et al., 1997),

* Reprinted from Brain Research Bulletin, Vol 57, EL Cantwell and VM Cassone, Daily and circadian fluctuation in 2-deoxy[^{14}C]-glucose uptake in circadian and visual system structures of the chick brain: effects of exogenous melatonin, Pages 603-611, Copyright © (2002), with permission from Elsevier.

although as a circadian pacemaker, the pineal gland varies in its importance among birds. For example, pinealectomy (PINX) abolishes locomotor activity (Gaston and Menaker, 1968; Gaston, 1971; Ebihara and Kawamura, 1981) and body temperature (Binkley et al., 1971) rhythms in house sparrows (*Passer domesticus*) and Java sparrows (*Padda oryzivora*) (Ebihara and Kawamura, 1981). In chickens, however, PINX fails to abolish feeding activity rhythms (McGoogan and Cassone, 1999). The retinae also produce and secrete melatonin rhythmically such that it is high during the night and low during the day in chickens, *Gallus domesticus* (Binkley et al., 1979; Hamm and Menaker, 1980; Reppert and Sagar, 1983), Japanese quail, *Coturnix coturnix* (Underwood and Siopes, 1984) and pigeons, *Columba livia* (Adachi et al., 1995). Bilateral enucleation (EX) of Japanese quail results in the loss of activity and body temperature rhythms. In pigeons, EX disrupts these rhythms while PINX/EX abolishes them (Ebihara et al., 1984). Periodic melatonin infusions or administration reestablish and maintain activity rhythms in PINX house sparrows (Lu and Cassone, 1993b; Heigl and Gwinner, 1995) and in PINX/EX pigeons (Chabot and Menaker, 1994). It has therefore been suggested that the variability among species concerning the effects of pinealectomy is due to the relative contribution of retinal melatonin (Underwood and Goldman, 1987).

There are two candidates for an avian homologue of the SCN, which have been established as the primary circadian pacemaker in mammals (Moore, 1979; Rusak and Zucker, 1979; Moore, 1982). The two areas of interest are the periventricular preoptic nucleus, also called the medial SCN (mSCN) (Norgren and Silver, 1990) and the visual

SCN (vSCN) (Cassone and Moore, 1987). The mSCN is positioned in the preoptic recess of the third ventricle and dorsal of the optic chiasm, which is close to the position of the mammalian SCN. The vSCN, on the other hand, is caudal and lateral to the mSCN. It is also positioned dorsal of the optic chiasm and sits between the ventrolateral geniculate nucleus and the supraoptic decussation. The vSCN of the house sparrow is rhythmic in its uptake of 2DG in both LD and DD. This rhythm is high during the day/subjective day and low in the night/subjective night. The mSCN displays no rhythm of uptake (Cassone, 1988). The 2DG uptake rhythm is also synchronized by daily melatonin administration to sparrows housed in DD. Uptake is low during the period of melatonin infusion and is significantly higher when melatonin infusion is discontinued (Lu and Cassone, 1993b). Further, melatonin injection during the day inhibits 2DG uptake (Cassone and Brooks, 1991). Finally, the vSCN, but not the mSCN, specifically bind the melatonin agonist 2[^{125}I]iodomelatonin (IMEL) with very high affinity in many species of bird (Rivkees et al., 1989; Cassone and Brooks, 1991; Brooks and Cassone, 1992; Cassone et al., 1995).

Central visual system structures are also sites of IMEL binding in many avian species (Rivkees et al., 1989; Cassone and Brooks, 1991; Cassone et al., 1995). The avian visual system is, as in mammals, comprised of four integrated pathways (Cassone and Moore, 1987; Nalbach et al., 1993), each of which bind IMEL at every level of sensory integration. The circadian/hypothalamic pathway consists of the retinohypothalamic tract and its terminus, the vSCN (Cassone and Moore, 1987). The tectofugal pathway, the avian homolog to the colliculoextrastriate pathway, involved in

gross visual detection, consists of the optic tectum, nucleus rotundus and ectostriatum (Engelage and Bischof, 1993). The thalamofugal pathway is involved in binocular and fine vision and is homologous to the geniculostriate pathway. This pathway comprises principal optic nucleus and visual Wülst (Güntürkün et al., 1993). Finally, the accessory optic pathway controls eye movement and consists of the nucleus of the basal optic root and associated structures, the oculomotor nucleus and the cerebellum. The nucleus of Edinger-Westphal is associated with the accessory optic pathway (Nalbach et al., 1993; Wallman and Letelier, 1993), since it regulates ocular physiology autonomically. In each case, retinorecipient and integrative structures of each pathway bind IMEL (Cassone et al., 1995).

In this paper, we show that 2DG uptake is rhythmic in the brain of the chicken, *Gallus domesticus,* in both LD and DD. Further, we demonstrate that administration of exogenous melatonin decreases daytime cerebral 2DG uptake, in some but not all rhythmic structures, similar to the situation in the house sparrow.

MATERIALS AND METHODS

Animals

Male White Leghorn chicks (*Gallus domesticus*) were obtained from Hy-Line Hatcheries (Bryan, TX) on their hatch date and were raised to two weeks of age in a heated brooder on a light:dark (LD) 12:12 cycle (lights on from 6:00 a.m. to 6:00 p.m. CST). Food and water were continuously available until the day before the experiment, at which time they were removed. All animal use protocols were reviewed and approved

by the University Laboratory Animal Care Committee (ULACC) at Texas A&M University.

Experiment 1: 2DG fluctuation in the chick brain over time of day

Chicks were injected with 2-deoxy [^{14}C]glucose (2DG; 200μCi/kg; 300mCi/mmol; American Radiolabeled Chemicals, St. Louis, MO) in the pectoral muscle at ZT6 (n=5) and ZT18 (n=5; Zeitgeber time, 6 and 18 hours after lights on, respectively). The birds were caged individually for one hour and then decapitated. Their brains were removed, frozen in 2-methylbutane and stored at –80^{o}C. Upon completion of this procedure at ZT18, the lights were disabled and the process of injection and decapitation was repeated in constant darkness (DD) at CT6 (n=5) and CT18 (n=5; Circadian time). These CT times were determined based on the preceding light cycle.

Experiment 2: Effects of melatonin on 2DG uptake

Chicks (n=10) were injected with ethanolic saline (0.5%; 1mL/kg) or melatonin (10μg/kg) in ethanolic saline and individually caged for fifteen minutes at ZT10. This timepoint was chosen because it is the peak time of 2-[^{125}I]iodomelatonin (IMEL) binding in the chick brain (Brooks and Cassone, 1992). The chicks were then injected with 200μCi/kg 2DG in the pectoral muscle and placed back into their cages for 45 minutes. At the end of this time, they were decapitated. Brains were removed and treated as in Experiment 1.

Brain sectioning and autoradiography

Brains were coronally sectioned (30μm) rostrocaudally from the ectostriatum to the *nucleus of Edinger-Westphal*. Sections were thaw-mounted onto gelatin-coated slides and apposed to Kodak BioMax MR film (VWR, Sugar Land, TX) along with ^{14}C standard slides (American Radiolabeled Chemicals, St. Louis, MO). One week after exposure, the films were developed with Kodak D19 developer, fixed, rinsed and dried. Sections were fixed in alcohol, stained with cresyl violet stain, dehydrated, cleared and coverslipped for histological localization.

Data analysis

The autoradiographic films were converted to computer images using the Java image analysis program (SPSS Inc., Chicago, IL). Representative sections from Experiments 1 and 2 are shown in Figures 1 and 2, respectively. Brain structures of specific interest, as well as structures showing prominent activity, were selected from all four visual pathways. From the circadian pathway, the vSCN was observed. We also chose to analyze the pineal gland (Pin) and periventricular preoptic nucleus (mSCN) as structures associated with circadian function. From the tectofugal pathway, we selected the optic tectum (TeO), ventrolateral geniculate nucleus (GLv), nucleus rotundus (Rot) and ectostriatum (E). Accessory optic pathway-associated components *nucleus of Edinger-Westphal* (EW) and cerebellum (Cb) were also chosen. Finally, from the thalamofugal pathway, the visual Wülst (HA) was selected. Using the Nissl-stained

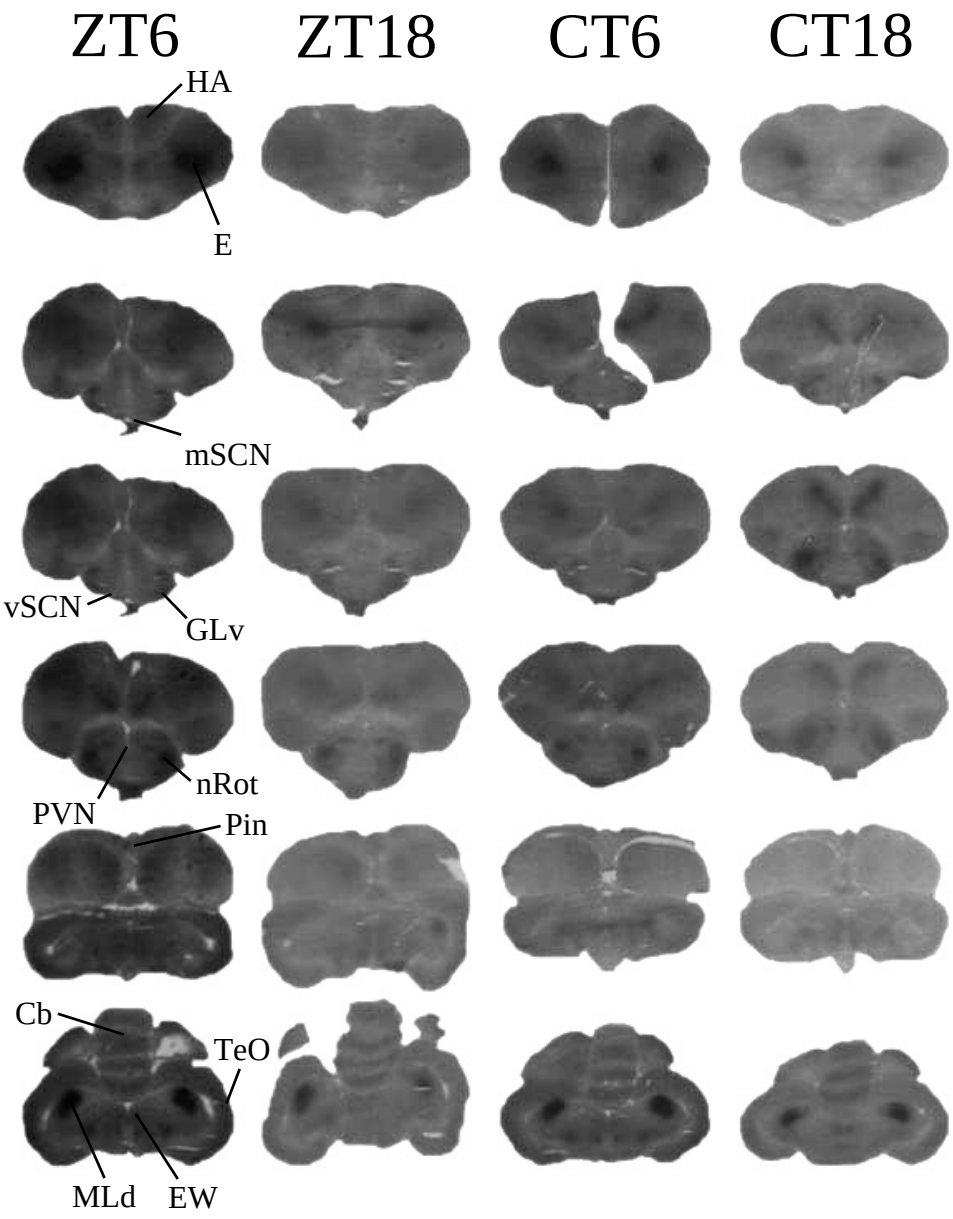

Fig. 1. Representative sections used to analyze 2DG uptake over time of day. Structures that were visible and of particular interest were analyzed for 2DG uptake in LD and DD. This figure shows representative brain sections video-digitized from autoradiographic films. Each column represents the time point indicated above it. From top to bottom, the sections progress rostrocaudally through the chicken brain. Each row represents one level in the chick brain. The structures studied are labeled on the ZT6 column. ZT6 corresponds to the middle of the day; ZT18 corresponds to the middle of the night. CT6 and CT18 correspond to mid-subjective day and mid-subjective night respectively in chicks maintained in constant darkness.

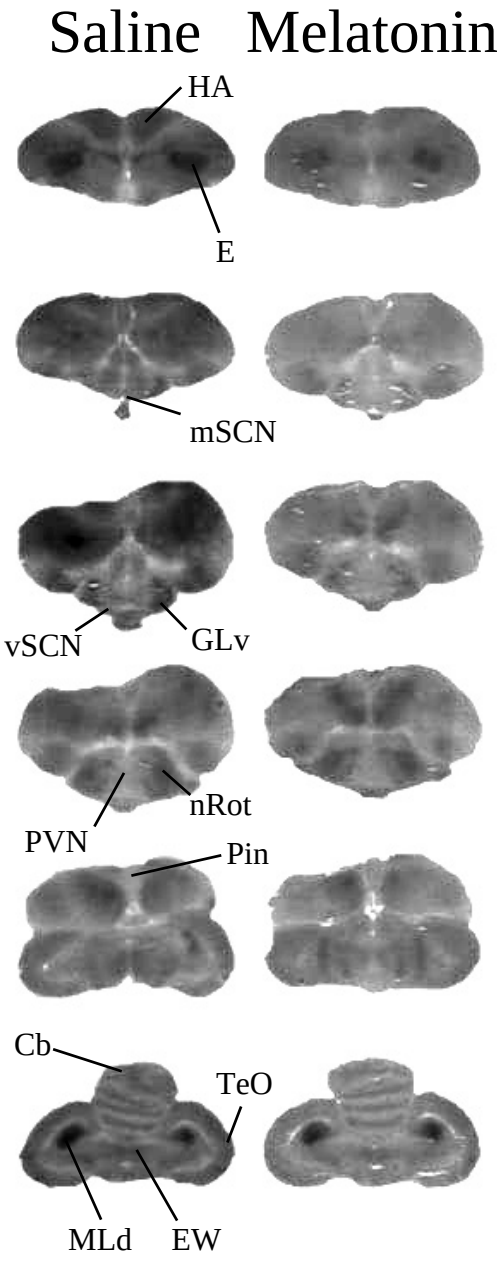

Fig. 2. Representative sections used to analyze effects of exogenous melatonin on 2DG uptake. Structures studied in Experiment 1 were further tested to determine whether an intramuscular injection of melatonin could affect 2DG uptake at ZT10, the peak time of 2-[^{125}I]iodomelatonin binding in the chick brain. Comparable brain sections from saline-injected and melatonin-injected chickens are presented side-by-side at six different levels, which are shown rostrocaudally from top to bottom. Structures are labeled in the Saline control column.

sections to localize structures, 2DG uptake was quantified densitometrically using the image analysis program, SigmaScan Pro (SPSS Inc., Chicago, IL). Densitometric values were converted to pmol/mg/hr. The densitometric values were then subjected to statistical analysis using SAS (SAS Institute, Inc., Cary, NC). A one-way analysis of variance procedure was performed to determine statistical significance within a 95% confidence interval ($p \leq 0.05$). Tukey's post hoc test was used to determine which values were significantly different from one another.

RESULTS

Experiment 1: 2DG fluctuation in the chick brain over time of day

Three structures associated with circadian function were observed—the vSCN, mSCN and Pin. Of these, only the vSCN displayed significant day/night differences of 2DG uptake in both LD and in DD (Fig. 3A). While uptake in the mSCN showed no significant daily change, even though a trend was apparent, a circadian difference of 2DG uptake was observed (Fig. 3B). Pin showed neither a daily nor a circadian difference in uptake (Fig. 3C).

2DG uptake was measured in seven visual system structures from the other three pathways. In the tectofugal pathway (Fig. 4), we found that GLv (Fig. 4B), nRot (Fig. 4C) and E (Fig. 4D) displayed daily changes in uptake, but that these differences were not maintained in DD. TeO displayed both daily and circadian fluctuations of 2DG uptake (Fig. 4A). From the thalamofugal pathway, HA displayed daily, but not circadian,

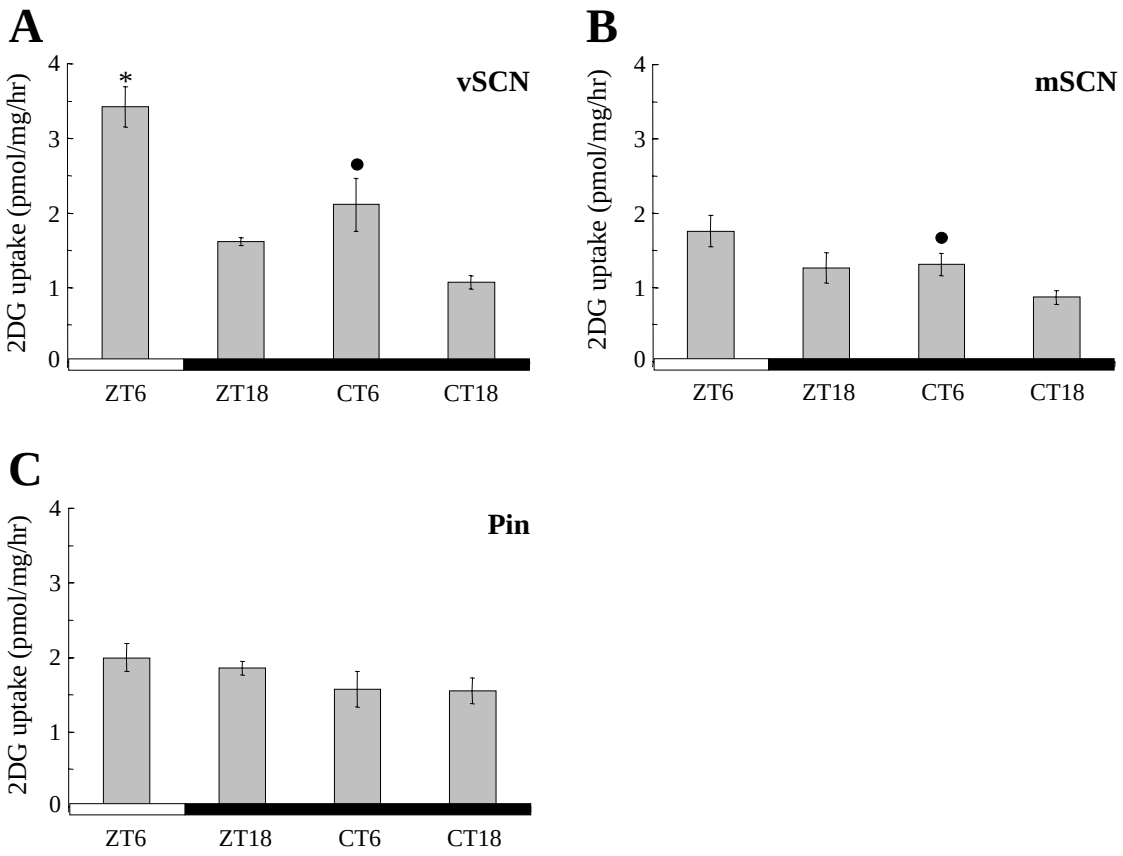

Fig. 3. 2DG uptake over time of day in circadian structures. Structures associated with the circadian system were analyzed for changes in 2DG uptake. The y-axis for each chart was set to the same scale such that amplitude differences between structures could be observed. **A** The vSCN showed daily and circadian differences in uptake. **B** mSCN varied in uptake in DD, but not LD. The amplitude of 2DG uptake in this structure was 40% lower than the vSCN at ZT6. The other time points were at similar levels. **C** Pin showed no significant differences in uptake. Uptake was comparatively low in this structure. Asterisks indicate a significant difference between ZT6 and ZT18 values, while dark circles indicate a significant difference between CT6 and CT18 values.

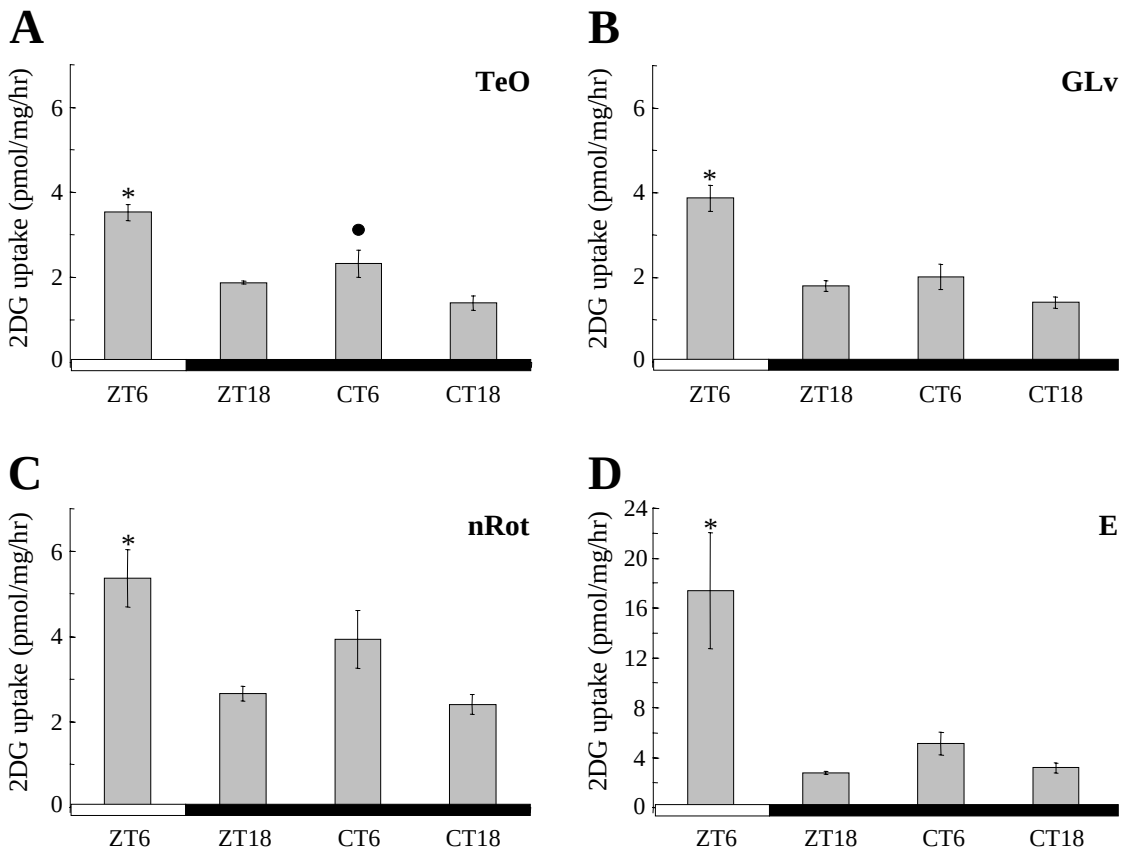

Fig. 4. 2DG uptake over time of day in tectofugal structures. The tectofugal pathway is represented. **A-C** have y-axes on the same scale. As E has a very high amplitude, its y-axis was given a separate scale. **A** TeO showed uptake differences in LD and DD. **B-D** GLv, nRot and E showed daily, but not circadian, changes in 2DG uptake. TeO and GLv show slightly less activity than nRot at all time points. Asterisks indicate a significant difference between ZT6 and ZT18 values, while dark circles indicate a significant difference between CT6 and CT18 values.

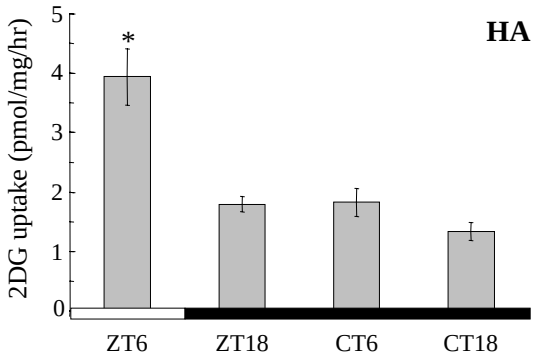

Fig. 5. 2DG uptake over time of day in thalamofugal structures. This pathway is represented by HA, which displayed daily, but not circadian, fluctuation in uptake. The amplitude of uptake in HA is comparable to that of TeO and GLv in Figure 4. Asterisks indicate a significant difference between ZT6 and ZT18 values, while dark circles indicate a significant difference between CT6 and CT18 values.

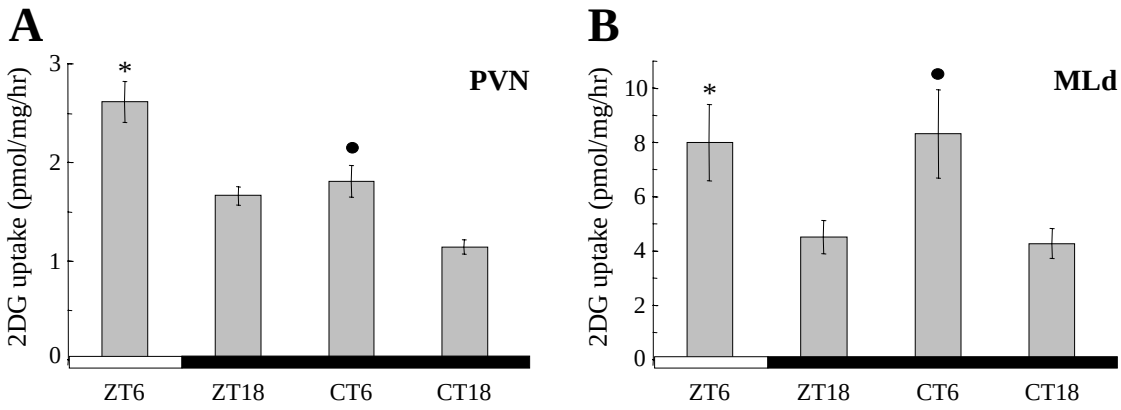

Fig. 6. 2DG uptake over time of day in accessory optic structures. The accessory optic pathway y-axes are on the same scale. **A** EW showed daily and circadian fluctuations of 2DG uptake, as well as higher amplitude uptake at ZT6 and CT6 compared to **B** Cb, which showed a daily, but not circadian, change in uptake. Asterisks indicate a significant difference between ZT6 and ZT18 values, while dark circles indicate a significant difference between CT6 and CT18 values.

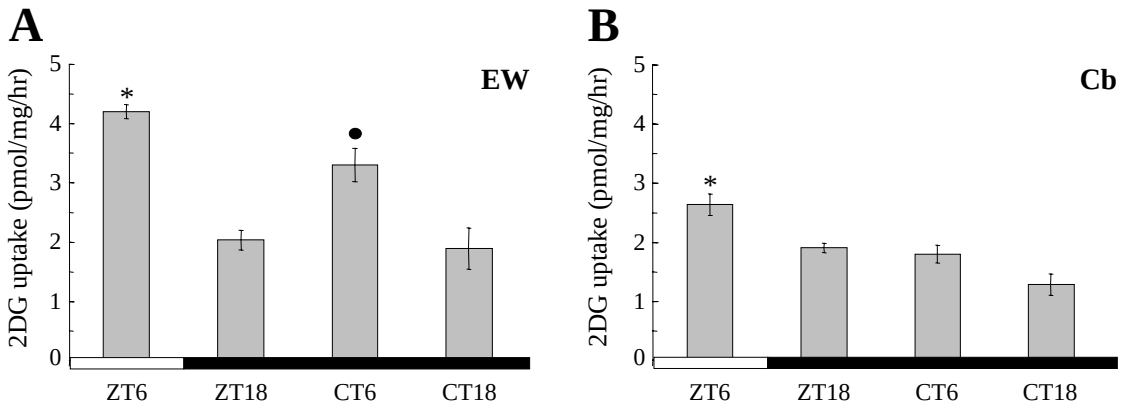

Fig. 7. 2DG uptake over time of day in other structures of interest. Two other prominent structures were measured. **A** PVN showed both daily and circadian changes in 2DG uptake. This uptake is low-amplitude when compared with the visual system structures. **B** MLd showed high amplitude uptake which varied both daily and in a circadian fashion. Asterisks indicate a significant difference between ZT6 and ZT18 values, while dark circles indicate a significant difference between CT6 and CT18 values.

TABLE 1. Analysis of 2DG uptake from Experiment 1

	Light:Dark 12:12			*Constant Darkness*		
structure	*ZT6 mean ± stderr*	*ZT18 mean ± stderr*	*p-value*	*CT6 mean ± stderr*	*CT18 mean ± stderr*	*p-value*
HA	3.898 ± 0.467	1.779 ± 0.131	0.0024	1.805 ± 0.233	1.323 ± 0.149	0.1196
E	17.207 ± 4.601	2.772 ± 0.131	0.0139	5.067 ± 0.885	3.169 ± 0.402	0.0867
mSCN	1.740 ± 0.210	1.251 ± 0.202	0.1435	1.294 ± 0.149	0.860 ± 0.091	0.0376
GLv	3.829 ± 0.307	1.784 ± 0.127	0.0003	1.991 ± 0.291	1.392 ± 0.131	0.0969
vSCN	3.389 ± 0.268	1.601 ± 0.051	0.0002	2.091 ± 0.353	1.060 ± 0.090	0.0221
PVN	2.588 ± 0.203	1.647 ± 0.093	0.0063	1.789 ± 0.160	1.131 ± 0.070	0.0417
nRot	5.313 ± 0.660	2.639 ± 0.172	0.0044	3.895 ± 0.667	2.385 ± 0.234	0.0653
Pin	1.979 ± 0.183	1.838 ± 0.094	0.5118	1.559 ±0.237	1.537 ± 0.171	0.9424
TeO	3.495 ± 0.188	1.859 ± 0.040	0.0001	2.299 ± 0.315	1.383 ± 0.170	0.0337
Cb	2.608 ± 0.177	1.886 ± 0.081	0.0052	1.778 ± 0.146	1.276 ± 0.177	0.0607
MLd	7.907 ± 1.386	4.470 ± 0.609	0.0410	8.231 ± 1.608	4.242 ± 0.542	0.0467
EW	4.159 ± 0.116	2.011 ±0.161	0.0001	3.267 ± 0.277	1.870 ± 0.347	0.0327

All values are given in pmol/mg/hr. For abbreviations, see list.

changes in uptake (Fig. 5). Of the accessory optic structures studied, EW displayed both daily and circadian changes in 2DG uptake (Fig. 6A). The cerebellum (Fig. 6B) showed daily fluctuations in uptake but none in DD.

The 2DG uptake of two other prominent structures of the brain was studied (Fig. 7). The MLd, an auditory system structure, displayed differences in both LD and DD (Fig. 7B). Finally we observed the PVN, which acts as a hypothalamic and autonomic relay center. This structure also displayed both daily and circadian changes in 2DG uptake (Fig. 7A). The means, standard errors and p-values of all comparisons between LD and DD timepoints are presented in Table 1.

Statistical analysis indicates that uptake values at the daytime time points, ZT6 and CT6, were significantly different from each other in the majority of structures studied. Of the three circadian structures, only the vSCN showed such a difference ($p=0.0190$). The visual structures HA ($p=0.0039$), E ($p=0.0321$), GLv ($p=0.0024$), TeO ($p=0.0115$), EW ($p=0.0411$) and Cb ($p=0.0082$) showed variance in their daytime values. PVN ($p=0.0059$) also showed significant changes in daytime uptake. Conversely, the majority of structures did not display significant differences in their values at ZT18 and CT18. Those that did, vSCN ($p=0.0008$), PVN (0.0028), TeO ($p=0.0259$) and Cb ($p=0.0141$), had also experienced significant differences in their daytime timepoint values.

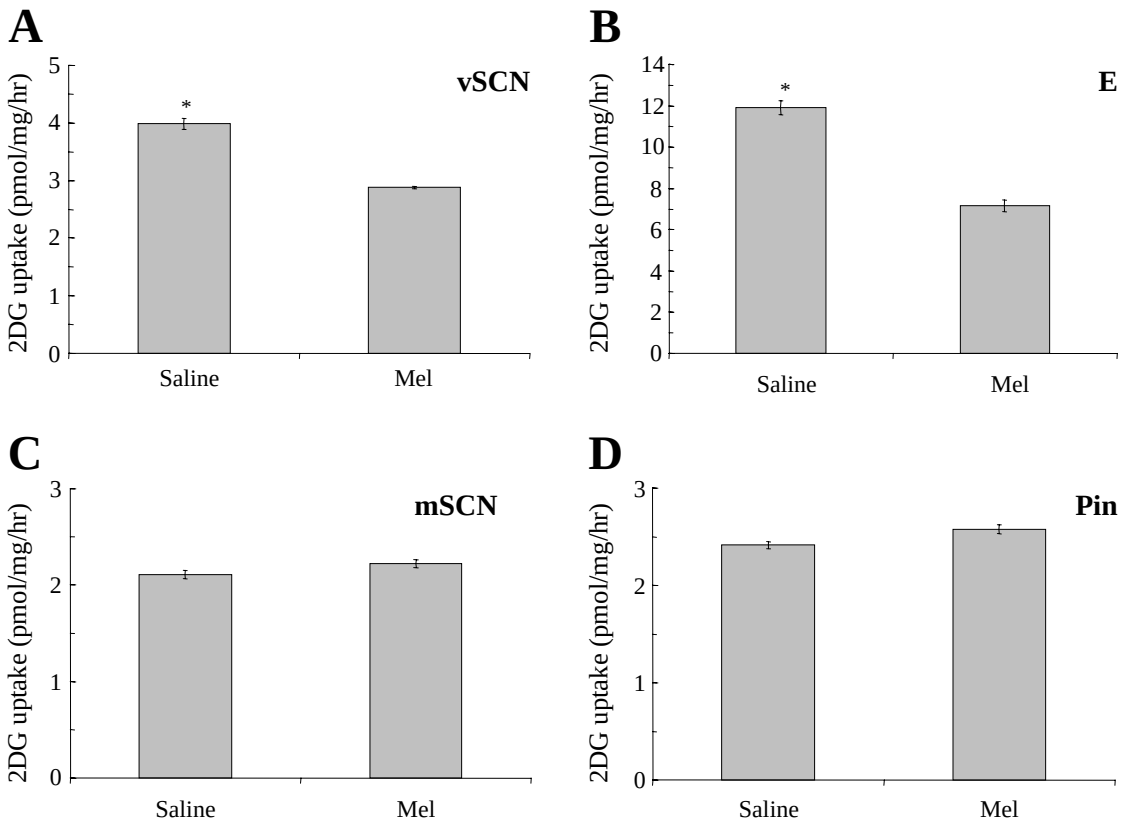

Fig. 8. Effects of exogenous melatonin on 2DG uptake. The effects of exogenous melatonin administration were observed in all structures analyzed in Experiment 1. Of these structures, only two—**A** vSCN and **B** E—showed a significant effect of melatonin. The two other circadian associated structures—**C** mSCN and **D** Pin—showed no effect of melatonin on 2DG uptake. Asterisks indicate a significant difference between ZT6 and ZT18 values.

TABLE 2. Analysis of 2DG uptake from Experiment 2

structure	*Saline* *mean ± stderr*	*Melatonin* *mean ± stderr*	*p-value*
HA	5.118 ± 0.369	3.979 ± 0.399	0.0695
E	11.786 ± 1.102	7.085 ± 0.908	0.0110
mSCN	2.107 ± 0.142	2.222 ± 0.133	0.5745
GLv	4.268 ± 0.402	3.776 ± 0.333	0.3743
vSCN	3.945 ± 0.310	2.855 ± 0.063	0.0089
PVN	3.156 ± 0.303	3.060 ± 0.285	0.8238
nRot	6.314 ± 0.558	5.447 ± 0.415	0.2476
Pin	2.414 ± 0.122	2.577 ± 0.142	0.4080
TeO	4.242 ± 0.350	3.973 ± 0.326	0.5894
Cb	3.237 ± 0.190	3.353 ± 0.245	0.7218
MLd	10.398 ± 1.295	10.432 ± 0.666	0.9816
EW	5.644 ± 0.773	4.755 ± 0.226	0.3029

All values are given in pmol/mg/hr. For abbreviations, see list.

Experiment 2: Effects of melatonin on 2DG uptake

Melatonin affected 2DG uptake in two structures at ZT10, the time at which all Saline/Melatonin comparisons are presented in Table 2. These structures were E and the vSCN (Fig. 8A,B). Uptake in these structures from animals injected by melatonin was significantly lower than in saline-injected animals. There was no effect of melatonin on 2DG uptake in either the mSCN or the pineal (Fig. 8C,D).

DISCUSSION

In this study we have shown that the vSCN of chickens display both daily and circadian changes in 2DG uptake such that it is high during the day and low at night. This finding is consistent with data from the vSCN of the house sparrow (Cassone,

1998) and from the SCN of mammals (Schwartz, 1990). The lowered amplitude of 2DG uptake at CT6, when a light cue was absent, compared with ZT6 suggests that 2DG uptake in the vSCN is influenced by light. This conclusion is supported by studies finding that the RHT terminates in the vSCN of birds (Meier, 1973; Bons, 1976; Cooper et al., 1983; Ehrlich and Mark, 1984; Shimizu et al., 1984; Cassone and Moore, 1987; Norgren and Silver, 1989; Shimizu et al., 1994). Melatonin injections inhibited daytime uptake of 2DG in the vSCN, as was previously shown in house sparrows (Cassone, 1991). This result is consistent with studies showing that, of the putative circadian structures, only the vSCN binds IMEL (Rivkees et al., 1989; Brooks and Cassone, 1992; Cassone et al., 1995).

The mSCN is interesting in that it displays circadian, but not daily, fluctuations in 2DG uptake (Fig. 3B). There are two possible explanations for this result. It is possible that a larger sample size would result in a statistically significant difference in LD uptake. Indeed, cursory inspection of the data leads one to believe that there is a daily change in mSCN 2DG uptake such that it is high during the day and low during the night. Alternatively, the avian SCN homolog may be a diffuse structure involving multiple regions in the hypothalamus including the mSCN and vSCN. This hypothesis may be likened to the discovery of sub-regions within the hamster SCN (LeSauter and Silver, 1999). Data in Chapter IV indicate that an astrocytic bridge and a neuronal connection link the mSCN and vSCN. Retinal input to the mSCN has been reported in the ringed turtledove, *Streptopelia risoria* (Norgren and Silver, 1990), pigeon (Shimizu et al., 1994), house sparrow (Hartwig, 1974), Java sparrow, (Ebihara and Kawamura,

1981) and Japanese quail (Oliver et al., 1978). With the exception of the Shimizu et al. study, this retinal projection is sparse. Recently, partial sequences of the putative clock genes *qclock*, *qper2* and *qper3* have been isolated and characterized in the Japanese quail (Yoshimura et al., 2001). *In situ* hybridization of these sequences in quail brain indicates rhythmic expression in the mSCN but not the vSCN. In contrast, in the house sparrow, expression of a *per2* ortholog is present in both structures, although the amplitude of the rhythm is greater in the mSCN than in the vSCN (Brandstatter et al., 2001). These findings clearly support the view that the mSCN is somehow involved in the circadian system.

The pineal gland shows no significant changes in 2DG uptake in LD or DD (Fig. 3C) consistent with findings in both the house sparrow (Cassone, 1998) and the rat (Rosenwasser et al., 1985). Previous studies have shown that glucose is transported to neurons from the extracellular space by the Glut3 glucose transporter. Interestingly, Glut3 levels are very low in the pineal gland when compared to the rest of the brain (Zeller et al., 1995). These data support an earlier finding that the pineal does not rely upon glucose as a primary fuel source but instead utilizes fatty acid oxidation as a major source of energy (Vannucci and Hawkins, 1983). It remains possible that fatty acid utilization is rhythmic, although this has not been determined. The pineal gland also showed no melatonin-induced change in 2DG uptake (Fig. 8D). This result seems odd due to the presence of Mel_{1C} melatonin receptor mRNA in the pineal (Reppert et al., 1995; personal communications). However, IMEL binding is not detectable in the pineal

(Brooks and Cassone, 1992), indicating that either melatonin binding in the pineal is weak or an alternative conformation of the receptor protein exists that prevents binding.

All seven of the visual structures studied showed a daily change in 2DG uptake (Fig. 4-6). With the exception of nRot, CT6 2DG uptake was significantly lower than ZT6 uptake. The nRot CT6 2DG uptake, while not significantly so, was also lower than ZT6 uptake. These data suggest that the metabolic activity of these visual structures is at least partially light dependent. Two visual structures, TeO and EW, showed a circadian fluctuation of 2DG uptake, also indicating circadian control of these two structures. TeO is the retinorecipient structure of the tectofugal pathway, which is involved in gross visual detection. This is interesting not only because it is the second retinorecipient structure to show circadian rhythmicity, but also because it is involved in the transduction of visual information. This observation is consistent with electrophysiological data indicating circadian variation in tectal-evoked potentials, in which responses to light pulses are higher during the day than during the night (Wu et al., 2000).

EW, on the other hand, is not retinorecipient. It receives projections from the oculomotor nucleus and the vSCN (Gamlin et al., 1982). However, EW sends projections back to the eye, regulating choroidal blood flow and retinal musculature via the ciliary ganglion (Gamlin and Reiner, 1991). The circadian change in 2DG uptake suggests that EW may be under circadian control such that the local atmosphere of the eye may be properly regulated. Only one visual structure, E of the tectofugal pathway, showed an effect by melatonin on uptake (Fig. 8B). E has been shown to strongly bind

IMEL, however so have other structures that were not significantly affected by melatonin (Lu and Cassone, 1993a). These data suggest that melatonin is not the only or even primary modulator of energy metabolism within the chick visual system.

PVN, which receives projections directly from the SCN in mammals, showed both daily and circadian changes in 2DG uptake (Fig. 7A). PVN also showed a significant ZT6/CT6 difference in uptake. These data suggest a role for the circadian system and light dependence in the control of PVN. Indeed it seems logical that such a multi-purpose structure would be under tight control in order to maintain proper brain function in DD. The MLd (Fig. 7C) showed both daily and circadian changes in uptake but did not show a significant difference between daytime time points, suggesting that it is controlled by the circadian system but is not light dependent. Neither of these structures showed an effect of melatonin on 2DG uptake, yet the MLd, at least, has been reported to contain melatonin receptors (Rivkees et al., 1989; Reppert et al., 1995).

It is clear that the circadian system is involved in the regulation of the visual system as a whole, although its importance to individual structures differs. Circadian fluctuation of 2DG uptake in the vSCN, mSCN, TeO, EW, PVN and MLd indicates that the circadian system is involved in the regulation of glucose metabolism. This regulation, however, would appear to occur in a subset of structures throughout the brain. Light seems to play a major role in the modulation of glucose metabolism: most of the studied structures presented higher daytime uptake when a light stimulus was present. Melatonin, on the other hand, did not affect uptake in many structures, suggesting that it is not a major regulator of energy production. It is important to

reiterate that melatonin was only injected at one time of day, ZT10. This time was chosen because it is the peak time of IMEL binding in the chick brain (Brooks and Cassone, 1992). Therefore it remains possible that melatonin injected at an alternate time would have more or less of an effect on 2DG uptake in the brain of the chick, suggesting useful experiments for the future. Overall, the data presented suggest that complex interactions of melatonin, light and, most certainly, other circadian and homeostatic factors regulate cerebral glucose utilization.

CHAPTER III

THE CHICKEN SUPRACHIASMATIC NUCLEI: EFFERENT AND AFFERENT CONNECTIONS

INTRODUCTION

Circadian systems are composed of multiple inputs, oscillators and outputs. Timing cues are transduced via input pathways to oscillators, which then drive rhythms and/or entrain sub-oscillators through output pathways (Menaker and Tosini, 1995). In vertebrates, these components comprise at least the retinae, the suprachiasmatic nuclei of the hypothalamus and the pineal gland, each of which vary in system-level importance among taxa and within each taxon (Menaker and Tosini, 1995).

In the mammalian circadian system, the suprachiasmatic nucleus (SCN) is the primary circadian pacemaker (Moore, 1979). First, the SCN receives significant direct retinal input via the retinohypothalamic tract (RHT) (Moore et al., 1971; Moore and Lenn, 1972; Moore, 1973), and the SCN of eutherian mammals (but not of marsupial mammals) may be subdivided, based on neuroanatomical and functional characteristics (Cassone et al., 1988b), into the retinorecipient ventrolateral SCN, known as the "core", and the dorsomedial region, the "shell" (Moore et al., 2002). Secondly, surgical destruction of the entire SCN results in arrhythmic locomotor behavior (Moore and Eichler, 1972; Stephan and Zucker, 1972; Moore and Klein, 1974; Klein and Moore, 1979), and transplantation of fetal SCN tissue into the third ventricle of arrhythmic, SCN-lesioned rodents restores rhythmicity in locomotor activity (Drucker-Colin et al., 1984; Sawaki et al., 1984; Lehman et al., 1987). Finally, many aspects of SCN

physiology oscillate with a circadian period, including glucose utilization *in vivo* and *in vitro* (Schwartz and Gainer, 1977; Schwartz et al., 1980; Newman et al., 1992), neuronal firing *in vivo* and *in vitro* (Inouye and Kawamura, 1979; Green and Gillette, 1982; Groos and Hendriks, 1982; Shibata et al, 1982), and gene expression *in vivo* and *in vitro* (Yamazaki et al., 2000; Hastings and Herzog, 2004).

Birds have a more complex circadian system than do mammals, since the pineal gland and retinae participate as independent oscillators and pacemakers as well. The pineal gland rhythmically synthesizes and secretes the hormone melatonin such that levels are high during the night and low during the day *in vivo* and *in vitro*, a rhythm that persists for up to four circadian cycles in constant darkness (DD; cf. Natesan et al., 2002). The retinae also rhythmically synthesize melatonin in chickens (Binkley et al. 1979, Hamm and Menaker 1980), Japanese quail (Underwood and Siopes 1984) and pigeons (Oshima et al., 1989; Adachi et al., 1995). This rhythm is important for overt circadian organization in some species. Bilateral enucleation results in the loss of rhythmic activity and body temperature in Japanese quail (Underwood and Siopes, 1984) and chickens (Nyce and Binkley, 1977). In pigeons, enucleation partially disrupts activity and body temperature rhythms but, when paired with pinealectomy, abolishes these rhythms (Ebihara et al., 1984; Chabot and Menaker, 1994).

Several features of circadian organization in birds suggest the presence of another oscillator in the anterior hypothalamus, possibly homologous to the mammalian SCN (Ebihara and Kawamura, 1981; Simpson and Follett, 1981; Takahashi and Menaker, 1982). Early cytoarchitectural evidence suggested that a region located near

the preoptic recess of the third ventricle is the avian SCN (Crosby and Showers, 1969). This structure has been labeled the periventricular preoptic nucleus (PPN; van Tienhoven and Jühász, 1962; Cassone and Moore, 1987; revised nomenclature, POP; Kuenzel and Masson, 1988), the SCN (Hartwig, 1974, Kuenzel and van Tienhoven, 1982; Brandstatter et al., 2001), the medial hypothalamic nucleus (MHN; Norgren and Silver, 1989), the medial hypothalamic retinorecipient nucleus (MHRN; Shimizu et al., 1994) and the medial SCN (mSCN; Kuenzel and Masson, 1988; Yoshimura et al., 2001). In the present study, we will refer to this structure as the mSCN. The mSCN has been reported to receive some retinal afferents, but the label is typically weak (Hartwig, 1974; Oliver et al. 1978) or undocumented with photomicrographs (Ebihara and Kawamura, 1981).

In contrast, a lateral hypothalamic nucleus is the primary, if not only, hypothalamic retinorecipient nucleus in a variety of species: ringed turtledove, *Streptopelia risoria* (Cooper et al., 1983; Norgren and Silver, 1989), house sparrow, *Passer domesticus* (Cassone and Moore, 1987), pigeon, *Columba livia* (Meier, 1973; Gamlin et al., 1982; Shimizu et al., 1994), duck, *Anas platyrhynchos* (Bons, 1976) and chicken, *Gallus domesticus* (Shimizu et al., 1984). This structure has been referred to in the literature as the SCN (Gamlin et al, 1982; Cooper et al., 1983), the lateral hypothalamic retinorecipient nucleus (LHRN; Norgren and Silver, 1989; Shimizu et al., 1994) and the visual SCN (vSCN; Cassone and Moore, 1987). In this study, we will use the term vSCN.

Antigen mapping has also been utilized to identify the avian SCN. The SCN of mammals is heterogeneous in its antigen distribution. In rodents, cells immunoreactive for vasoactive intestinal polypeptide (VIP) are found in the core, while arginine vasopressin (AVP) immunoreactive cells are found in the shell (Moore et al., 2002). Similarly, in the house sparrow, AVP (avian homolog, arginine vasotocin) immunoreactive cells are found ventral to the vSCN, while VIP positive cells are found at the medial border of the vSCN (Cassone and Moore, 1987). Other antigens found in the mammalian SCN include gastrin releasing peptide, glutamic acid decarboxylase, neuropeptide Y, neurotensin, serotonin, somatostatin and substance P (Moore et al., 2002), all of which are found in the vSCN of the house sparrow (Cassone and Moore, 1987). While the chemoarchitecture of the vSCN is similar to that of the eutherian mammalian SCN, it is not identical; therefore, it was proposed by Cassone and Moore (1987) that the vSCN is the retinorecipient portion of a suprachiasmatic complex in which one or more other structures may be involved.

The present study is an analysis of the synaptic connections of both the vSCN and the mSCN of the chicken, *Gallus domesticus*, and examines whether efferent and afferent connections of and between the mSCN and vSCN indicates whether one or both may be homologous to the mammalian SCN. We present here a new working model of the avian SCN based on the current and previous studies.

MATERIALS AND METHODS

Animals

Female Spangled Old English Bantams (*Gallus domesticus*) were acquired at Ideal Poultry (Cameron, TX) on their hatch date. Male White leghorn chicks (*Gallus domesticus*) were obtained, also on their hatch date, from Hy-Line Hatcheries (Bryan, TX). Birds were housed on a light:dark 12:12 cycle (lights on from 6:00 a.m. to 6:00 p.m. CST) until the injections took place. Both strains were raised in heated brooders: the White leghorns remained in the brooders, while the bantams were moved to unheated cages and grown to adulthood, about two to three months, to achieve a stable weight (450-720 g) before surgery. Injections were performed on White leghorns once their weight reached 275-310 g, which took four to five weeks. Food (Purina Start and Grow; Brazos Feed & Supply, Bryan, Texas) and water were continuously available until the day of the surgery, at which time it was removed. All animal use protocols were reviewed and approved by the University Laboratory Animal Care Committee (ULACC) at Texas A&M University (Animal Use Protocol #2001-163).

Determination of stereotaxic coordinates

Stereotaxic coordinates for the vSCN and mSCN were determined using 26 White leghorn chicks. Chicks were deeply anesthetized with ketamine/xylazine drug cocktail (90 mg/kg ketamine, 10 mg/kg xylazine) and placed into a stereotaxic apparatus equipped with ear and beak bars specialized for birds. In order to ensure a stable angle, coordinates were taken from three points: ear bar zero was used as the reference point,

eye corner zero represented the coordinates of the posterior corner of the eye and lambda designated the coordinates at the intersection of the lambdoid and sagittal sutures of the cranium. A stable slope was established and test lesions were performed. After each lesion, the birds were immediately sacrificed; their brains were removed and flash frozen. Brains were sectioned frontally at 30 μm, thaw-mounted onto slides, fixed in alcohol, stained with cresyl violet, dehydrated, cleared and coverslipped for localization of the lesions. After obtaining a rough location for the mSCN and vSCN, the coordinates were refined such that we could reliably target these structures with the thin micropipettes used for intracerebral iontophoresis.

Tract tracing agents

Cholera Toxin B-subunit (CTB; List Biological Laboratories, Campbell, CA) is a sensitive tracing agent widely used in anatomical studies. It functions as an anterograde (Wu et al., 1999) and retrograde (Calaza and Gardino, 2000) tracer when injected intravitreally. Injected intracerebrally, CTB also traces anterogradely and retrogradely. There is some evidence that suggests CTB is avidly taken up by fibers of passage (Chen and Aston-Jones 1995); therefore, it is more useful as a retrograde tracer. CTB has been used extensively in mammalian mapping studies, and many studies have demonstrated comparable efficacy in birds (Shimizu et al., 1994; Wu et al., 2003; Gardino et al., 2004). We also used 10,000 kD biotin dextran amine (BDA; Molecular Probes, Eugene, OR) as an anterograde tracing agent. Previous studies have shown its ability to label both axons and terminals in efferent structures in birds (Veenman et al., 1992; Tombol et

al., 2003). Neither CTB nor BDA cross synapses over short incubation periods, thus, labeling identifies direct afferents or efferents to injected and iontophoresed sites.

Intravitreal injection of CTB

Five birds were anesthetized with ketamine/xylazine drug cocktail. The eyelid was deflected and 20 μl 0.5% CTB was injected into the vitreous chamber of the eye with a 50 μl Hamilton syringe. The syringe was left in place for two minutes while the CTB diffused away from the tip, at which time it was removed. These birds were maintained in a separate cage for two (n=4) or five (n=1) days until they were sacrificed.

Iontophoretic CTB injections

The first set of CTB iontophoretic injections was performed in the Bantam chickens. Glass micropipettes (tip diameter 5-10 μm) were backfilled with 1% CTB solution after which 5 μl were loaded into each micropipette using a 10 μl Hamilton syringe. Twenty-six Bantams were anesthetized with ketamine/xylazine drug cocktail and the proper head angle in a stereotaxic apparatus was achieved as described above. The micropipette was slowly lowered to the proper coordinates and allowed to settle for ten minutes. A 5 μA current was then applied to the CTB solution for a five-minute cycle of 7 seconds on/7 seconds off using a Midgard power supply (Stoelting Co., Wood Dale, IL). In Bantams, we directed twelve unilateral injections at the vSCN and fourteen at the mSCN. Upon completion of iontophoresis, the micropipette was left in place and the CTB solution was allowed to diffuse away from the tip of the electrode for at least

ten minutes, at which time the micropipette was removed from the brain and the scalp was stitched closed.

White leghorns (n=13) were injected in a second round of similar surgeries after the Bantam brains were processed and visualized. Micropipettes were loaded, as described above, but this time with 0.5% CTB. Eight injections were directed at the vSCN, five at the mSCN. A 5 μA current, alternating on and off for 7 seconds, was applied to the CTB solution for ten minutes. After ten minutes of diffusion time, the micropipette was removed while the CTB solution was under a continuous -5 μA current to further ensure that none leaked into the track made by the micropipette.

Iontophoretic BDA injections

Glass micropipettes (tip diameter 20-30 μm) were backfilled with 10% BDA in 0.01 M phosphate buffer after which 5 μl were loaded into each micropipette using a 10 μl Hamilton syringe. White leghorn chicks (n=23) were anesthetized with ketamine/xylazine drug cocktail and the surgical insertion of the micropipettes was performed as described above. A +5 μA current was applied to the BDA solution for twenty minutes in 7-second on/off cycles. Twelve injections were directed at the vSCN, eleven were aimed at the mSCN. After iontophoresis, the micropipette was left in place and the BDA solution was allowed to diffuse away from the tip of the electrode for at least ten minutes. The micropipette was removed from the brain under constant negative current and the scalp was stitched closed.

Tissue preparation

Birds with CTB injections were maintained for five days; BDA injected birds, for eight days. The birds were then anesthetized with ketamine/xylazine drug cocktail, which was supplemented as needed with halothane. White leghorn eyes were removed prior to fixation and the retinae were removed and fixed in 4% paraformaldehyde. Birds were transcardially perfused with 50-100 ml phosphate buffered saline (PBS; 10mM), followed by 300-500 ml 4% paraformaldehyde fixative. Brains were subsequently removed and post-fixed for 4-16 hours. They were then cryoprotected in serial solutions of 10%, 20% and 30% sucrose.

Brain tissue processing

Cryoprotected brains were frozen, frontally sectioned at 30 μm on a Lipshaw cryostat (Pittsburgh, PA) and rinsed in PBS. Endogenous peroxidase activity was inhibited with a 15-minute incubation of 30% methanol and 0.75% hydrogen peroxide in PBS followed by a blocking step in PBS containing 0.3% Triton-X-100 and 1% normal rabbit serum (PBSRT) for 1 hour. Sections processed for CTB immunoreactivity were incubated with goat anti-choleragenoid antibody (1:5000; List Biological Laboratories, Campbell, CA) in PBSRT for 48-72 hours at 4^{o}C, followed by biotinylated rabbit anti-goat secondary antibody (1:200; Vector Laboratories, Burlingame, CA) in PBSRT for two hours at room temperature. Sections were incubated with avidin-biotin complex from a peroxidase standard kit (1:55; Vector Laboratories, Burlingame, CA) in PBSRT, in the case of CTB, or PBS containing 0.4% Triton-X-100, in the case of BDA, for 90

minutes at room temperature. Sections were incubated in 0.5% 3-3'-diaminobenzidine solution in 100 mM Tris buffer for five minutes after which 0.21% hydrogen peroxide was added to the solution. The color reaction was stopped as soon as background coloration became evident. Sections were rinsed, put into order, mounted onto gelatin-coated slides and dried overnight. The slides were then rinsed in PBS and the color reaction was stabilized in 1% cobalt chloride solution. The slides were rinsed, dehydrated, cleared and coverslipped for analysis.

Retinal processing

Intact retinae were processed for visualization of BDA and CTB in the manner described above. After the color reaction, the retinae were float mounted onto slides. They were then processed and coverslipped in the same manner as the brain sections.

Microscopy and Photography

An Olympus BH-2 light microscope (Melville, NY) was used to examine processed tissues. CTB immunoreactivity was observed with differential interference contrast optics, while BDA immunoreactivity was viewed under dark field. Photomicrographs were taken with an Olympus C-35AD-4 camera on Kodak Gold 200 film (Rochester, NY). Prints were scanned at 600 DPI and opened in Adobe Photoshop 7.0.1 (Adobe Systems, Mountain View, CA), where they received minor brightness and contrast adjustments.

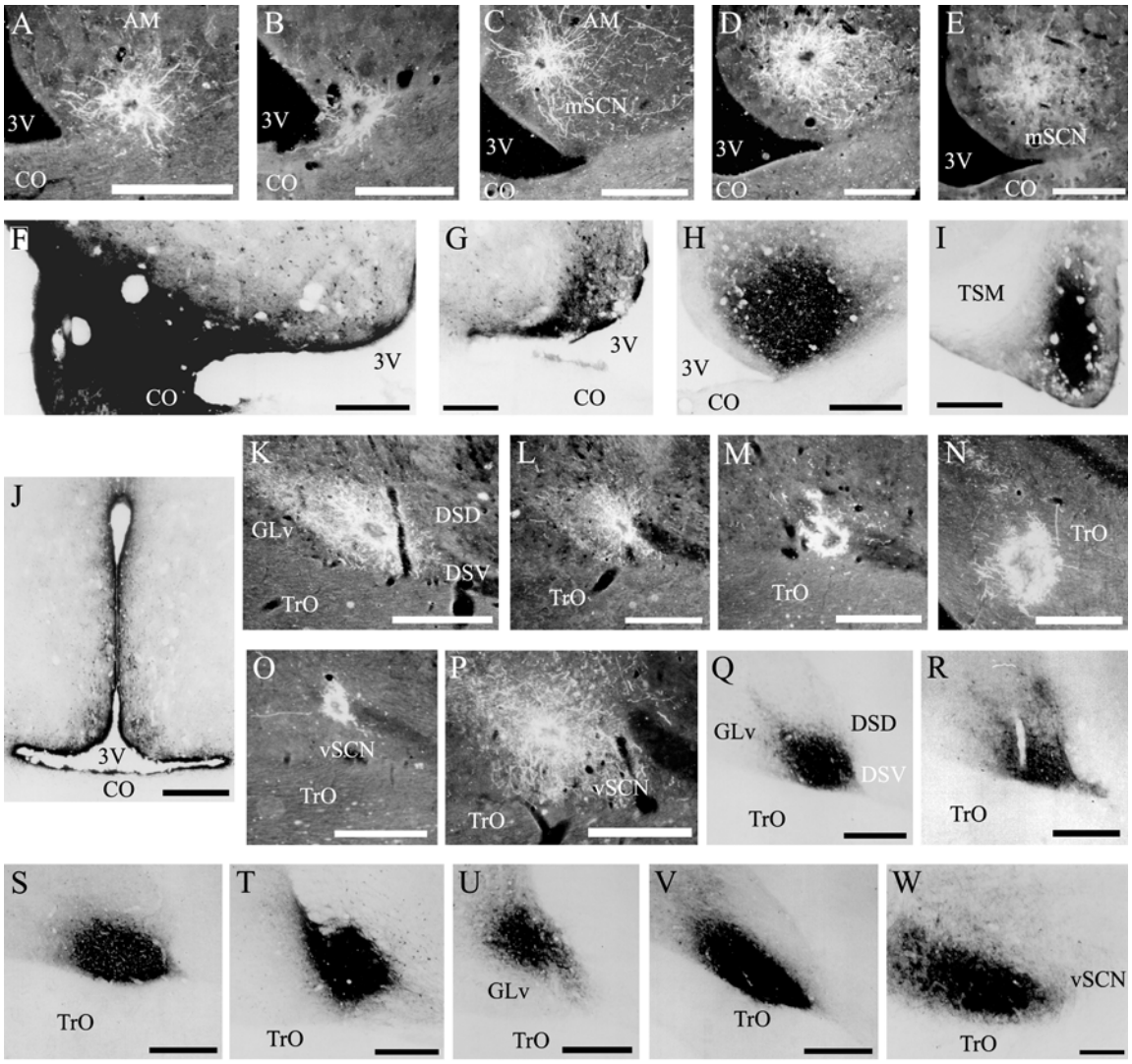

Fig. 9. Photomicrographs documenting all biotin dextran amine (BDA) and cholera toxin B subunit (CTB) iontophoretic injections reported in Tables 4 and 5. BDA injections directed toward mSCN landed as follows: **A,B** mSCN, **C** mSCN/AM, **D** AM, **E** AM/POA. CTB injections directed at mSCN landed as follows: **F** mSCN/POA/CO, **G** mSCN/3V, **H** mSCN/AM, **I** POA, **J** 3V. BDA injections directed toward mSCN landed as follows: **K-M** vSCN, **N** TrO, **O** DSV, **P** dorsal to vSCN. CTB injections directed toward vSCN landed as follows: **Q-S** vSCN, **T** vSCN, dorsal to vSCN and WM (defined in Results), **U** ICT, **V** vSCN/GLv, **W** GLv. For abbreviations, see list. Scale bar = 1 mm in C-V; 400 μm in A,B,W.

Evaluation of injection sites and tracing

CTB and BDA injection sites appeared similar to one another and were readily identified by dense immunoreactive fields surrounding central necrotic areas. Previous studies have demonstrated that CTB and BDA are taken up and transported from the most densely labeled region (Leak and Moore, 2001). Photomicrographs of reported injection sites are available in Figure 9. Injection sites outside the border of these structures were used for two purposes. First, Bantam and White leghorn afferents and efferents were compared in brains that had similar injection sites. In this way, we were able to determine that there are no significant differences between the connections of the vSCN and mSCN of these two strains. Secondly, injections that missed the SCN entirely were used to assess the accuracy of our maps. In the analysis of tract tracing, we also took into account whether BDA labeled fibers were terminal or fibers of passage. Terminal fibers were identified by the presence of varicosities and fibers of passage by their thick, smooth appearance.

Mapping

CTB cells and fibers and BDA fibers were hand drawn and then digitized onto plates adapted from a published chick stereotaxic atlas (Kuenzel and Masson, 1988). Brain structures were identified according to the nomenclature of Kuenzel and Masson (1988) and several published partial atlases (Kuenzel and van Tienhoven, 1982; Ehrlich and Mark, 1984; Reiner et al., 2004).

In order to produce a map of the retina, a slide was placed on a light box and the outline was drawn onto a transparency. The traced image was put onto an overhead projector for enlargement. The enlarged image was scanned into Photoshop where the distribution of retinal ganglion cells was digitally recorded.

RESULTS

Retinal projections

Four intravitreal injections resulted in strong labeling of retinal terminals in the chick brain, including the injection that was allowed to transport for five days. Sections from these brains were used to produce maps (Fig. 10) and photomicrographs (Fig. 11). We observed retinal terminals and, in the case of the isthmo-optic nucleus, cells, in many structures previously identified by tract-tracing methods and retinal degeneration. A summary of these structures is provided in Table 3. Of particular interest in this study was a terminal field in the vSCN (Fig. 10C-E). This region was more strongly labeled after five days of transport (Fig. 11E) than it was after two days (Fig. 11F). Labeled sparse cells were also identified within vSCN, and were more easily identified after two days of CTB transport (Fig. 11F inset) than they were after five days. Sparse label in the lateral mSCN indicated both terminal fibers and fibers of passage (Figs. 10A, 11C). Staining in several other structures identified has not been previously reported. Retinal terminals were also observed in the region dorsal to the mSCN, including the ventral aspect of the hypothalamic anterior nucleus (AM) and the region between mSCN and

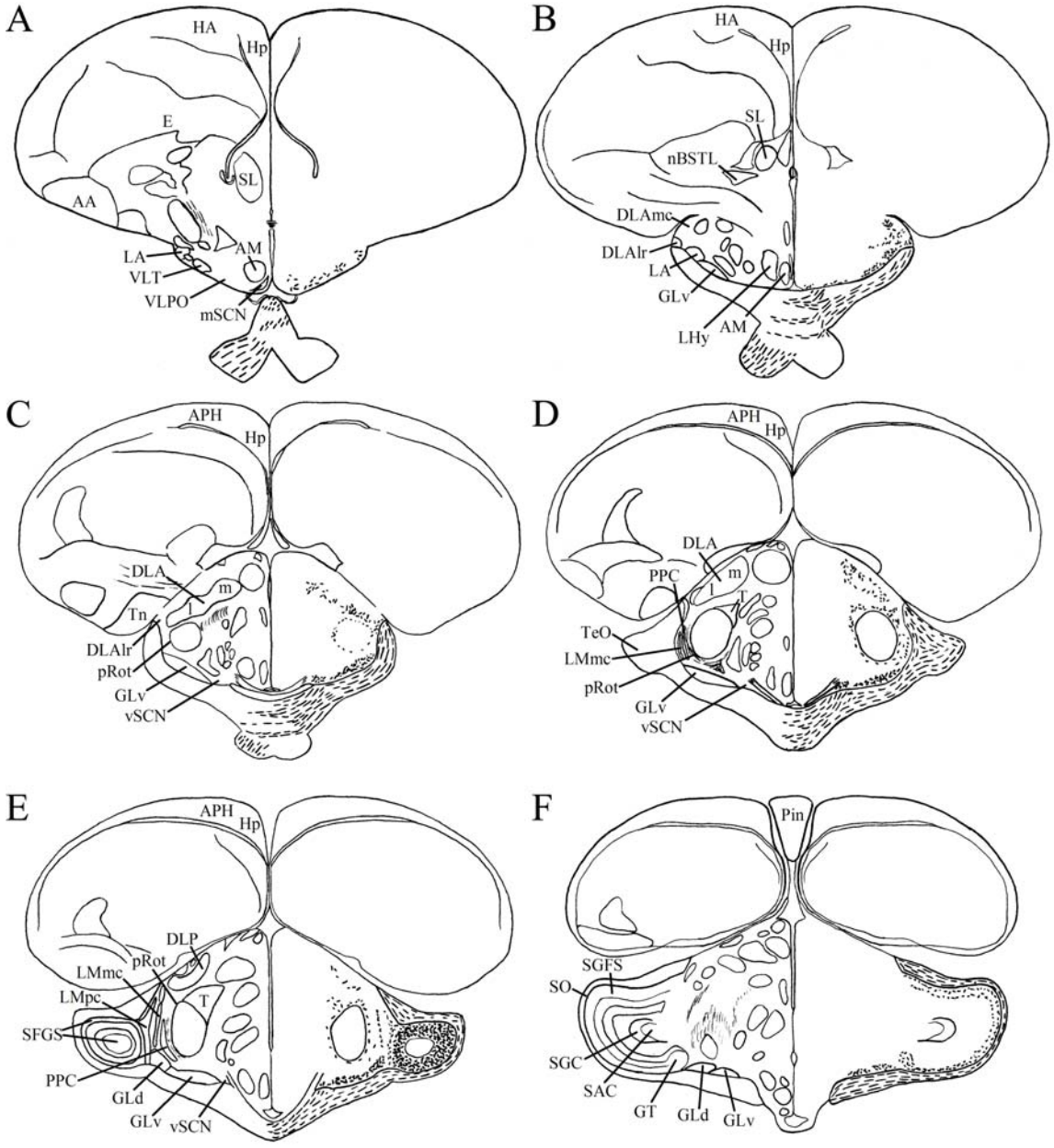

Fig. 10. Maps of retinal input throughout its rostrocaudal extent following CTB injection to the vitreous chamber of the eye. Structures of interest are labeled on the left hemisphere of each brain and retinal fibers are indicated on the right hemispheres with short lines. All fibers shown are terminal fibers. The distribution of lines represents the relative strength of input to each area, but do not represent measured values. For abbreviations, see list.

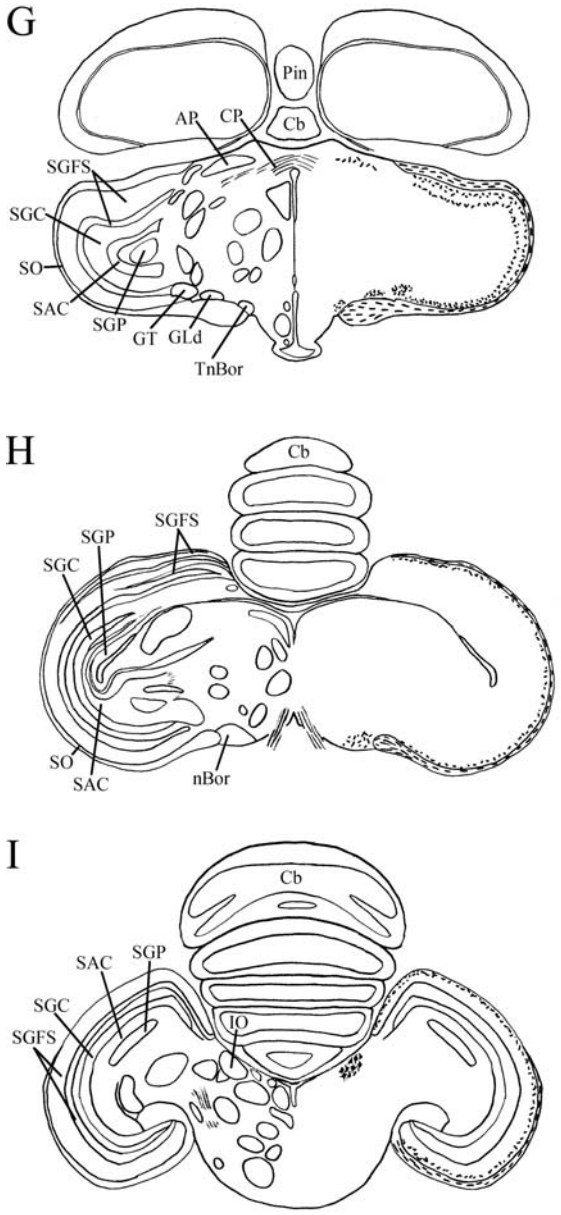

Fig. 10 Continued

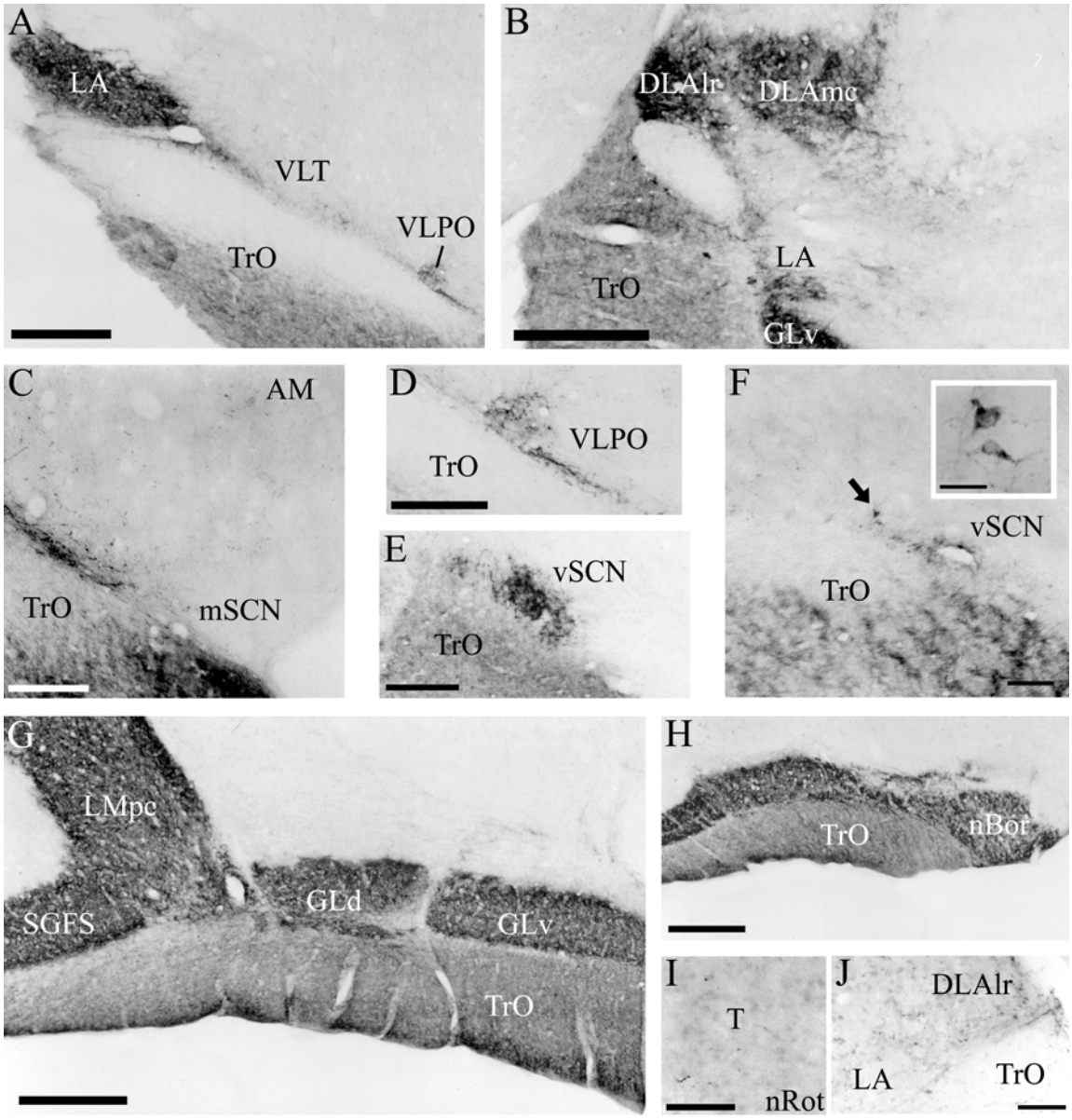

Fig. 11. Representative photomicrographs of retinal input to the brain following CTB injection to the vitreous chamber of the eye. Note the sparse terminal fibers in the lateral mSCN, as well as a dense grouping of fibers of passage on the lateral border (**C**) and the presence of cells in the anterior vSCN (**E**). For abbreviations, see list. Scale bar = 1 mm in A,B,G,H; 400 μm in E,C,D; 200 μm in I,J; 100 μm in F inset.

TABLE 3. Previously reported retinorecipient avian brain structures.

Diencephalon
Medial suprachiasmatic nucleus (mSCN)[4,7,9,10]
Visual suprachiasmatic nucleus (vSCN) [1-3,10,11]
Lateral anterior nucleus (LA)[5,10]
Ventrolateral thalamic nucleus (VLT)[5]
Ventrolateral geniculate nucleus (GLv)[5,10]
Rostrolateral dorsolateral nucleus (DLAlr)[5,13]
Magnocellular dorsolateral nucleus (DLAmc)[5,10]
Lateral dorsolateral nucleus (DLAl)[5,10]
Medial dorsolateral nucleus (DLAm)[5]
Dorsolateral geniculate nucleus (GLd)[5,10]
Mesencephalic lentiform nucleus, magnocellular part (LMmc)[5,6]
Mesencephalic lentiform nucleus, parvicellular part (LMpc)[5,6]
Perirotundal area (pRot)[5,10]
Diffuse pretectal nucleus (PD)[5,6]
Pretectal area (AP)
contralateral[5,6,10]
ipsilateral[10]
Mesencephalon
Superficial gray and fiver layer of the optic tectum (SGFS), layers 2-7[5,6,10]
Tectal gray (GT)[5]
Nucleus of the basal optic root (nBor)
contralateral[5,10]
ipsilateral[8]
Isthmo-optic nucleus (IO)[5,10,12]

Strength of CTB signal in retinal terminals: +++, strong; ++, moderate; +, sparse. For abbreviations, see list. Species and reference: 1, duck, Bons, 1976; 2, house sparrow, Cassone and Moore, 1987; 3, ringdove, Cooper et al., 1983; 4, Java sparrow, Ebihara and Kawamura, 1981; 5, chicken, Ehrlich and Mark, 1984; 6, pigeon, Gamlin and Cohen, 1988; 7, house sparrow, Hartwig, 1974; 8, chicken, Mey and Johann, 2001; 9, quail, Oliver et al., 1978; 10, pigeon, Shimizu et al., 1994; 11, chicken, Shimizu et al., 1984; 12, quail, Uchiyama, 1989; 13, quail, Watanabe, 1987.

AM (Fig. 11C). We also found terminal fibers in a contralateral region of the anterior diencephalon that we believe may be homologous to the mammalian ventrolateral preoptic nucleus (VLPO). Modest staining in the form of discernible terminal fibers was observed in this structure roughly 500 μm anterior to the vSCN and 750 μm lateral of the mSCN, which was in the same frontal planes of section (Figs. 10A, 11A,C). Finally, terminals were found in the ipsilateral nucleus triangularis (T; Fig. 11I), dorsolateral

anterior nucleus, rostrolateral part (DLAlr; Fig. 11J) and the lateral anterior nucleus (LA; Fig. 11J). All of these structures also receive strong contralateral input.

Iontophoretic injections

Two BDA injections were identified within the medial suprachiasmatic nucleus (mSCN). One was located in the mSCN with minor leakage caudally (Fig. 9A), while the second impinged upon the optic chiasm with some possible leakage into the third ventricle (Fig. 9B). Projections that were identified in both mSCN-injected brains are reported in Table 4. Projections present in one brain and not the other are not described. Of the nine remaining injections, two were discarded due to poor tracer administration. Four injections were completely misplaced, resulting in projection patterns bearing no similarity to the mSCN efferents observed. They are not reported. The final three injections were analyzed in order to critically evaluate our potential mSCN efferents. The first injection was located in the mSCN, but extended dorsally to the ventral aspect of AM (Fig. 9C). The second injection was localized specifically to AM (Fig. 9D), while the third was also located in AM, but extended rostrally into the preoptic area (POA; Fig. 9E). The efferents identified as a result of these injections are noted in Table 4.

Two CTB injections were identified within the borders of the mSCN. The first extended laterally into the preoptic area and ventrally into the optic chiasm (CO) with a small amount of leakage into the third ventricle (Fig. 9F). The second was relatively well-contained, with only a small amount of leakage into the third ventricle (Fig. 9G).

TABLE 4. Efferent connections of the avian and mammalian suprachiasmatic nuclei

Structures	Chick mSCN	Chick vSCN	Corresponding Mammalian SCN Efferent	Misplaced injections near mSCN: mSCN/AM	AM	AM/POA	Misplaced injections near vSCN: TrO	DSV	Dorsal to vSCN
Telencephalon									
SL	+	-	SL[#*§]	++	+	+		-	-
nBST	+	-	BST[#*]	++	+	+		-	-
Diencephalon									
Preoptic area	+	+	POA[#*§]	++	+++	+++		-	-
Hypothalamus									
AM	++	+	AHA[§]	+++	injected	injected		-	-
LHy	+	+	LHA[§]	++	+++	+++		+	-
mSCN	injected	++		-	++	++		-	+
mSCN, contra	+	-		+	+	-		-	-
VLPO	-	++	VLPO[#*]	-	-	-		-	++
VMN	++	-	VMH[#*§]	+++	+++	+++		-	-
VMN, contra	+	-		-	-	-		-	-
vSCN	+	injected		+	+	+	@	+	+++
vSCN, contra	+	++		+	-	-		-	+
AL	-	++		-	-	-		-	-
IH	++	-	TM[§]	++	+	++		-	-
IN	++	-		++	++	+		-	-
DMN	++	-	DMH[#*§π]	++	++	++		-	-
MM	+	-		+	+	+		-	-
PVN	+++	-	PVN[#*§π]	+++	+++	++		-	-
Thalamus									
VLT	-	++		++	++	+		+	++
LA	-	+		+	+	+		-	+
GLv	-	++		+	+	+	@	+	+
GLv, contra	-	+		-	-	-		-	-
ICT	-	+++		+	-	-		+	++
DLAmc	-	+++		++	+	+		+	++
DLAl	-	+++		+	+	+		+	++
DLAm	-	+++		+	-	-		-	++
DLAlr	-	+++		-	-	-		-	+
DLP	-	+++		-	-	-		-	+
PVT	+++	-	PVT[#*§]	+++	++	++		-	-
nCPa	+	-		+	+	-		-	-
OV	-	+		-	-	-		-	+
GLd	-	+		-	-	-	@	-	+
Pretectum									
pRot	+	++	IGL[#*]	+	+	+		-	+
SP	-	+		-	-	-		-	+
PPC	-	++		-	-	-		+	+
AP	+	+++		+	+	++		-	+
LMmc	-	+++		-	-	-		+	++
LMpc	-	+++		-	-	-	@	+	++
Habenula	++	-	Habenula[§]	+++	+++	+++		-	-
Mesencephalon									
SGP	+	+		+	+	+		+	+
SAC	+	+		+	+	+		+	+
SGC	-	+		-	-	-		+	+
SGFS	-	+		-	-	-	@	-	-
GCt	+	+	PAG[#*]	++	++	++		+	+
nBor	-	+		-	-	-	@	+	+
PPT	-	+		-	-	-		++	++
AVT	-	+		+	+	+		++	++
Ru	-	+		-	-	-		+	+
EW	-	+		-	-	-		-	-
Rhombencephalon									
Pap	-	++		-	-	-		++	++

Strength of BDA signal in terminal fibers: +++, strong; ++, moderate; +, sparse. Misplaced injections are described in the Results section. Structures labeled by the BDA injection to TrO are indicated simply (@) and represent a subset of the retinal projections delineated in Table 3. For chick structure abbreviations, see list. Corresponding mammalian structure abbreviations: AHA, anterior hypothalamic area; BST, bed nucleus of the stria terminalis; DMH, dorsomedial hypothalamic nucleus; IGL, intergeniculate leaflet; LHA, lateral hypothalamic area; POA, preoptic area; PAG, periaqueductal gray; PVN, hypothalamic paraventricular nucleus; PVT, thalamic paraventricular nucleus; SL, lateral septal nucleus; TM, tuberomamillary hypothalamus; VLPO, ventrolateral preoptic nucleus; VMH, hypothalamic ventromedial nucleus. Species and reference of mammalian structures: #, rat, Leak and Moore, 2001; *, hamster, Kriegsfeld et al., 2004; §, mouse, Abrahamson and Moore, 2001; π, human, Dai et al., 1998.

TABLE 5. Afferent connections of the avian and mammalian suprachiasmatic nuclei

				Misplaced injections near mSCN			Misplaced injections near vSCN			
Structures	Chick mSCN	Chick vSCN	Corresponding Mammalian SCN Afferent	AM/ mSCN	POA/CO	3V	dorsal vSCN/WM	ICT	GLv/ vSCN	Medial GLv
Telencephalon										
HA	-	+++		++	-	++	++	+	++	++
Hp	+	-	H*	++	+	++	+	-	+	-
APH	+	++		++	-	-	+	-	+	-
SL	++	-	SL#*	++	-	++	+	-	-	-
nBST	+++	-		+	+	++	-	-	-	-
Tn	++	-		-	-	-	-	-	-	-
Diencephalon										
Preoptic Area	+++	-	POA#*	++	+++	+++	+	-	-	-
Hypothalamus										-
AM	++	+	AHA#*	injected	-	+	+	+	+	-
AM, contra	-	+		+	-	-	-	-	-	-
LHy	++	+		++	-	+	+	-	+	-
mSCN	injected	+		++	++	++	+	-	+	-
mSCN, contra	+	-		++	-	++	-	-	-	-
VLPO	++	++		+	-	+	++	-	-	-
VMN	++	++	VMH#*	+++	+	+	+	+	+	-
vSCN	+	injected		+	-	-	++	++	+	-
vSCN, contra	-	++		-	-	-	+	-	+	-
AL	-	++		-	-	-	++	+	+	+
IH	++	++		+++	++	++	++	-	+	-
IN	++	-	Arc#	++	++	++	-	-	-	-
DMN	++	-		+	+	++	-	-	-	-
MM	++	-		+	+	++	-	-	-	-
ME	++	-		-	-	++	-	-	-	-
PVN	++	+	PVN*	+	+	+++	+	+	+	-
Thalamus										
VLT	+	++		+	-	-	++	++	+	+
LA	+	+++		+	-	+	+	+	++	-
LA, contra	-	++		-	-	-	+	-	+	-
GLv	-	+++	vLGN*	+	-	-	+++	++	injected	injected
GLv, contra	-	++		-	-	-	+	+	++	+
ICT	-	++		-	-	-	+	injected	-	+
DLAmc	-	++		+	-	-	++	+	+	+
DLAl	-	++		+	-	-	+	-	++	+
DLAm	-	++		+	-	-	-	-	+	+
PVT	+++	++	PVT#*	+	+	+++	++	-	+	-
PVT, contra	+++	-		-	-	-	+	-	-	-
nCPa	++	++		+	-	+++	+	+	+	-
T	-	++		-	-	-	+	-	-	-
GLd	-	++		-	-	-	+	+	-	-
Pretectum			Pretectal nuclei#							
pRot	-	++	IGL#	++	-	-	+	-	+	+
PPC	-	++		-	-	-	++	++	+++	+
AP	-	++		-	-	-	+	+	+++	-
PD	-	++		-	-	-	+	-	+	-
LMmc	-	+++		-	-	-	++	+++	+++	++
LMpc	-	+++		-	-	-	++	+++	+	++
Habenula	+++	-		+	+	+	-	-	-	-
Mesencephalon										
SGP	+	++		++	-	-	++	+	-	-
SAC	+	+		++	-	-	++	+	+	-
SGC	-	+++		-	-	-	+	++	-	-
SGFS	-	++	Superficial SC#	-	-	-	+	+	-	+
GT	-	+++		-	-	-	++	+	+	+
GCt	++	++	PAG#	++	-	-	++	+	+	-
GCt, contra	-	+		-	-	-	+	-	-	-
LoC	-	+	LoC#*	+	-	-	+	+	++	-
SCE	-	+		++	-	-	+	+	+	-
nBor	-	+		-	-	-	+	-	-	-
AVT	++	-	VTN*	-	-	-	+	-	-	-
Rhombencephalon										
Pap	-	+++		-	-	-	+	+	+	+
OM	-	+		+	-	-	++	++	++	+

Strength of CTB signal: +++, strong; ++, moderate; +, sparse. Misplaced injections are described in the Results section. For chick structure abbreviations, see list. Corresponding mammalian structure abbreviations: AHA, anterior hypothalamic area; Arc, arcuate nucleus; H, hippocaumpus; IGL, intergeniculate leaflet; LoC, locus coeruleus; POA, preoptic area; PAG, periaqueductal gray; PVN, hypothalamic paraventricular nucleus; PVT, thalamic paraventricular nucleus; SC, superior colliculus; SL, lateral septal nucleus; vLGN, ventral lateral geniculate nucleus; VMH, hypothalamic ventromedial nucleus; VTN, ventral tegmental nucleus. Other abbreviation: WM, white matter, defined in the results section. Species and reference of mammalian structures: #, rat, Moga and Moore, 1997; *, hamster, Pickard, 1982.

The resulting afferent projections to the mSCN are listed in Table 5. Of the seventeen remaining injections, five were discarded due to large scale leakage of tracer into the pipette track, two were discarded because tracer delivery was not apparent, likely due to a clogged micropipette tip, and one was discarded because the micropipette was deflected to a distal region, the afferents of which are significantly different than those resulting from the mSCN injections. The final eight injections were sorted into three groups—one very large injection encompassing most of AM and the dorsal aspect of mSCN (Fig. 9H), three injections to POA with impingement on CO (Fig. 9I) and four injections that delivered tracer to the third ventricle (3V; Fig. 9J) were used to evaluate our reported mSCN afferents and are included in Table 5. One injection to CO was analyzed and it was found that no cellular staining resulted; therefore, we did not include this injection in Table 5.

Three BDA injections were limited to the borders of the vSCN (Fig. 9K-M). One of these injections was situated dorsally compared to the other two (Fig. 9L) and one impinged slightly on DSV (Fig. 9M), but there were no significant differences in their efferent projections, which are reported in Table 4. Of the remaining nine injections, two were discarded due to lack of tracer delivery, while four injections were misplaced into either white matter tracts or distal areas bearing no efferent projection similarity to the three vSCN injections. Three injections were of particular interest and were used in our assessment of vSCN efferents. The first injection was located in the optic tract (TrO; Fig. 9N), while the other two were situated atop the vSCN dorsal

border, one in the ventral supraoptic decussation (DSV; Fig. 9O) and the other into gray matter dorsal and slightly lateral to vSCN, between GLv and DSV (Fig. 9P).

Three CTB injections were identified within the borders of the vSCN. One of these injections was very well confined within the nuclear border (Fig. 9Q). The other two injections overflowed the border slightly into adjacent gray matter (Fig. 9R-S). No significant differences were evident in their afferents, which are reported in Table 5. Of the seventeen remaining injections, three were discarded due to tracer leakage into the track or deficient tracer delivery and four were discarded as the injection location was distal and the resulting afferent projections were significantly different than those found with vSCN injection. The remaining injections were grouped into four categories. One large injection included the dorsal vSCN, the gray matter dorsal to vSCN and four fiber tracts (white matter; WM): the dorsal supraoptic decussation (DSD), DSV, the medial forebrain bundle and the quinto-frontal tract (Fig. 9T). A second injection was located further dorsal in the intercalated nucleus (ICT; Fig. 9U). Two CTB injection sites encompassed the vSCN and impinged upon the medial aspect of GLv (Fig. 9V). Four injections were located within GLv (Fig. 9W), two of which extended slightly into the ventrolateral thalamic nucleus (VLT). The final two injections were located within TrO. No afferent cells were identified as a result of these injections and they are therefore not included with the reported injections of interest in Table 5.

Most labeling from both BDA and CTB iontophoretic injections was ipsilateral. Therefore, unless specifically identified as contralateral, all structures described are ipsilateral to the injection site.

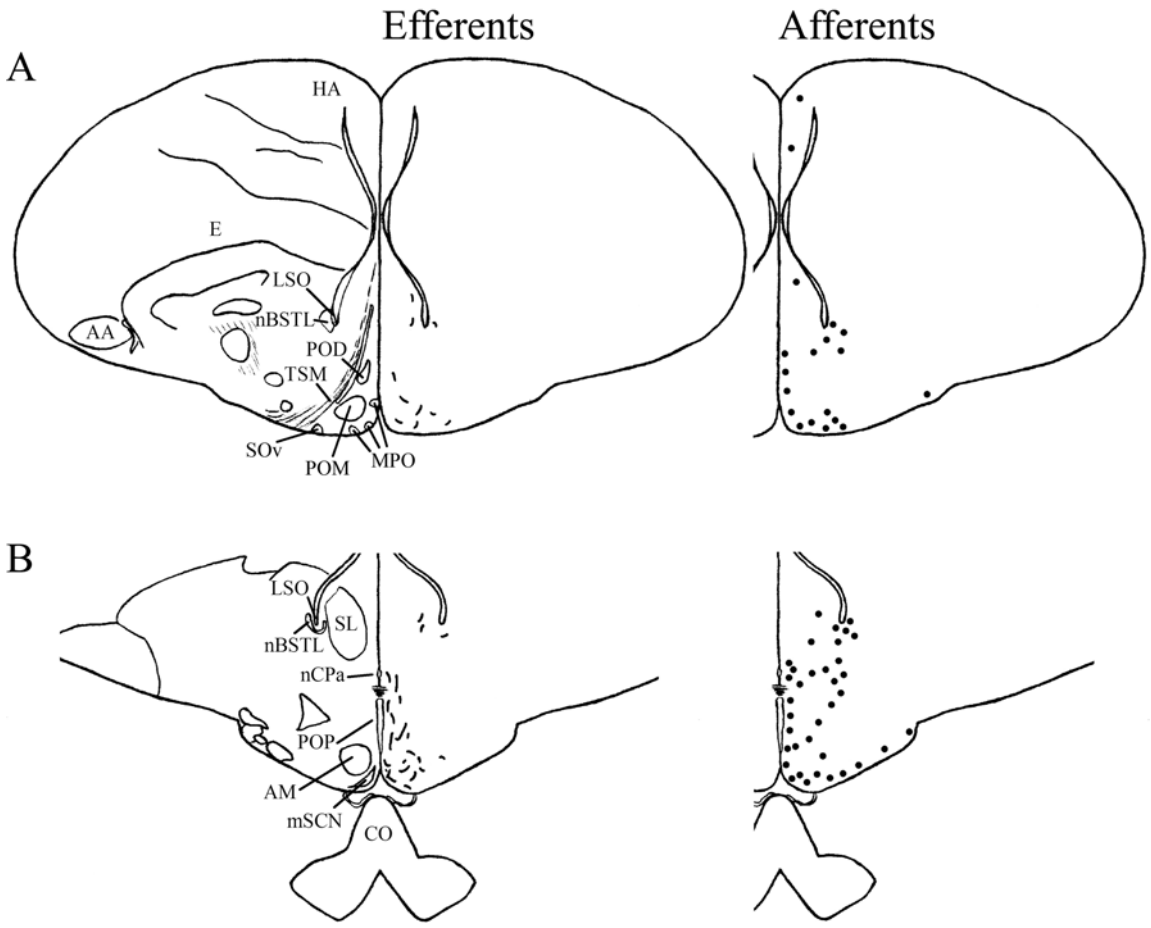

Fig. 12. Maps of mSCN efferents and afferents throughout the rostrocaudal extent of the brain following BDA and CTB iontophoretic injections, respectively. Structures of interest are labeled on the left hemisphere of the brains in the left panel. Fibers in mSCN efferents are indicated on the right hemispheres of the left panel by short lines. No distinction is made between terminal fibers and fibers of passage. A summary of terminal efferents is available in Table 4. Afferents are indicated on the right panel by dark circles representing cells and are summarized in Table 5. The distribution of fibers and cells on these maps represent the relative strength of staining in these areas, but do not reflect measured values. For abbreviations, see list.

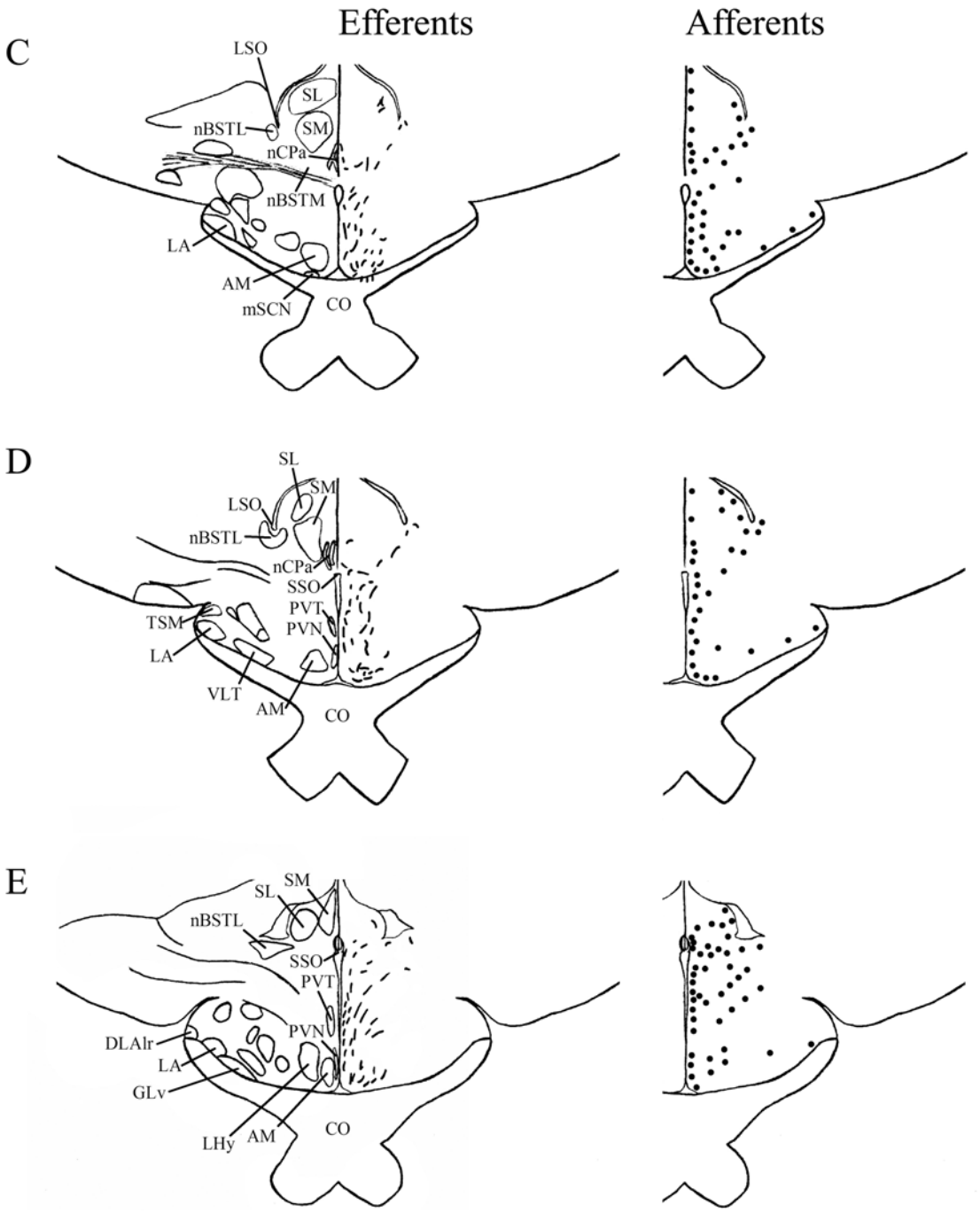

Fig. 12 Continued

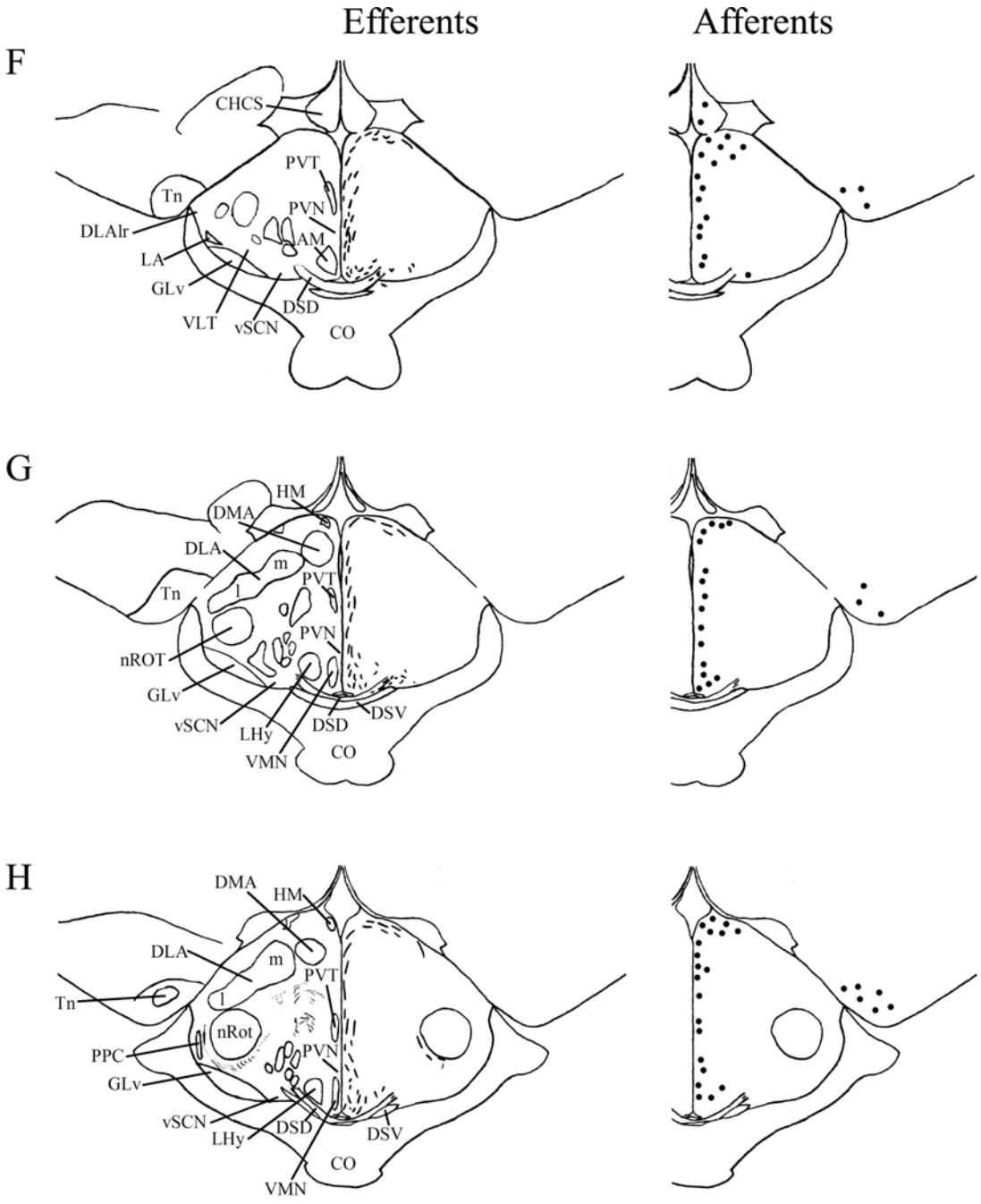

Fig. 12 Continued

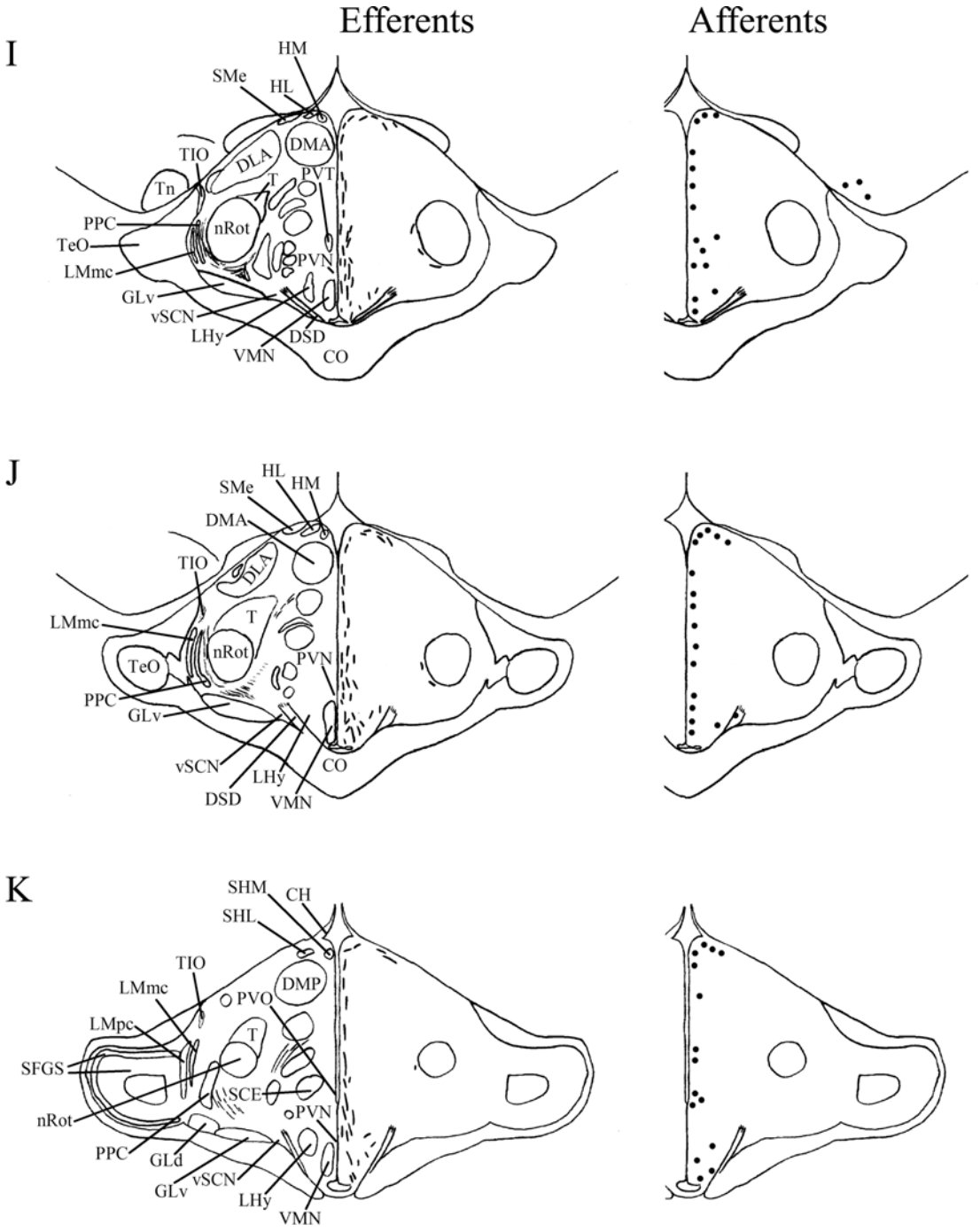

Fig. 12 Continued

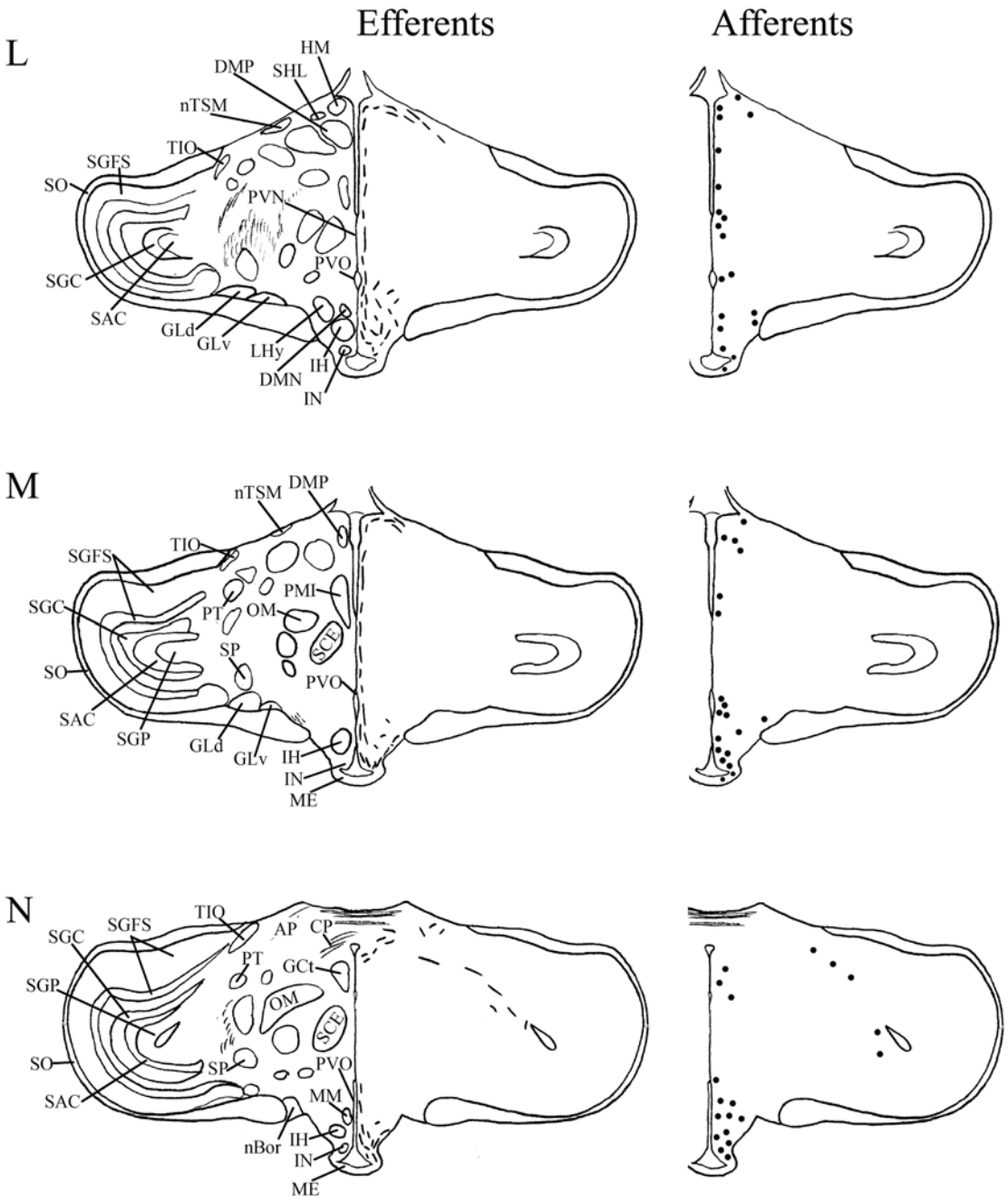

Fig. 12 Continued

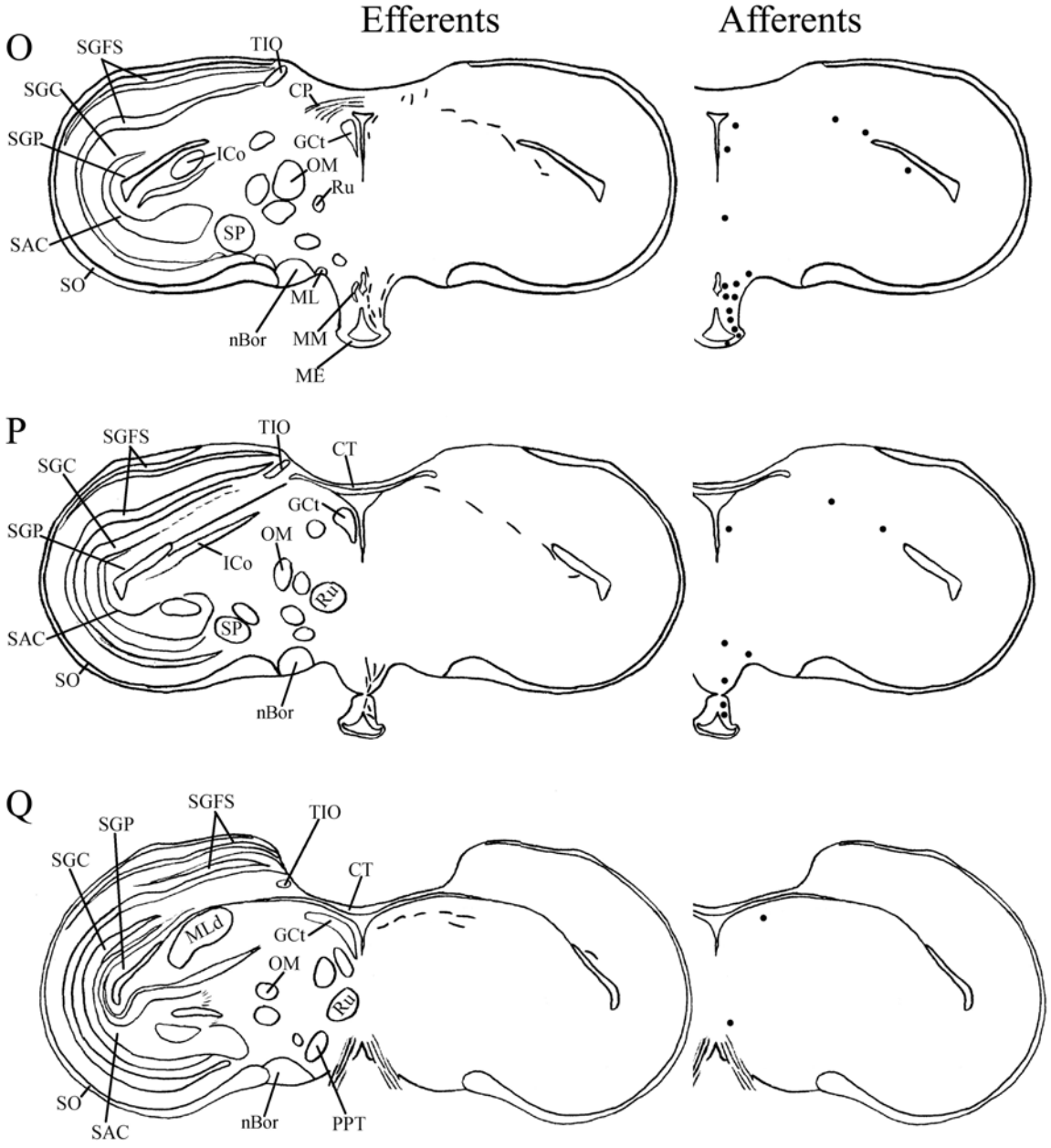

Fig. 12 Continued

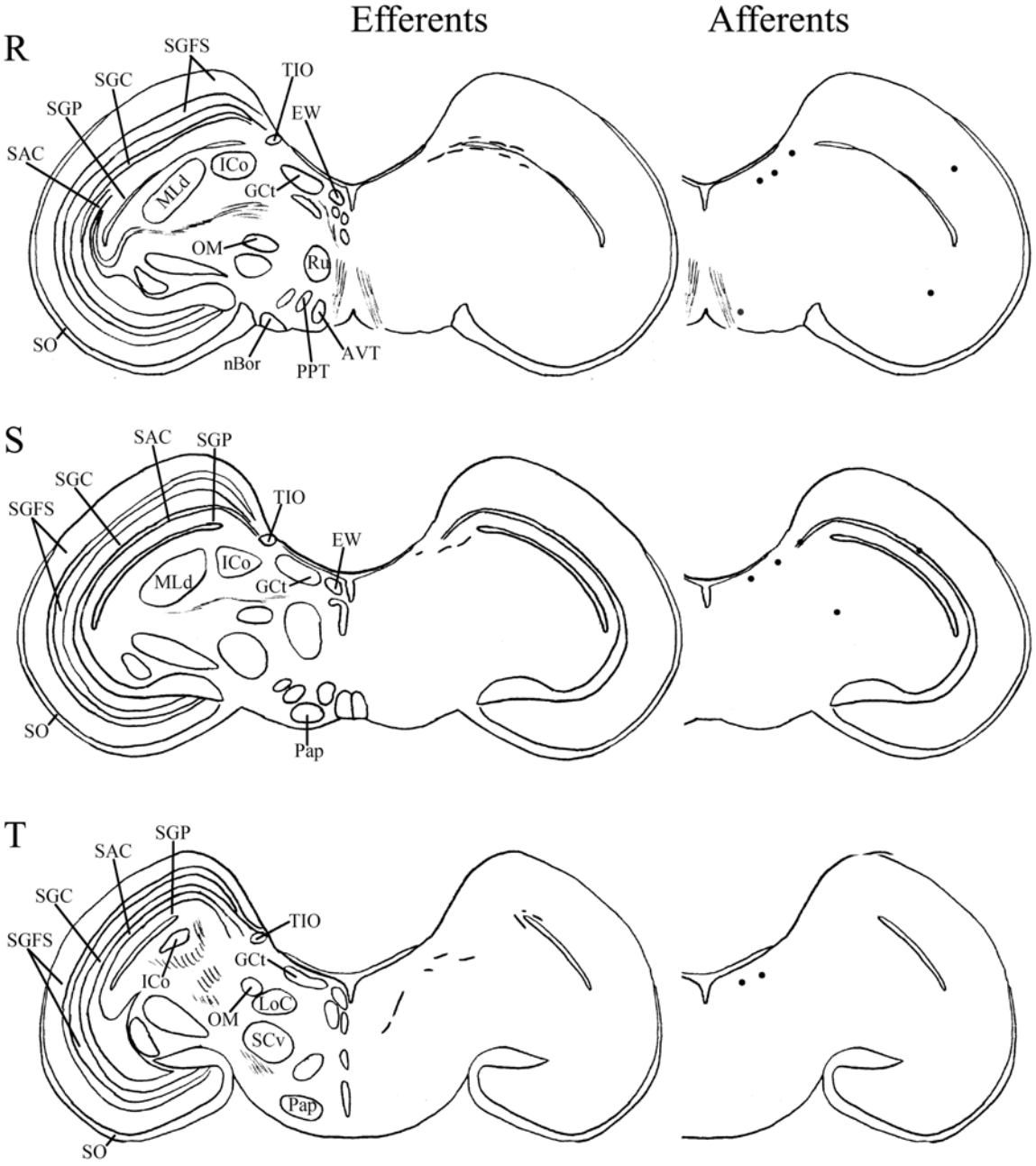

Fig. 12 Continued

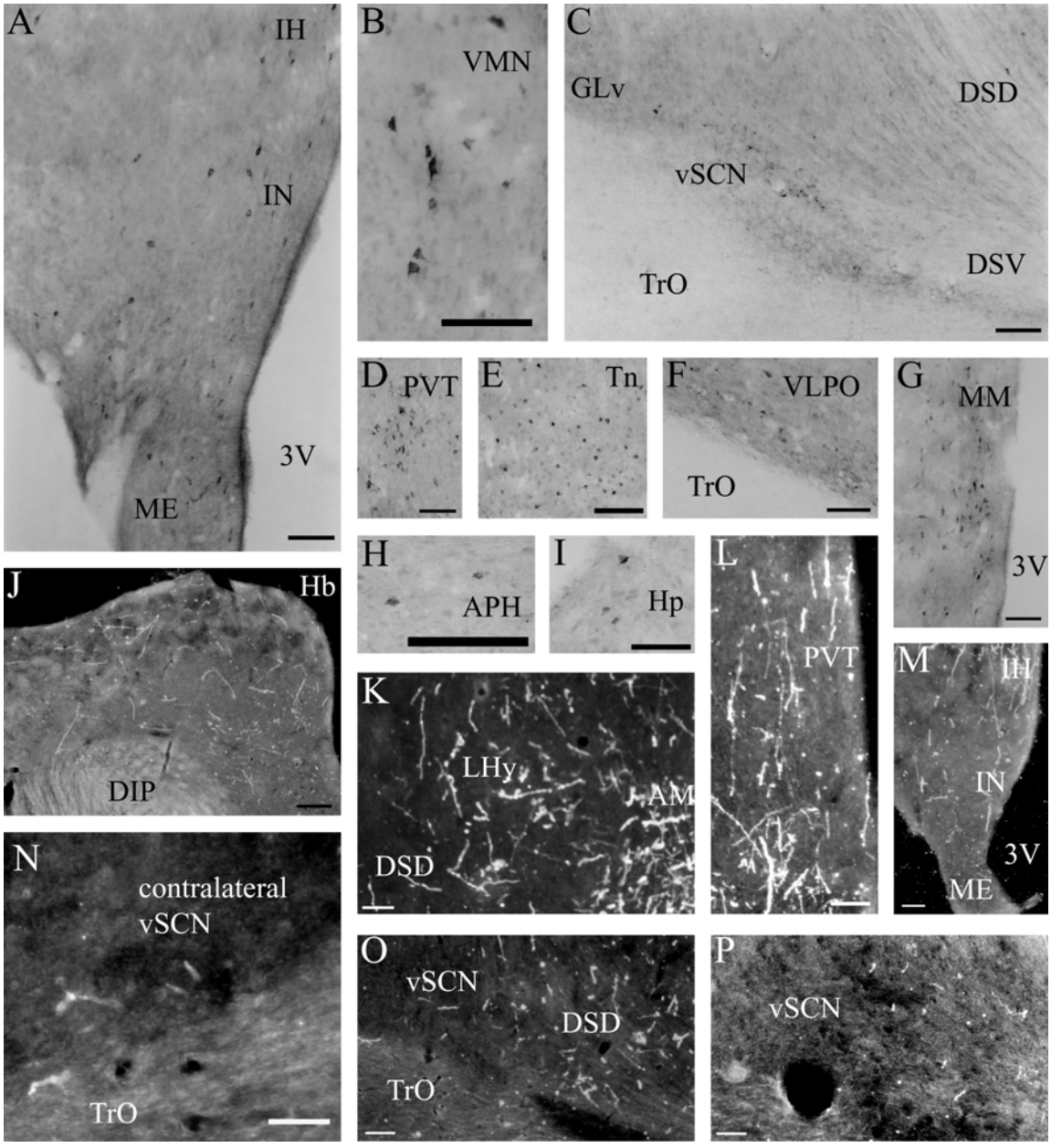

Fig. 13. Representative photomicrographs of mSCN afferents and efferents. **A-G**: Labeled afferents following CTB iontophoretic injections to the mSCN. Note the label in the vSCN (C) and MM (G). **H-M**: mSCN efferents following BDA iontophoretic injections. Note the presence of terminals in both the ipsilateral (O,P) and contralateral (N) vSCN. For abbreviations, see list. Scale bar = 1 mm in J; 400 μm in A-H,K-M,O; 200 μm in I,N,P.

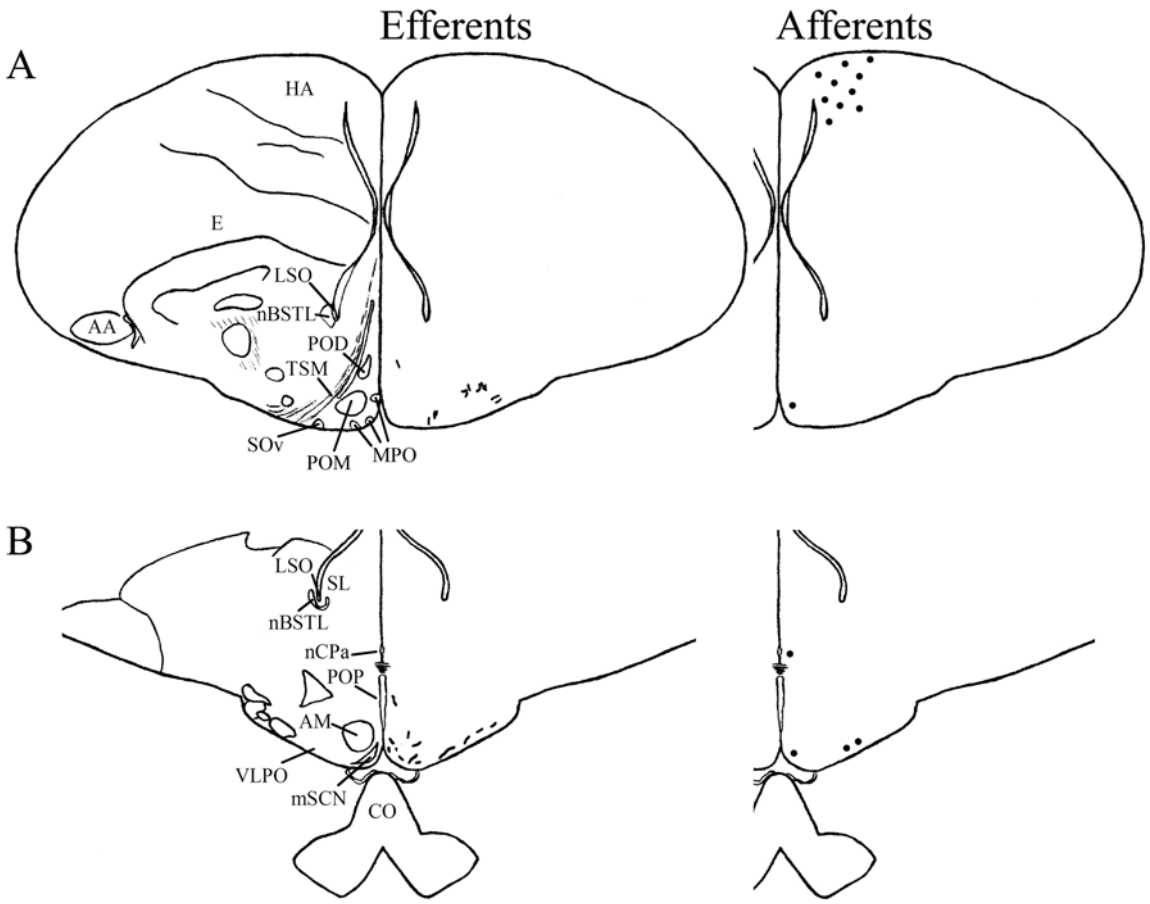

Fig. 14. Maps of vSCN efferents and afferents throughout the rostrocaudal extent of the brain following BDA and CTB iontophoretic injections, respectively. Structures of interest are labeled on the left hemisphere of the brains in the left panel. Fibers in vSCN efferents are indicated on the right hemispheres of the left panel by short lines. No distinction is made between terminal fibers and fibers of passage. A summary of terminal efferents is available in Table 4. Afferents are indicated on the right panel by dark circles representing cells and are summarized in Table 5. The distribution of fibers and cells on these maps represent the relative strength of staining in these areas, but do not reflect measured values. For abbreviations, see list.

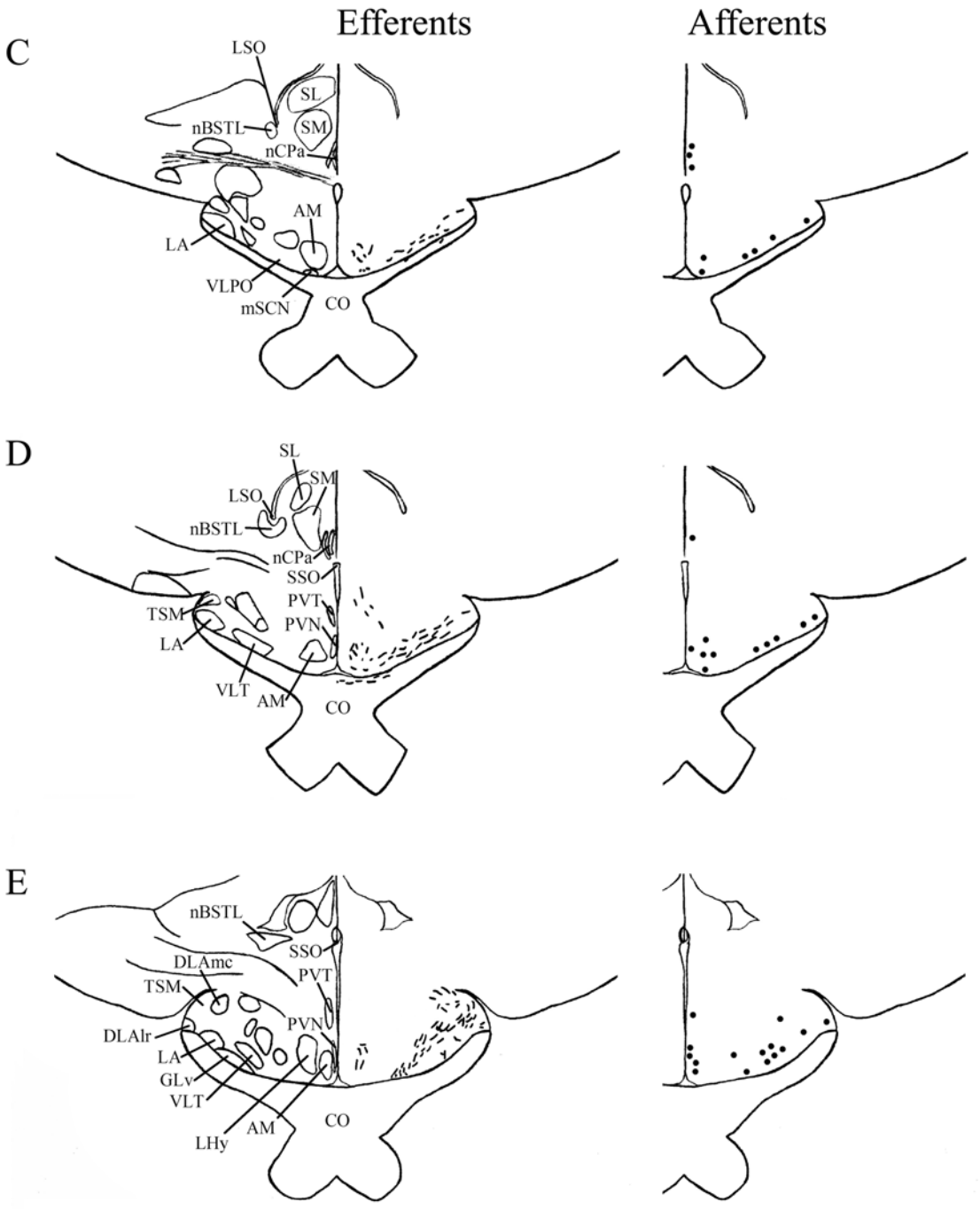

Fig. 14 Continued

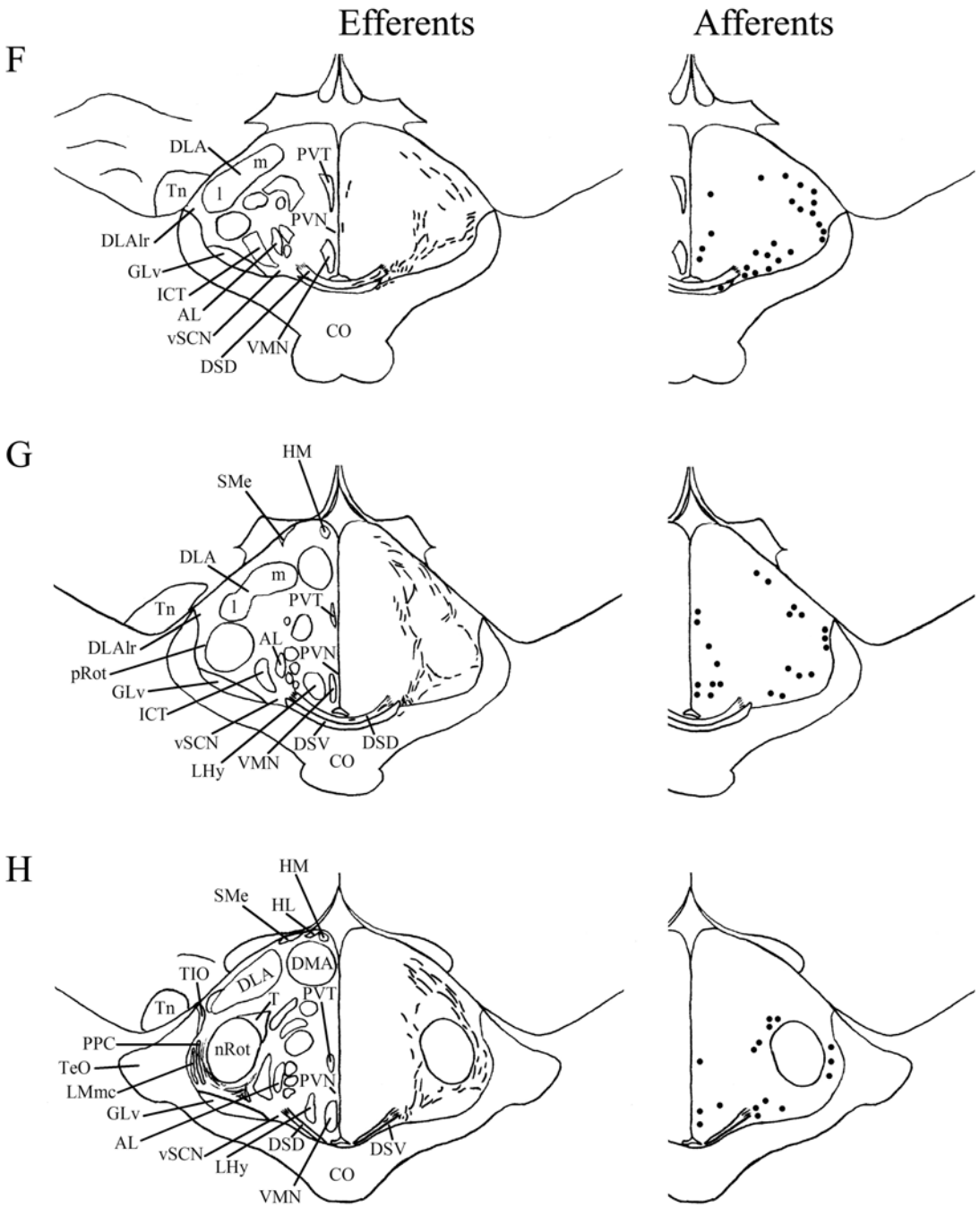

Fig. 14 Continued

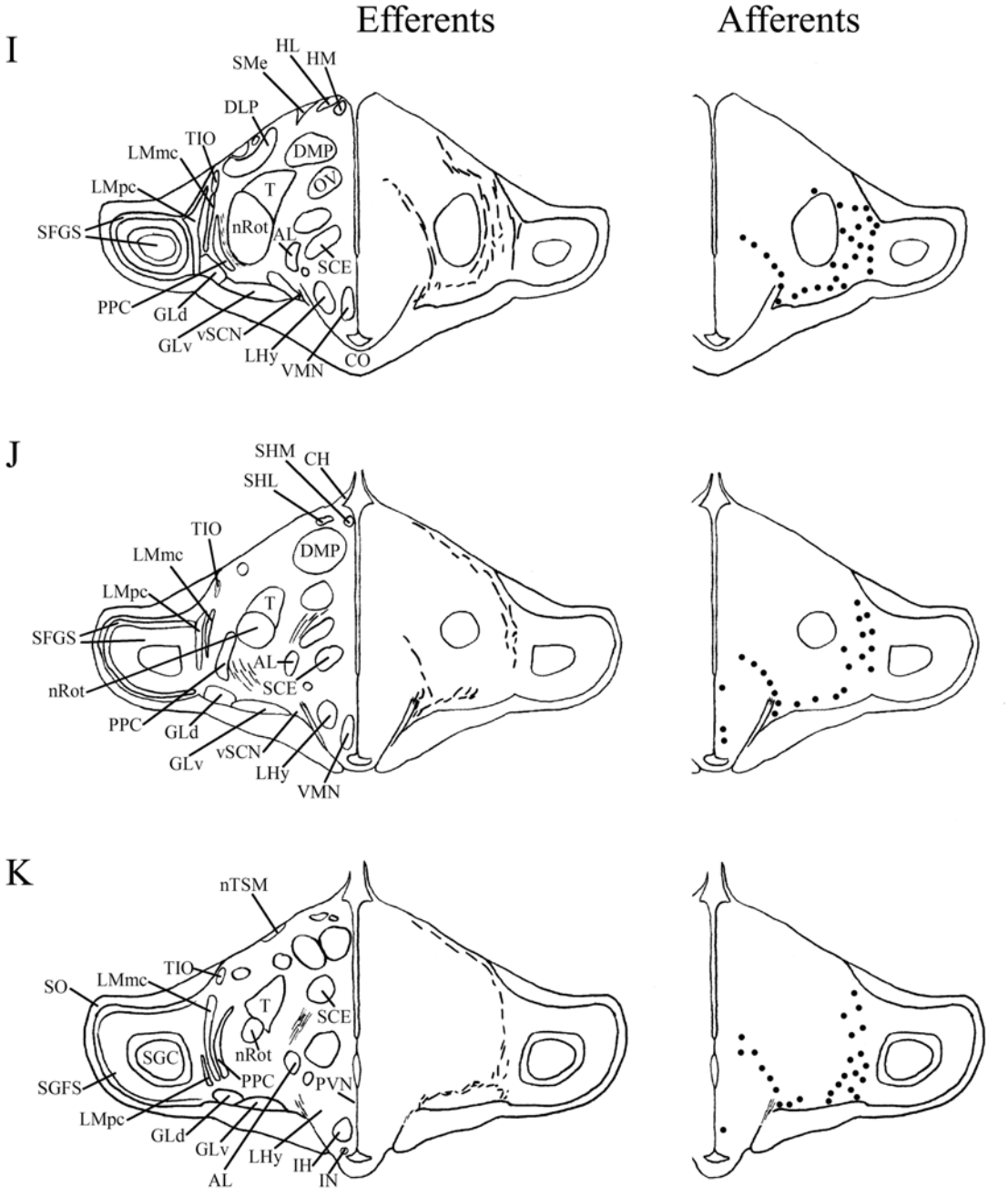

Fig. 14 Continued

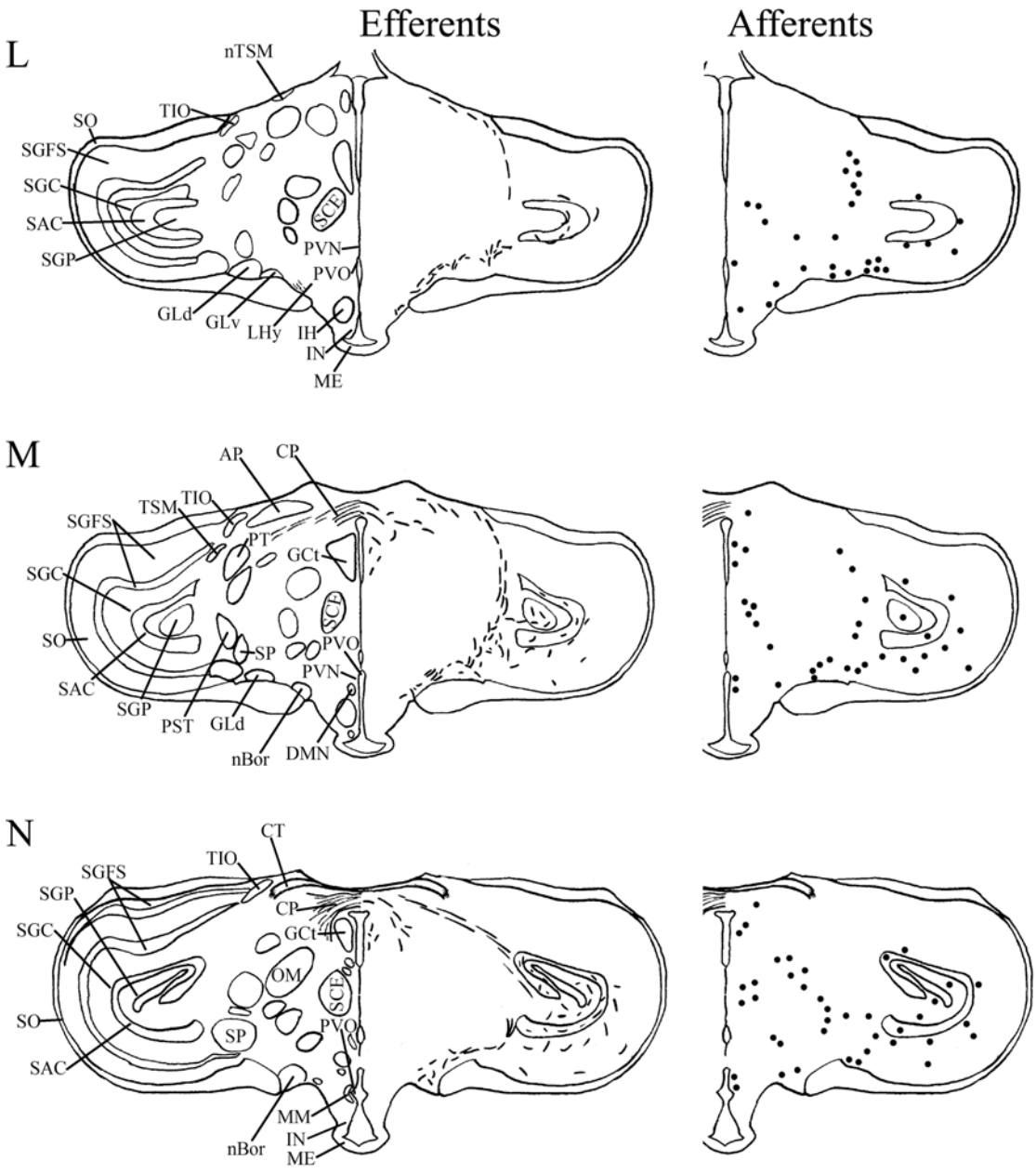

Fig. 14 Continued

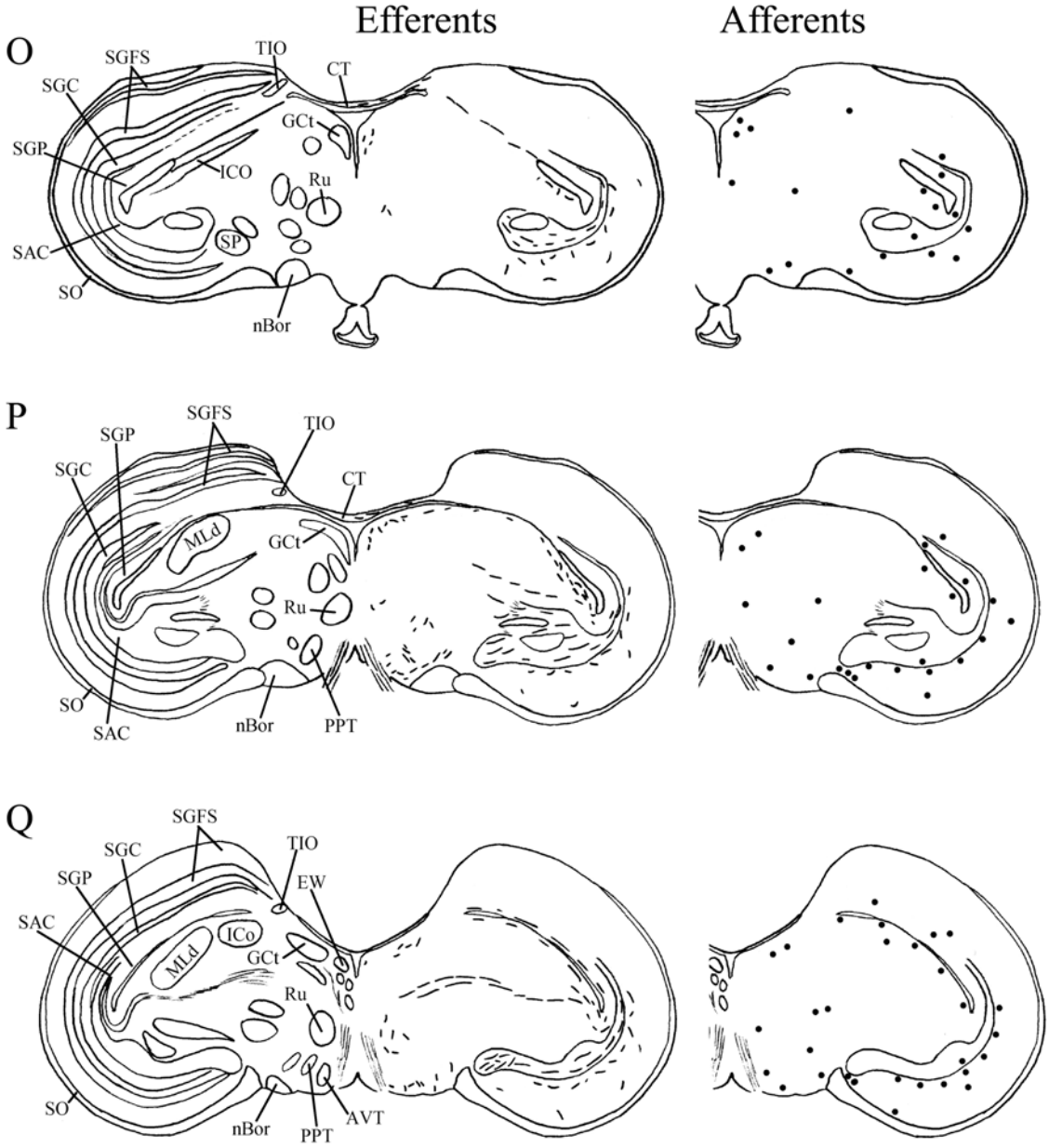

Fig. 14 Continued

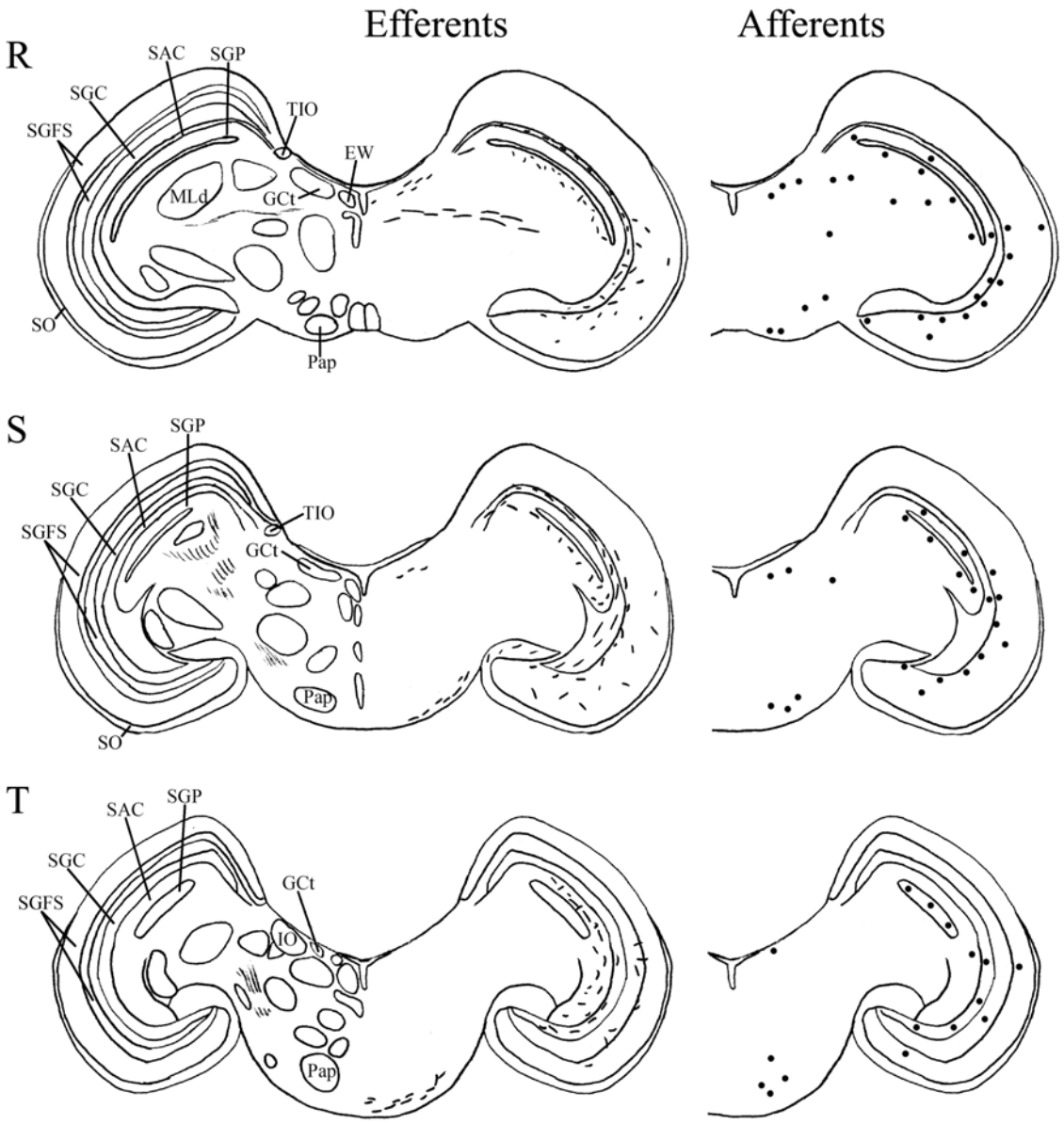

Fig. 14 Continued

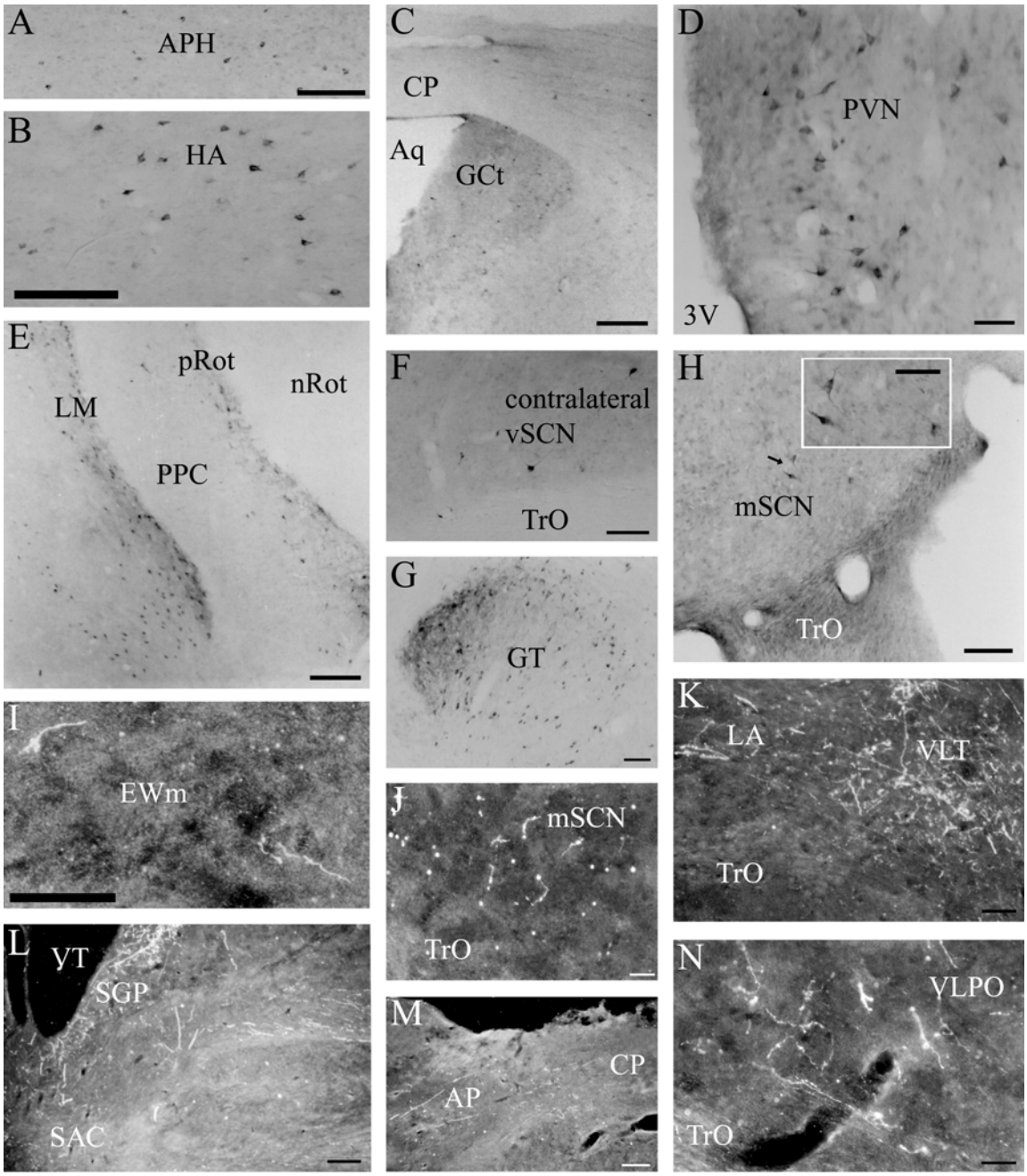

Fig. 15. Representative photomicrographs of vSCN afferents and efferents. **A-H**: Labeled afferents following CTB iontophoretic injections to the vSCN. Note the label in the contralateral vSCN (F) and mSCN (H). **I-N**: vSCN efferents following BDA iontophoretic injections. Note the presence of terminals in the mSCN (J). For abbreviations, wee list. Scale bar = 1 mm in C,E,L,M; 400 μm in A,B,F-H,K; 200 μm in D,H inset,I,J.N.

Efferent connections

The mSCN and vSCN efferents in which terminal fibers were identified are summarized in Table 4. Maps of mSCN efferents are shown in the right hemispheres of the left-hand panels of Figure 12, and representative photomicrographs are compiled in Figure 13. Efferents from the vSCN are mapped in Figure 14 left panels and representative photomicrographs are shown in Figure 15.

We found mSCN efferent terminal fibers primarily in structures along the midline of the chick brain. Fibers terminate in the lateral septal nucleus (SL; Fig. 12A-E) and the bed nucleus of the stria terminalis (nBST; Fig. 12A-E) of the telencephalon. In the diencephalon, terminal fibers are found in the preoptic area (POA), including the medial preoptic nucleus (POM; Fig. 12A), preoptic periventricular nucleus (POP; Fig. 12B), dorsolateral preoptic nucleus (POD; Fig. 12A) and ventral supraoptic nucleus (SOv; Fig. 12A). Hypothalamic efferents include AM (Figs. 12B-F, 13K), the lateral hypothalamic area (LHy; Figs. 12E-L; 13K) and the ventromedial nucleus (VMN; Fig. 12G-K). The contralateral mSCN receives input, as does the ipsilateral (Figs. 12F,G, 13O,P) and contralateral (Fig. 13N) visual suprachiasmatic nucleus (vSCN). In the tuberal hypothalamus, efferent fibers terminate in the hypothalamic inferior nucleus (IH) (Figs. 12L-N, 13M), the infundibular nucleus (IN; Figs. 12L-N, 13M), dorsomedial nucleus (DMN; Fig. 12L) and the medial mammillary nucleus (MM; Fig. 12O). Finally, strong signal is present in the hypothalamic paraventricular nucleus (PVN; Fig. 12D-I), from which fibers of passage oriented toward the thalamic paraventricular nucleus (PVT; Figs. 12D-K, 13L) originate. PVT is labeled and fibers of passage in the dorsal portion

of PVT are directed toward nBST of the telencephalon. The habenular region is stained with terminal fibers (Figs. 12G-M, 13J). A few structures associated with the visual system are labeled, including the perirotundal area (pRot; Fig. 12H-K) and the pretectal area (AP; Fig. 12N). The periventricular gray layer (SGP; Fig. 12N-T) and the central album layer (SAC; Fig. 12N-P) of the optic tectum contain labeled fibers. Finally, terminal fibers are located in the bed nucleus of the pallial commissure (nCPa; Fig. 12B-D) and the central gray (GCt; Fig. 12N-Q).

Efferent projections identified by the mSCN/AM injection included all of the efferents identified by mSCN injection alone. Many of these projections were more abundant from this more dorsal injection site, particularly efferents to SL, nBST and the habenula. In addition to these projections, mSCN/AM injection identified efferents in several thalamic structures as well as the ventral tegmental area (AVT). These additional efferents were also identified by AM injection alone and by the AM/POA injection.

Efferents from the vSCN are generally found more laterally in the chick brain. In POA of the diencephalon, terminals are found in SOv and POM (Fig. 14A). Many structures receiving efferents from the vSCN are in the hypothalamus, including AM (Fig. 14B-E), anterior LHy (Fig. 14E), mSCN (Figs. 14B,C, 15J), VLPO (Figs. 14B,C, 15N), ansa lenticularis (AL; Fig. 14F-J) and the contralateral vSCN. Fibers of passage in DSD and the ventral supraoptic decussation (DSV; Fig. 14F-I) are apparent. Many structures associated with visual function receive efferents from the vSCN. In the thalamus, VLT (Figs. 14B-E, 15K), LA (Figs. 14B-E, 15K), the dorsal border of GLv

(Fig. 14E-L), the intercalated nucleus (ICT; Fig. 14F,G), dorsolateral anterior nucleus magnocellular part (DLAmc; Fig. 14E), lateral part (DLAl; Fig. 14F-H), medial part (DLAm; Fig. 12F-H) and rostrolateral part (DLAlr; Fig. 14E-G), the dorsolateral posterior nucleus (DLP; Fig. 14I) and the dorsal border of the dorsolateral geniculate nucleus (GLd; Fig. 14I-M), contain terminal fibers. In the pretectum, efferent terminals are in pRot (Fig. 14F-I), the subpretectal nucleus (SP; Fig. 14M,N), principal precommissural nucleus (PPC; Fig. 14H-K), pretectal nucleus (PT; Fig. 14M), AP (Figs. 14M, 15M), LMmc (Fig. 14H-K) and LMpc (Fig. 14I-K). In the mesencephalon, terminal fibers are found in the optic tectum (Fig. 14L-T)—SGP and SAC (Fig. 15L), the central gray layer (SGC) and superficial fiber and gray layer (SGFS) all contain terminal fields. SGP and SAC fibers are primarily ventral, although sparser staining is present dorsally. In the SGC and SGFS, fibers are localized only to the ventral portion of the optic tectum. Nucleus ovoidalis (OV; Fig. 14I), GCt (Fig. 14M-S), the nucleus of the basal optic root (nBOR, Fig. 14M-Q), the pedunculopontine tegmental nucleus (PPT; Fig. 14P,Q), AVT (Fig. 14Q), the red nucleus (Ru; Fig. 14O-Q) and the medial nucleus of Edinger-Westphal (EWm; Figs. 14Q,R, 15I), as well as the papillioform nucleus (Pap; Fig. 14R-T) of the rhombencephalon receive efferent projections.

The misplaced injection to TrO labeled a limited subset of retinorecipient regions, as is delineated in Table 4. Two injections dorsal to vSCN were analyzed. Injection to DSV resulted in efferent projections that are similar to vSCN efferents, but are much less abundant. Injection to the gray matter just dorsal to the vSCN identified,

again, a similar set of efferent projections that were generally less abundantly labeled, while strongly labeling the vSCN itself.

Afferent connections

Afferents of the mSCN and vSCN are summarized in Table 5. Maps of mSCN afferents are shown in the right-hand panels of Figure 12, and representative photomicrographs are displayed in Figure 13. Afferents from the vSCN are mapped in Figure 14 right panels and representative photomicrographs are shown in Figure 15.

Telencephalic afferents to the mSCN include the hippocampus (Hp; Figs. 12A, 13I), parahippocampal area (APH; Fig. 13H), nucleus taeniae (Tn; Figs. 12F-I, 13E), SL (Fig. 12A-E) and nBST (Fig. 12A-E). In the diencephalon, POA afferents include MPO, SOv and POD (Fig. 12A) and POP (Fig. 12B). In the hypothalamus, AM (Fig. 12B-F), PVN (Fig. 12D-L), the contralateral mSCN, VLPO (Figs. 12B,C, 13F), LHy (Fig. 12C-K), VMN (Figs. 12G-K, 13B) and the anterior vSCN (Figs. 12F, 13C) are also labeled. In the tuberal hypothalamus, IH (Figs. 12L-N, 13A), IN (Figs. 12L-N, 13A), DMN (Fig. 12L), MM (Figs. 12O, 13G) and the median eminence (ME; Figs. 12L-P, 13A) contain afferent cells. In the thalamus, cells are seen in LA (Fig. 12B-E), VLT (Fig. 12B-E), nCPa (Fig. 12B-D) and PVT (Figs. 12D-I, 13D). The habenular region is also afferent to the vSCN (Fig. 12G-L). In the mesencephalon, SGP (Fig. 12N,O) and SAC (Fig. 12O-S) of the optic tectum are labeled. Finally, afferent cells are found in GCt (Fig. 12N-T) and AVT (Fig. 12R).

A large, misplaced injection that encompassed AM and the dorsal portion of mSCN identified a set of afferents similar to that of mSCN. In some cases, afferents were more abundant after mSCN injection, in others, they were more abundant after AM/mSCN injection. This is different from the situation with efferents, where we found that mSCN/AM injection resulted in generally more abundant projections than mSCN only. Additional afferents identified after AM/mSCN injection presumably originate from AM itself; however, no injection to AM was limited within that nucleus only. POA/CO injection resulted in a limited subset of stained afferents, which are also afferent to mSCN, in addition to mSCN itself. In general, these afferents were less abundant from POA/CO. Delivery of the entire volume of CTB to the third ventricle labeled a set of cell bodies similar to the afferents that project to mSCN; however, the appearance of this staining was markedly different from cellular stain resulting from CTB injection to the mSCN. In the case of transport from the mSCN, labeled fibers associated with the projecting cell bodies were oriented dorsoventrally and were relatively light in their appearance. In contrast, cell bodies stained by uptake of CTB from the third ventricle were more closely associated with the cavity than were those labeled by transport from mSCN injections. Further, the processes associated with these cells were very dark and were oriented mediolaterally, extending from the ependymal border of the third ventricle to the closely apposed cell bodies. Staining of cell bodies in more distal regions such as Hp, nBSTL, SL an the visual Wulst (HA) is presumably a result of transport of CTB within the cerebrospinal fluid, which contacts all structures identified.

Telencephalic structures afferent to the vSCN include HA (Figs. 14A, 15B) and APH (Fig. 15A). The hypothalamic AM (Fig. 14B-E), rostral LHy (Fig. 14E-H), mSCN (Figs. 14B,C, 15H), rostral and caudal, but not middle PVN (Figs. 14D,E,J-N, 15D) and VMN (Fig. 14F-J) contain afferent cells. Label is also found in VLPO (Fig. 14C,D), AL (Fig. 14F-K), contralateral vSCN (Fig. 15F) and IH (Fig. 14K,L). Afferents in the thalamus include LA (Fig. 14C-E), the dorsal border of GLv (Fig. 14E-L), nCPa (Fig. 14B-D), VLT (Fig. 14D,E), ICT (Fig. 14F,G), PVT (Fig. 14E-H), DLAmc (Fig. 14E), DLAl (Fig. 14F-H), DLAm (Fig. 14F-H), GLd (Fig. 14I-M) and T (Fig. 14H,I). In the pretectum, afferent cells are found in pRot (Figs. 14G-J, 15E), PPC (Figs. 14H-K, 15E), PD (Fig. 14L), PT (Fig. 14M), AP (Fig. 14M), LMmc (Figs. 14H-K, 15E) and LMpc (Figs. 14I-K, 15E). In the mesencephalon, all four layers of the optic tectum are afferent (Fig. 14L-T). Cells are denser in the ventral region of the tectum, with sparser staining in the dorsal regions. SGFS cells are found only it its ventral aspect. Afferent cells are found in the tectal gray (GT; Figs. 14L,M, 15G), GCt (Figs. 14M-S, 15C), locus coeruleus (LoC; Fig. 14S), the external cellular layer (SCE; Fig. 14L-N), nBOR (Fig. 14M-Q), Pap (Fig. 14R-T) and the oculomotor tract (OM; Fig. 14N).

The misplaced injection to the dorsal vSCN/WM resulted in labeling of a very similar set of afferents as the vSCN injection itself, and they were either of comparable abundance or were less abundant. Injection to ICT labeled a much more limited set of afferents, all of which we identified as vSCN afferents, and are, in general, less abundant than those of the vSCN. Afferents labeled from the medial GLv and lateral vSCN are

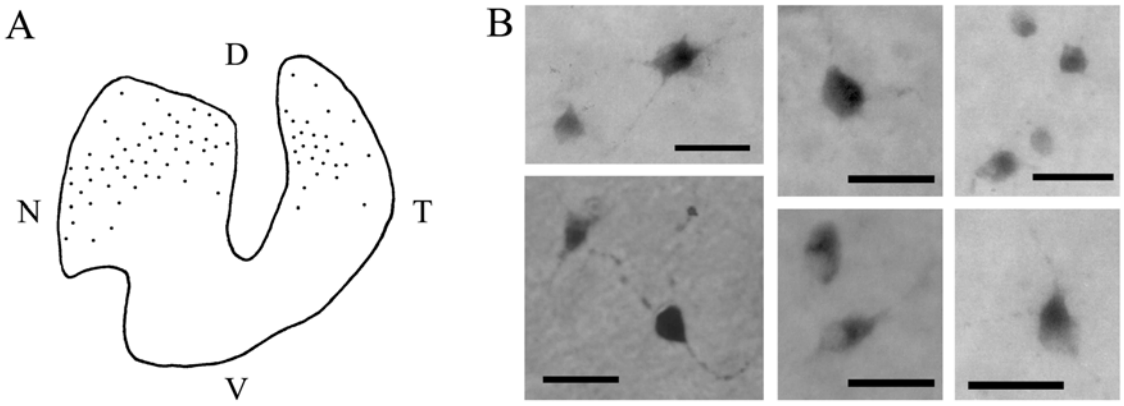

Fig. 16. Retinal ganglion cell (RGC) label following CTB injection to the vSCN. **A**: A distribution map of RGCs involved in the retinohypothalamic tract (RHT). CTB was iontophoresed into the vSCN and allowed to trace back to the retina. RGCs projecting to the vSCN are present only in the dorsal retina. **B**: Photomicrographs of representative RGCs, which have a variety of morphologies. Chick RGCs have not been characterized by function. Abbreviations: D, dorsal; V, ventral; N, nasal; T, temporal. Scale bars in B = 100 μm.

also similar, but less abundant, than vSCN afferents. Finally, very few afferents were identified after injection to the medial GLv.

The retinae from CTB-injected birds were examined for retinal ganglion cells (RGCs). Afferent RGCs were identified in the retinae contralateral to the vSCN injections and were used to create a distribution map (Fig. 16A) and photomicrographs of representative RGCs (Fig. 16B). RGCs are located throughout the dorsal portion of the retina. The distribution appears as a dense band with a sparse region of cells surrounding it. The cells are more dense centrally and less dense around the periphery of the dorsal retina. The cells are smaller toward the central region of the distribution, with slightly larger cells in the periphery. No RGCs were found in the retinae of mSCN- or mSCN/AM-injected birds.

DISCUSSION

Similarities to the mammalian SCN exist within both the mSCN and the vSCN. Data from the work presented here and previous studies, taken as a whole, indicate that both the mSCN and vSCN are involved in the avian circadian system. We propose below a new working model of the avian suprachiasmatic nucleus based on these observations.

Retinal projections

The data presented here indicate that the vSCN receives completely contralateral retinohypothalamic input. Following iontophoretic injections of CTB to the vSCN, numerous RGCs are labeled in the contralateral retina only. The finding that this retinal input derives from RGCs in the dorsal retina differs significantly from what has been found in the hamster, which sends a retinohypothalamic projection from RGCs that are distributed evenly throughout the retina (Pickard, 1982). The dorsal distribution of retinohypothalamic RGCs in chick, however, may be expected, since the dorsal region of the chick retina contains a denser population of RGCs than does the ventral aspect (Chen and Naito, 1999). As has been reported previously (see Table 3), sparse retinal input to the mSCN was also observed; however, the paucity of labeled terminal fibers in this structure and the absence of CTB-labeled RGCs in the retinae of mSCN-injected birds indicate that the vSCN is the primary retinorecipient structure in the chick hypothalamus.

Interestingly, a classical study, employing autoradiographic techniques, reported abundant retinopetal cells present throughout the suprachiasmatic region of the pigeon and the jackdaw, *Corvus monedula*, including both the vSCN and the mSCN (Meier, 1973). In our study, cells were retrogradely labeled in the vSCN alone. These cells were clearly visible after two days of CTB transport but were generally obscured by the retinal terminal field after five days of transport. We attempted to confirm an efferent from the vSCN to the retina by viewing retinae from chicks in which BDA was injected into the vSCN but, because of the pigmentation in the retina, background was too high under dark field microscopy to identify BDA immunoreactive fibers. The data nevertheless suggest a putative modulatory role for the vSCN on the retina.

Retinal terminals identified in other structures have been reported previously (Table 3). Because they are outside the scope of this study and have already been described, we will not discuss them. We did, however, identify a previously unreported contralateral retinal projection that is of particular interest. This structure is in the same frontal plane as, and is lateral to, the rostral mSCN. This region contains γ-aminobutyric acid (GABA) immunoreactive cells with fibers visible at the dorsal margin (EL Cantwell and VM Cassone, unpublished data). The mammalian VLPO is retinorecipient (Lu et al., 1999) and one of its primary antigens is GABA (Sherin et al., 1998); therefore, we believe this structure may be homologous to the mammalian VLPO, which has been implicated in regulation of sleep:wake cycles in mammals (Lu et al., 1999).

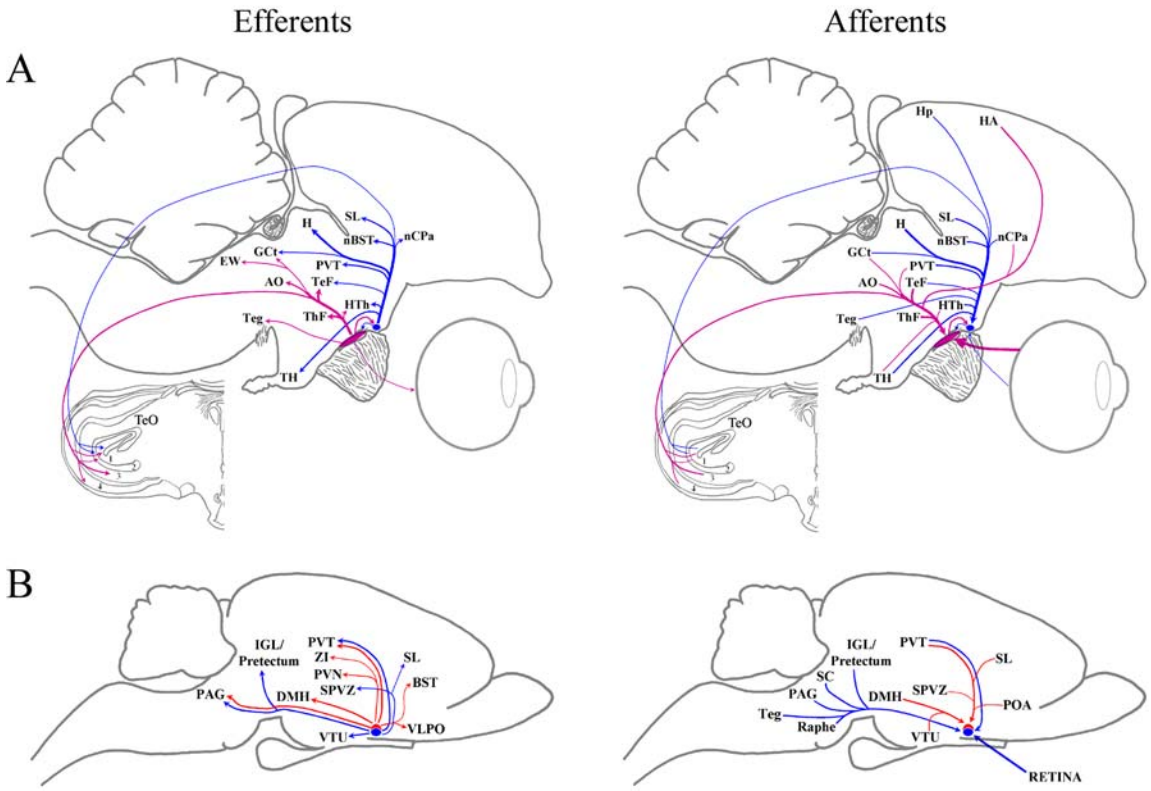

Fig. 17. These schematic diagrams in the sagittal plane summarize what is known about the efferent and afferent connections of the chick (A) and rodents (B). The thickness of the lines represents the relative density of each projection. **A**: These drawings represent the connections of the vSCN (purple) and mSCN (blue). TeO layers: 1, SGP; 2, SAC; 3, SGC; 4, SGFS. Due to space constrictions, structures of TeF, ThF, AO and HTh were grouped together. These structures are considered individually in Tables 2 and 3. For chick structure abbreviations, see list. **B**: Summary of projections from the core (blue) and shell (red) of the mammalian suprachiasmatic nucleus (SCN). Mammalian structure abbreviations: BST, bed nucleus of the stria terminalis; DMH, dorsomedial hypothalamic nucleus; IGL, intergeniculate leaflet; PAG, periaqueductal gray; POA, preoptic area; PVN, hypothalamic paraventricular nucleus; PVT, thalamic paraventricular nucleus; SC, superior colliculus; SL, lateral septal nucleus; SPVZ, subparaventricular zone; Teg, tegmentum; VLPO, ventrolateral preoptic nucleus; VTU, ventral tuberal hypothalamus; ZI, zona incerta.

Efferents of the suprachiasmatic nuclei

With the exception of one investigation into human hypothalamic efferents of the SCN (Dai et al., 1998), studies investigating efferent connectivity of the SCN have focused on three rodents—rat, hamster and mouse (Stephan et al., 1981; Watts and Swanson, 1987; Watts et al., 1987; Kalsbeek et al., 1993; Morin et al., 1994; Abrahamson and Moore, 2001; Leak and Moore, 2001; Kriegsfeld et al., 2004). In a few of these studies, efferents from the core and the shell regions have been divided in order to compare the two subdivisions of the nucleus. This division of mammalian SCN efferents may be seen in Figure 17B. In the present study, mSCN and vSCN projections are predominantly ipsilateral, as is the case in all mammals studied, and they are summarized in Figure 17A.

The mSCN and the rodent SCN exhibit several common efferents. Of particular interest are the projections to SL and nBST: the mammalian SCN also sends efferents to nBST and SL of the basal forebrain. These efferents are interesting because they are closely apposed to the lateral septal organ (LSO) in the chick. Previous studies have suggested that encephalic photoreceptors are located in LSO (Vigh-Teichmann et al., 1980; Silver et al., 1988; Kuenzel, 1993; Li et al., 2004; Rathinam and Kuenzel, 2005). The current data indicate a possible means of interaction between the mSCN and these putative encephalic photoreceptors. The vSCN makes fewer connections that are comparable to rodent SCN efferents. Most notable is a connection to VLPO, which receives projections from the SCN in the hamster (Kriegsfeld et al., 2004) and the rat

(Chou et al., 2002). Several mammalian SCN efferents are comparable to structures efferent from both the mSCN and vSCN in the chick, as is delineated in Table 4.

The total number of structures efferent from the mSCN and vSCN combined exceeds the number of known mammalian SCN efferents. One vSCN efferent reported here, EWm has been well characterized in the pigeon (Gamlin et al., 1982). Because our BDA-labeled efferents were significantly more sparse than those previously identified, we referred to CTB-labeled fibers from vSCN injected birds and observed a much more abundant efferent connection, presumably due to the larger CTB injection sites. EWm has been shown to regulate choroidal blood flow in the eye via parasympathetic circuits involving the ciliary ganglion (Fitzgerald et al., 1990; Reiner et al., 1990). A few efferent connections are made by the mSCN to tectofugal pathway structures; however, the vSCN exhibits a high degree of connectivity with visual structures of the tectofugal, thalamofugal and accessory optic pathways. Previous studies have indicated a role for the circadian system in the regulation of the visual system. In pigeons, parameters of both visually evoked potentials in the optic tectum and electroretinograms are rhythmic in both a 12:12 light:dark cycle (LD) and in constant darkness (DD; Wu et al., 2000). The distribution of vSCN efferents in the optic tectum, homologous to the mammalian superior colliculus, is particularly interesting because SGFS fibers are located on its ventral aspect (Fig. 14). Electroretinogram parameters are also rhythmic in LD and DD in chicks (McGoogan and Cassone, 1999). Although the avian retina clearly contains the machinery for endogenous oscillation (Bailey et al., 2004), it is intriguing to speculate modulation of retinal function directly via vSCN efferents (Fig. 11E). The

scope of efferent connectivity from the vSCN to visual system structures strongly supports the view that it is involved in circadian visual regulation in the retina, in retinorecipient structures and in integrative structures associated with visual processing.

Afferents of the suprachiasmatic nuclei

Few studies have mapped the afferents of the mammalian SCN (Pickard, 1982; Morin at al, 1994; Moga and Moore, 1997). Table 5 provides a list of structures afferent to the mammalian SCN that correspond to structures identified in the chick. As was found with efferents, afferent structures to the mSCN and vSCN are more numerous than is the case in the mammalian SCN. Figure 17 provides a schematic representation of rodent and chicken afferents.

The reception of afferents from SL completes a circuit between that structure and mSCN. Input to the mSCN from SL is corroborated by a study of efferents traced from that structure (Montagnese et al., 2004). A similar bidirectional interaction with SL exists in rats (Moga and Moore, 1997; Leak and Moore, 2001). While nBST is not an afferent structure of the rodent SCN, its afferent input to the chick mSCN supports the hypothesis that encephalic photoreceptors of the LSO project indirectly to the mSCN. The mSCN also receives afferent input from hypothalamic structures apposed to the periventricular organ (PVO), another putative encephalic photoreceptive structure (cf. Silver et al., 1988), suggesting another putative pathway by which light information may reach the avian suprachiasmatic nucleus.

As is the case in the mammalian SCN, the primary afferent to the vSCN is the retina. In mammals, some light information is carried to the SCN from the lateral geniculate nucleus via the geniculohypothalamic tract (Card and Moore, 1982, 1989; Moore et al., 1984; Harrington et al., 1985; Moore and Speh, 1993; Moore and Card, 1994). Our data suggest a similar relationship between the geniculate nuclei and the vSCN. Further, the nuclei of the pretectal area project to the rat SCN (Mikkelsen and Vrang, 1994), while, in the chick, many pretectal and visually active thalamic structures project to the vSCN, indicating an abundant afferent input to the vSCN by structures of the tectofugal, thalamofugal and accessory optic pathways. A few structures associated with the tectofugal and thalamofugal pathways also project to the mSCN, suggesting a minor modulatory role in its function.

Taken together, mSCN and vSCN afferents are very similar to the afferents of the mammalian SCN. As is seen with the core and shell of the mammalian SCN, there is significant overlap between the connections of the two avian structures.

Connections between mSCN and vSCN

We found that the mSCN and vSCN communicate bidirectionally and bilaterally. Projections from the vSCN to the mSCN are stronger than they are in the converse. In rodents, the core of the SCN communicates with the shell, but the shell doesn't send efferents to the core (Abrahamson and Moore, 2001). Thus, although the details of the relationship between putative sub-regions of the avian suprachiasmatic nucleus are different than the situation in the mammalian circadian system, the general scheme

suggests an asymmetric flow of retinal information from the vSCN to the mSCN. This scheme is generally similar to the relationship of the "core" and "shell" of the rodent SCN.

Evaluation of projections based on misplaced injections

Assessment of efferent connections was made possible by several injections. In the region dorsal to the mSCN, we found that AM has several common efferents with mSCN. An injection that encompassed the dorsal mSCN and the ventral aspect of AM identified an efferent population that is an amalgam of the two structures' efferents. Interestingly, several of the efferents common to the mSCN and mSCN/AM are more abundant when traced from the more dorsal injection site, most notably SL, nBSTL and the habenula. There are several possible explanations. First, more abundant projections may arise from the dorsal mSCN. Second, the presence of BDA in two structures with common targets may have had an additive effect. Finally, AM may be involved in multisynaptic pathways originating in or involving the mSCN. The fact that ventral mSCN injection labels AM supports the third hypothesis, although all three possibilities may be responsible for the greater abundance of stain in mSCN/AM injections. In mammals, one structure involved in such pathways is the subparaventricular zone (SPZ), which is just dorsal to the SCN. The mammalian SCN sends a considerable efferent projection to the SPZ, which then sends efferents to a variety of downstream structures. Thus, injection to SPZ often results in an efferent pattern similar to SCN, but with more abundant terminal fibers present in those structures (Watts et al., 1991). The data

presented here imply that a similar, albeit less intense, relationship may exist between mSCN and the region immediately dorsal to mSCN, perhaps including AM. This possibility is made all the more intriguing by the presence of sparse retinal terminals in and between the two structures. By way of contrast, injection to the gray matter just dorsal to the vSCN does not produce any amplification of efferent abundance, although the structures receiving efferents from this injection are very similar to those obtained from vSCN injections. This similarity of efferent staining is probably at least partially due to uptake by efferent fibers of the vSCN.

In studies of suprachiasmatic afferents, misplaced injections again serve an important role in the analysis of our results. A large CTB injection that included the entirety of AM and the dorsal portion of mSCN transported to an afferent population very similar to what was found in the ventral mSCN injections. None of the injections were delivered to AM only; however, based on efferent findings, one may reasonably suspect that the more lateral thalamic afferents are those of AM itself. In contrast to what was found in the efferent study, some afferent projections are stronger when traced from mSCN alone and some stained more abundantly after injection to AM/mSCN. This suggests that, if AM is involved in mSCN-mediated communication with output structures, it is only involved in this capacity with a subset of structures and that it is more active in the conveyance of efferent messages than in the reception of afferent signals. Because we may only speculate given the data here, studies designed to determine the precise relationship between AM and mSCN are necessary in the exploration of the suprachiasmatic nucleus of birds.

Our missed injections were able to confirm a few efferent and afferent projections reported based on mSCN and vSCN injection. First, injection of BDA into AM led to efferent staining in mSCN, supporting our finding that there are cells afferent to mSCN within that nucleus. Second, injection of CTB into POA confirmed mSCN efferents to that structure. Third, injection of CTB to ICT confirmed its reception of vSCN efferents. Finally, CTB injections contained within GLv resulted in a large fiber plexus within vSCN. While we did not choose to report efferent projections from CTB injections, opting to use BDA instead, no BDA injections were placed in the GLv, so we used the CTB injections for confirmation of a geniculohypothalamic tract to the vSCN (Fig. 9W). Reciprocal injection to other efferents and afferents will be necessary to assess their full extent and validity.

Functional comparisons of the mSCN and vSCN

Lesion studies support the involvement of the mSCN in expression of circadian locomotor rhythms. Initial lesions of the anterior hypothalamus resulted in loss of locomotor activity rhythms in house sparrows (Takahashi and Menaker, 1982), Japanese quail (Simpson and Follett, 1981) and Java sparrows (Ebihara and Kawamura, 1981). These lesions comprised a large portion of the anterior hypothalamus, likely destroying both the mSCN and vSCN. To resolve this issue, Ebihara et al. (1987) produced individual lesions to the vSCN and mSCN in pigeons; these lesions, by themselves, had little effect. However, lesions of the mSCN in pigeons that had also received either pinealectomy or enucleation (each of which only disrupts rhythmicity) abolished or

further disrupted free running rhythms in constant dim light (dimLL). Lesions of the vSCN failed to abolish free running rhythms in dimLL. In contrast, Cassone et al. (1990) found that specific lesions in the vSCN abolished circadian patterns of norepinephrine turnover in the chick pineal gland, but that mSCN had no effect on this output.

Conversely, physiological analyses of rhythmic function points to the vSCN as a circadian oscillator. The vSCN, but not the mSCN, of the house sparrow exhibits circadian rhythms of 2-deoxy[^{14}C]glucose (2DG) uptake, such that 2DG uptake is high during the subjective day and low during the subjective night (Cassone, 1988; Lu and Cassone, 1993a). In the chick, 2DG uptake is rhythmic in constant darkness in both structures (Cantwell and Cassone, 2002), such that uptake is highest during subjective day. This phase of peak uptake is similar to the situation in the mammalian SCN (Schwartz et al. 1980). In Japanese quail, the vSCN exhibits rhythmic electrical activity *in vitro* (Juss et al., 1994), with activity greater during the subjective day, also similar to the situation for the mammalian SCN (Green and Gillette, 1982). Finally, the early immediate gene *c-fos*, which is induced in the mammalian SCN by a one-hour light pulse during the night (Rea, 1989), is similarly induced in the vSCN, but not in the mSCN, of quail and starlings (King and Follett, 1997).

Of course, the role of an avian SCN must be integrally linked to the role of pineal melatonin in circadian organization (Cassone, 1998), and the vSCN fits this criterion rather well. First, exogenous melatonin administration during the day acutely inhibits 2DG uptake in the vSCN, but not the mSCN, of sparrows (Cassone and Brooks, 1991)

and chickens (Cantwell and Cassone, 2002). This is similar to the situation in rodents (Cassone et al., 1988a). Secondly, pinealectomy of house sparrows not only abolishes circadian locomotor patterns but also abolishes the circadian rhythms of 2DG uptake in the vSCN (Lu and Cassone, 1993a). Thirdly, rhythmic administration of melatonin to arrhythmic, pinealectomized sparrows restores both a rhythm of locomotion and a rhythm of 2DG uptake in the vSCN, but not the mSCN, such that 2DG uptake is lower during melatonin administration than during vehicle administration (Lu and Cassone, 1993b). Finally, the vSCN of more than 20 species of birds express high density, high affinity binding of radiolabeled 2-[^{125}I]-iodomelatonin (IMEL) (Rivkees et al., 1989; Stehle, 1990; Cassone and Brooks, 1991; Siuciak et al., 1991; Brooks and Cassone, 1992; Cassone et al., 1995). The mSCN do not.

Recent advances in the molecular biology of circadian clocks have offered yet another avenue for the comparative study of the SCN. In rodents, several transcription factors and kinases, labeled "clock genes", are involved in a complex transcriptional-translational feedback loop that is at the core of a model explaining the generation of biological rhythms (Reppert and Weaver, 2002). Included in this loop are *period* genes (*pers*), *cryptochromes* (*crys*), *clock*, *bmal1* and *E4bp4*, which have been identified within the mammalian SCN (cf. Hastings and Herzog, 2004). Avian orthologs for these genes have been identified (Bailey et al., 2003, 2004). Several of these genes have been identified in the mSCN but not the vSCN in Japanese quail (Yoshimura et al. 2001; Yasuo et al., 2003). In the house sparrow, *pPer2* expression is rhythmic in both the

mSCN and the vSCN such that it is highest during the mid-day (Brandstatter et al., 2001), which is similar to the phasing seen in the mouse SCN (Tei et al. 1997).

A working model of the avian SCN

The present data and literature suggest to us that there is a role for both the mSCN and the vSCN in the avian circadian system. As with the pineal and the retinae, these structures will likely have varying levels of importance in different avian species. We hypothesize that both the mSCN and the vSCN are involved in a suprachiasmatic complex that serves as a functional equivalent of the mammalian SCN. At this stage, attribution of "homology" to these structures is premature. Further developmental and more comparative analyses of extant amniote vertebrate species will be necessary to truly address this issue.

Our model (Fig. 18) states that light information is transmitted to the suprachiasmatic complex via three separate input pathways. The first of these is the retinohypothalamic tract (RHT), which has been well characterized in the vSCN of many avian species. Sparse RHT input also transmits light information to the mSCN. The second photic input to the vSCN is indirect, through the lateral geniculate nuclei via a pathway homologous to the mammalian GHT, described above. The third and final light input to our suprachiasmatic complex is input to the mSCN via the encephalic photoreceptors of LSO and PVO. While sufficient data has not been produced to bear out the existence of a specific connection, the hypothesis is supported by the finding of Yoshimura et al. (2001) that a one-hour light pulse during the subjective night is capable

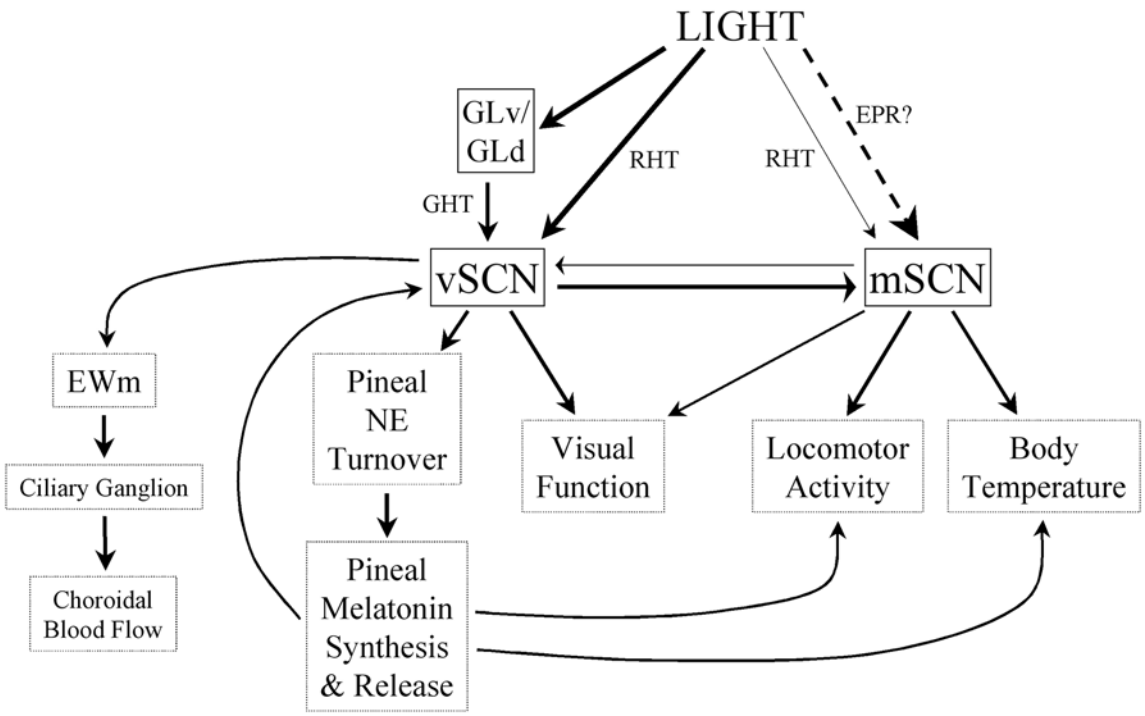

Fig. 18. A working model of the avian SCN. This model addresses the transduction of light to the SCN and summarizes what we hypothesize are the roles of the vSCN and mSCN in the circadian system. Solid lines represent connections reported in the current study and the literature. The dashed line represents speculation based on indirect evidence. For abbreviations, see list.

of inducing *per2* RNA expression in the mSCN of quail whose eyes are covered by opaque black rubber caps, barring RHT and GHT transduction of the signal. The mSCN and vSCN have bilateral and bidirectional communication, allowing them to share light information with one another.

Both the mSCN and vSCN have been implicated in the literature as circadian pacemakers. Our model suggests that the mSCN drives locomotor activity and body temperature rhythms, based on lesion studies (Ebihara et al., 1987; Yoshimura et al., 2001). Conversely, we propose that the vSCN regulates choroidal blood flow via EWm, drives and/or entrains circadian rhythms of visual function and regulates pineal melatonin secretion via the sympathetic nervous system. As was shown in this study, there is abundant connectivity between the vSCN and structures of the thalamofugal, tectofugal and accessory optic visual pathways.

Why are there two structures in birds undertaking the role of the mammalian SCN? We hypothesize that the evolution of this organization involves the development of the supraoptic decussation, which is extensive in birds and first visible in the chick on embryonic day 8 (E8). By E15, it is quite thick and has visible subdivisions (Ehrlich et al., 1988). The retinohypothalamic innervation of the hypothalamus, on the other hand, is not visible until E15 or E16 (Shimizu et al., 1984). We propose that, because of the conflicting developmental timing of the supraoptic decussation and RHT, mSCN innervation by retinohypothalamic terminals is not physically permitted. Instead, retinal afferents innervate the vSCN, which in turn innervate the mSCN. If this is the case, this anatomical configuration may be a derived feature and unique to birds, which express a

greater inter-hemispheric interaction of visual information than do other taxa (Ehrlich et al., 1988) with the possible exception of crocodilians (Crosby and Showers, 1969). If this is the case, then we might expect a similar organization in crocodilians as birds, which share archosaurian ancestry (Rogers, 1999), but it is likely that the SCN of other reptile taxa are co-localized in the preoptic recess. Clearly, more comparative research on non-mammalian vertebrates will be required to test this hypothesis.

Further, analysis of the chemoarchitecture of these two structures in this and other avian species will be important in understanding avian circadian organization as well as the evolution of the diencephalons. More detailed studies of the development of the retinohypothalamic tract in birds and other non-mammalian vertebrates may provide a window into knowledge of suprachiasmatic nucleus function and evolution.

CHAPTER IV

THE CHICKEN SUPRACHIASMATIC NUCLEI: AUTORADIOGRAPHIC AND IMMUNOHISTOCHEMICAL ANALYSIS

INTRODUCTION

The suprachiasmatic nucleus (SCN) of the hypothalamus is the primary pacemaker in all mammals studied (Moore, 1979). The SCN receives primary visual input via the retinohypothalamic tract (RHT; Moore et al., 1971; Moore and Lenn, 1972; Moore, 1973), as well as indirect retinal input from the lateral geniculate nucleus via the geniculohypothalamic tract (GHT; Card and Moore, 1982, 1989; Moore et al., 1984; Harrington et al., 1985; Moore and Speh, 1993; Moore and Card, 1994). Surgical destruction of the SCN produces arrhythmicity in locomotor behavior (Moore and Eichler, 1972; Stephan and Zucker, 1972; Moore and Klein, 1974; Klein and Moore, 1979) and transplant of fetal SCN tissue into the third ventricle restores rhythmicity to SCN-lesioned animals (Drucker-Colin et al., 1984; Sawaki et al., 1984; Lehman et al., 1987). Further, many functional properties of the SCN are known to oscillate, including glucose utilization *in vivo* and *in vitro* (Schwartz and Gainer, 1977; Schwartz et al., 1980; Newman et al., 1992), neuronal firing *in vivo* and *in vitro* (Inouye and Kawamura, 1979; Green and Gillette, 1982; Groos and Hendriks, 1982; Shibata et al., 1982) and gene expression *in vivo* and *in vitro* (Yamazaki et al., 2000; Hastings and Herzog, 2004).

Antigen distribution in the mammalian SCN is well established; however, it is variable among the few species studied thus far (Card and Moore, 1982; van den Pol and

Tsujimoto, 1985; Cassone et al., 1988b). For example, the eutherian mammalian SCN may be subdivided into the ventrolateral, retinorecipient "core", which is immunoreactive for arginine vasopressin (AVP), and the dorsomedial "shell", which contains neurons positive for vasoactive intestinal polypeptide (VIP; Cassone et al., 1988b; Moore et al., 2002). In contrast, the marsupial SCN differs from the eutherian SCN in that the dorsomedial aspect of the structure is retinorecipient and co-localizes with both AVP and VIP immunoreactivity (Cassone et al., 1988b). Thus, specific details of immunohistochemical distributions in the SCN are phylogenetically labile even among mammals.

In birds, there is evidence that a circadian oscillator, presumed to be homologous to the mammalian SCN, resides in the anterior hypothalamus of birds (Ebihara and Kawamura, 1981; Simpson and Follett, 1981; Takahashi and Menaker, 1982). Early cytoarchitectural studies identified a structure near the preoptic recess of the third ventricle that was thought to be homologous to the mammalian SCN. While this structure has been referred to in the literature by a variety of designations (Chapter III), we will refer to this structure as the medial suprachiasmatic nucleus (mSCN), as indicated by Kuenzel and Masson (1988). Some studies have reported retinal afferents in the mSCN, but the label is weak (Hartwig, 1974; Oliver et al., 1978) or undocumented with photomicrographs (Ebihara and Kawamura, 1981).

A lateral hypothalamic nucleus is the primary, if not only, retinorecipient nucleus in the hypothalamus in the ringed turtledove (*Streptopelia risoria*; Cooper et al., 1983; Norgren and Silver, 1989), house sparrow (*Passer domesticus*; Cassone and Moore,

1987), pigeon (Meier, 1973; Gamlin et al., 1982; Shimizu et al., 1994), duck (*Anas platyrhynchos*; Bons, 1976), and chicken (Shimizu et al., 1984; Chapter III). As with the mSCN, it has been given many different names (cf. Chapter III); we will refer to this structure as the visual suprachiasmatic nucleus (vSCN).

In Chapter III, we addressed the efferent and afferent connections of both the mSCN and vSCN. Using cholera toxin B-subunit and biotin dextran amine tract tracing, we determined that the mSCN and vSCN jointly possess more efferents and afferents than does the mammalian SCN. A subset of these connections correlates well with those that have been established in rodent species, and the mSCN and vSCN are equally similar to the eutherian mammalian SCN. Based on the information currently available on the avian mSCN and vSCN, we presented a working model in which both structures participate in a suprachiasmatic complex. We will revisit this model in our discussion of the data presented here.

The chemoarchitecture of both the mSCN and vSCN has been studied in other bird species. The most extensive study concentrated on only the vSCN of the house sparrow (Cassone and Moore, 1987). The work presented here focuses on three aspects of suprachiasmatic organization in the chicken, *Gallus domesticus*: 1) cytoarchitecture, 2) retinohypothalamic projections, which corroborates previously reported data using different techniques (Chapter III), and 3) chemoarchitecture. The purpose of this study was to further address the question of homology between the putative avian SCN and the mammalian SCN.

MATERIALS AND METHODS

Animals

White leghorn cockerels (*Gallus domesticus*) were obtained on their hatch date from Hy-Line Hatcheries (Bryan, TX) and were kept in heated brooders on a light:dark (LD) 12:12 cycle (lights on from 6:00 a.m. to 6:00 p.m. CST). Food (Purina Start & Grow, Brazos Feed & Supply, Bryan, Texas) and water were available ad libitum. At two to three weeks of age, the chickens were used for tract-tracing and immunohistochemical procedures.

Retinohypothalamic projections and cytoarchitecture

Two birds were anesthetized and received an intraocular injection of 10 μCi ^{3}H-proline in 6 μL 0.75% saline with a 10 μL Hamilton syringe. Birds were allowed to survive 24 hours before they were administered a large dose of pentobarbital and perfused with Bouin's fixative. Brains were removed, dehydrated, embedded in paraffin and sectioned frontally at 15 μm through the diencephalon. Slides were coated with Kodak NTB-2 (Rochester, NY) emulsion and stored in light-tight boxes for two weeks at 4^{o}C. They were developed with Kodak D-19 developer, fixed and counter stained with cresyl violet.

For cytoarchitectural analysis, all sections containing the mSCN or vSCN were identified using differential interference contrast optics on a Zeiss Axioplan 2 microscope (Thornwood, NY). Data regarding retinal terminal fields in the vSCN were used to aid in its location. A digital image of each structure was taken with a Hamamatsu Color Chilled 3CCD Camera (Bridgewater, NJ). The area of each structure

was analyzed using Image J (National Institutes of Health, Bethesda, MD) and total cell number was counted in Adobe Photoshop (Adobe Systems, Mountain View, CA). Total volume was obtained by multiplying the area of each measured structure by the thickness of tissue represented by the section (45 μm) and adding those sectional volumes together. Identified cell types were measured by determining the circumference of 50 cells, and size is expressed as the mean diameter ± standard error of the mean. Values reported indicate the cytoarchitectural characteristics of the mSCN or vSCN from one cerebral hemisphere.

Immunohistochemistry

Chicks (n=35) were anesthetized with a ketamine/xylazine drug cocktail (90 mg/kg ketamine, 10 mg/kg xylazine) and perfused transcardially with 50-100 ml saline followed by 150-300 ml Zaborsky or 4% paraformaldehyde fixative in 0.1M phosphate buffer. Their brains were removed, post-fixed for one hour and cryoprotected in a series of sucrose solutions (10%, 20% and 30%).

Some brains (n=15) were sectioned frontally (30μm) and floated into phosphate buffered saline (PBS; 10mM). One bin each from six birds were stained with cresyl violet at 150μm intervals. These sections were used to locate structures of interest. The remaining sections were processed immunohistochemically with primary antisera, developed in rabbit, against vasopressin (AVP; avian homolog, arginine vasotocin), gastrin releasing peptide (GRP), glutamic acid decarboxylase (GAD), glial fibrillary acidic protein (GFA), gonadotropin releasing hormone (GnRH), neuropeptide Y (NPY),

oxytocin (OT; avian homolog, mesotocin), serotonin (5HT), somatostatin (SS), substance P (SubP), tyrosine hydroxylase (TH) and vasoactive intestinal polypeptide (VIP). The GRP antibody was a gift from Dr. N. Brecha. The GAD antiserum was a gift from Drs. I. Kopin and W. Oertel (Oertel et al., 1982). The NPY antiserum was provided by Dr. J. McDonald. Some antisera against AVP, GFA, GnRH, OT, 5HT, SS, SubP, TH and VIP were purchased from INCSTAR (formerly Immunonuclear, now DiaSorin, Stillwater, MN).

The rest of the brains (n=20) were sectioned into PBS at 30 μm on a nearly horizontal plane that included both the mSCN and the vSCN. Sections were processed with primary antibodies against AVP, VIP, 5HT, GFA, NPY, GAD, SP, SS, and γ-aminobutyric acid (GABA; Chemicon International, Temecula, California).

Immunohistochemistry was performed on these sections. Briefly, floating sections were blocked in PBS containing 0.3% Triton-X-100 and 1% normal goat serum (PBSGT) for 1 hour and then incubated in primary antibody (1:1000) in PBSGT for 48 to 72 hours at 4^{o}C. Sections were then incubated in biotinylated rabbit anti-goat secondary antibody (1:500; Vector Laboratories, Burlingame, CA) in PBSGT for two hours at room temperature, followed by a 90 minute incubation in avidin-biotin complex from a peroxidase standard kit (1:55; Vector Laboratories, Burlingame, CA) in PBSGT. Sections were incubated in 0.5% 3-3'-diaminobenzidine solution in 100 mM Tris buffer for five minutes after which 0.21% hydrogen peroxide was added to the solution. The color reaction was stopped when minimal background coloration became evident. Sections were rinsed, ordered, mounted onto gelatin-coated slides and dried. The slides

were rinsed in PBS and the color reaction was stabilized in 1% cobalt chloride solution. The slides were then rinsed, dehydrated, cleared and coverslipped for analysis.

Microscopy and photography

An Olympus BH-2 light microscope (Melville, NY) was used to examine processed tissues. Immunohistochemically processed sections were observed using a phase contrast condenser with differential interference contrast optics, while autoradiographic tract tracing was viewed under dark field. Photomicrographs were taken with an Olympus C-35AD-4 camera on Kodak Gold 200 film. Prints were scanned at 300 DPI and opened in Adobe Photoshop 7.0.1, where they received minor brightness and contrast adjustments.

RESULTS

Cytoarchitecture

The mSCN is just dorsal to the optic chiasm in the most anterior portion of the hypothalamus, apposed to the preoptic recess of the third ventricle, about 0.5 mm lateral of the midline. It is a crescent-shaped band with tapered ends, about 100-175 μm thick and 400-800 μm wide. It is 300 μm long rostrocaudally. It contains roughly 5,300 cells in a 0.014 mm^3 volume, giving a total cell density of 385 ± 14 cells per 100 μm^3. The cells in this structure are small, measuring 10.6 ± 0.2 μm.

The vSCN is slightly more caudal than the mSCN and is roughly 1.5 mm lateral of the midline. It sits atop the optic chiasm, lateral to the dorsal supraoptic decussation

and medial of the ventrolateral geniculate nucleus. There is a blood vessel frequently associated with this nucleus. It is roughly triangular in rostral coronal sections, but becomes more rounded and smaller caudally. Therefore, it measures from 150-500 μm dorsoventrally and 150-500 μm mediolaterally, with a mean diameter of 350 μm. It is 950 μm on its rostrocaudal axis. The small neurons of the vSCN (13.2 ± 0.3 μm) are slightly larger than those in the mSCN and are less densely packed. Total cell density is 211 ± 4 cells per 100 μm^3, representing about 22,000 cells in a volume of 0.105 mm^3. Larger neurons (16.8 ± 0.4 μm) are found at the ventral and medial borders of the vSCN.

Retinohypothalamic projections

A completely contralateral retinohypothalamic projection (RHT) to the vSCN is evident (Fig. 19B). The RHT has the same spatial distribution as the nucleus itself: the borders of the nucleus are defined by the projection and are described above. No label was observed in the mSCN (Fig. 19A). A schematic representation of visual projections in the planes of interest is shown on the left-hand panels of Figure 20.

Immunohistochemistry

Immunohistochemical results are shown schematically in Figure 20. Sparse fibers and modest amounts of cellular label positive for AVP-like immunoreactivity (LI) were found within mSCN (Fig. 20). The vSCN contained only a few sparse large

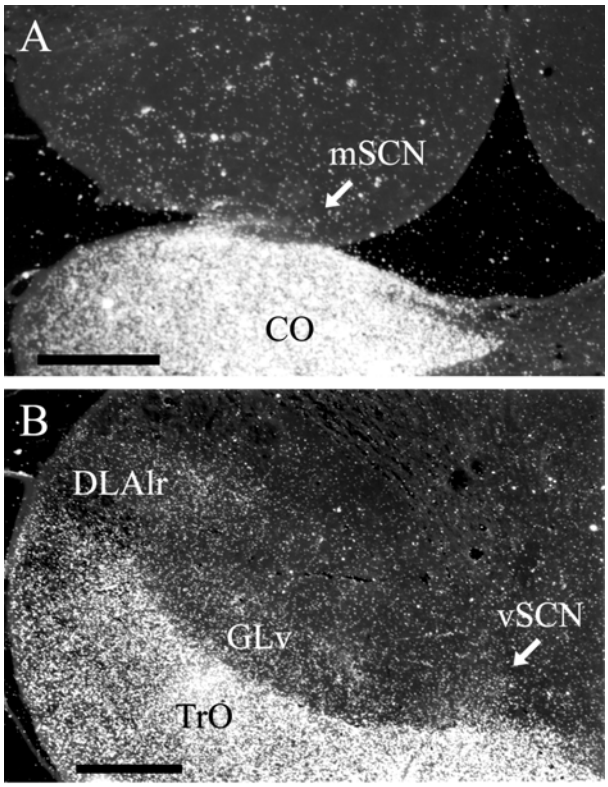

Fig. 19. Representative photomicrographs of retinal input to the brain following injection of tritiated proline to the eye. Note the lack of visible retinal input to the mSCN (A) and the presence of retinal terminals throughout the vSCN (B). For abbreviations, see list. Scale bar = 1 mm.

AVP-LI cells, however, a dense plexus of fibers exits the vSCN from its dorsal border and spans the distance to PVN (Figs. 20, 21D). VIP-LI and 5HT-LI fibers are sparsely present in the mSCN. However, they are not arranged in a discernible nuclear arrangement (Fig. 20). In the vSCN, large VIP-LI cells are present on the dorsomedial border and a moderate fiber plexus is present in the rostral portion of the nucleus (Figs. 20, 21E). 5HT-LI fibers form a dense plexus in the vSCN, which becomes less dense in the caudal region of the nucleus (Figs. 20, 21J). Sparse GRP-LI fibers and cellular staining are present within the mSCN (Figs. 20, 21A), with only sparse fibers present in the vSCN (Fig. 20). NPY-LI and Sub-P-LI fibers are found in the medial portion of mSCN (Fig. 20). In the vSCN, a moderate NPY-LI fiber plexus is more dense in the rostral half of the nucleus (Figs. 20, 21H). Small SubP-LI cells are found in the ventral vSCN, along with a dorsal fiber plexus that extends beyond the dorsal border (Figs. 20, 21F). GFA-LI cells are present within the medial portion of the mSCN (Fig. 20), while they form a dense aggregation within the vSCN (Figs. 20, 21G). SS-LI fibers are sparse in mSCN (Fig. 20). SS-LI small cells and fibers are dense in the rostral portion of the vSCN (Figs. 20, 21I). GAD-LI follows the general pattern of retinal input, while staining additional areas such as the lateral bed nucleus of the stria terminalis and the ventral region of the anterior hypothalamus (Fig. 20). GAD-LI fibers in this region include mSCN and the anterior hypothalamic nucleus, without forming discernible aggregations in any one structure. In the vSCN, small GAD-LI cells and fibers are dense throughout the nucleus (Figs. 20, 21K). Cells and fibers are also present in the ventrolateral geniculate nucleus and the rostrolateral part of the dorsolateral anterior

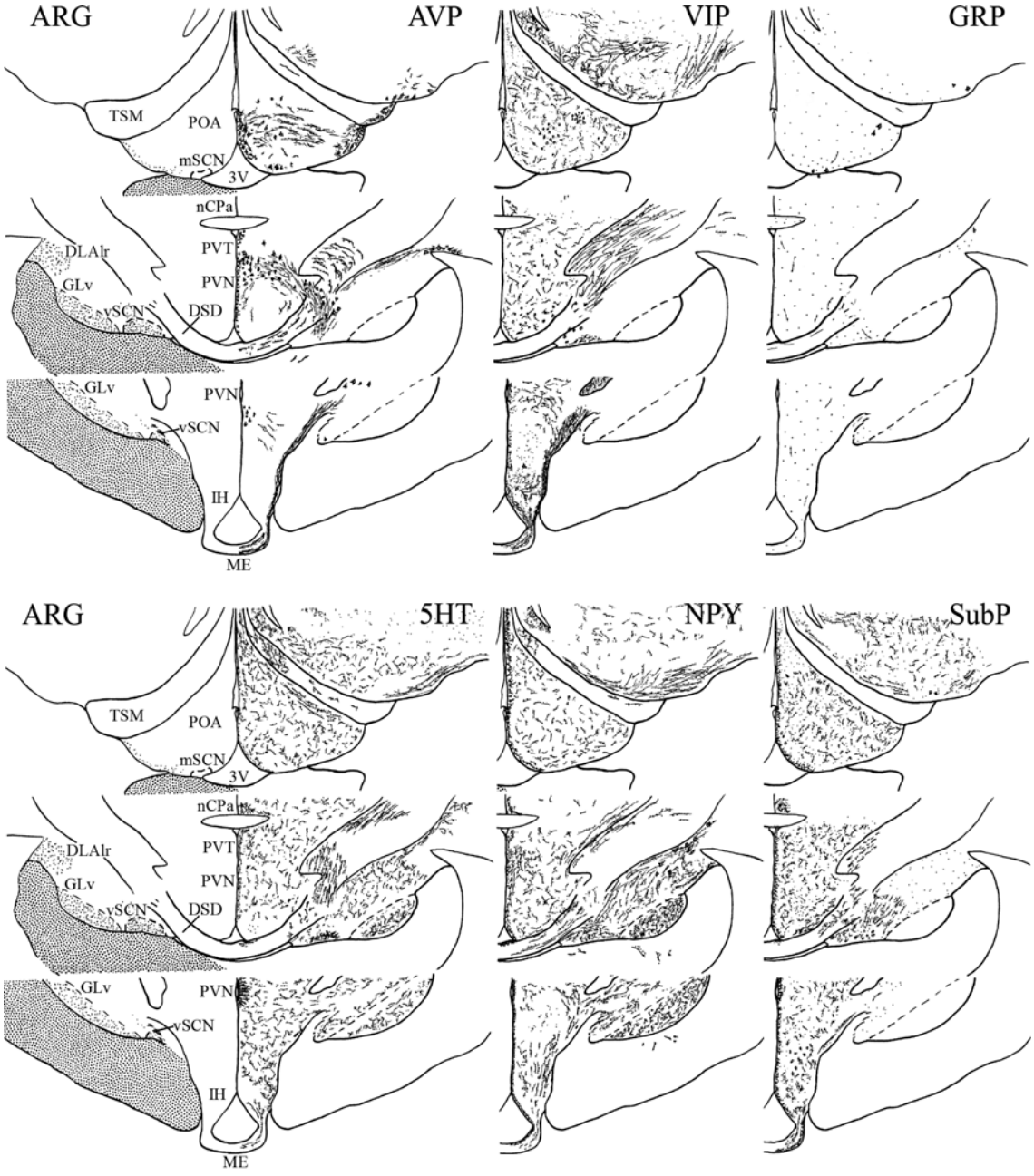

Fig. 20. Schematic illustration of retinal terminals and antigen distribution at three levels of the hypothalamus. Structures of interest are labeled and retinal terminals are mapped on the left hemisphere of the sections in the left panel. Fibers and cells identified immunohistochemically are indicated for a variety of antibodies. A summary of this information is available in Table 6. The distribution of fibers and cells on these maps represent the relative strength of staining in these areas, but do not reflect measured values. Abbreviations: ARG, ^{3}H-proline autoradiography; all others, see list.

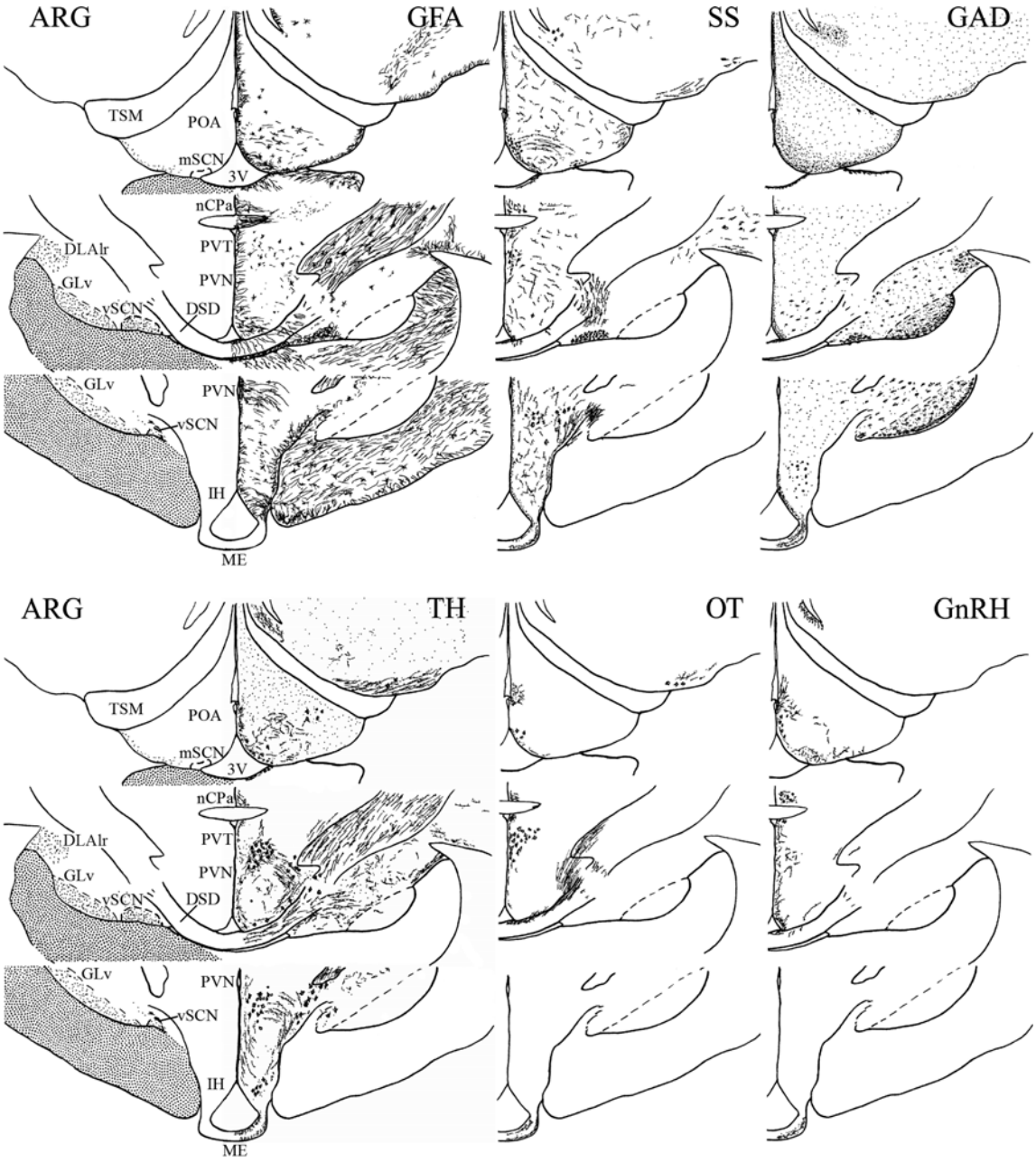

Fig. 20 Continued

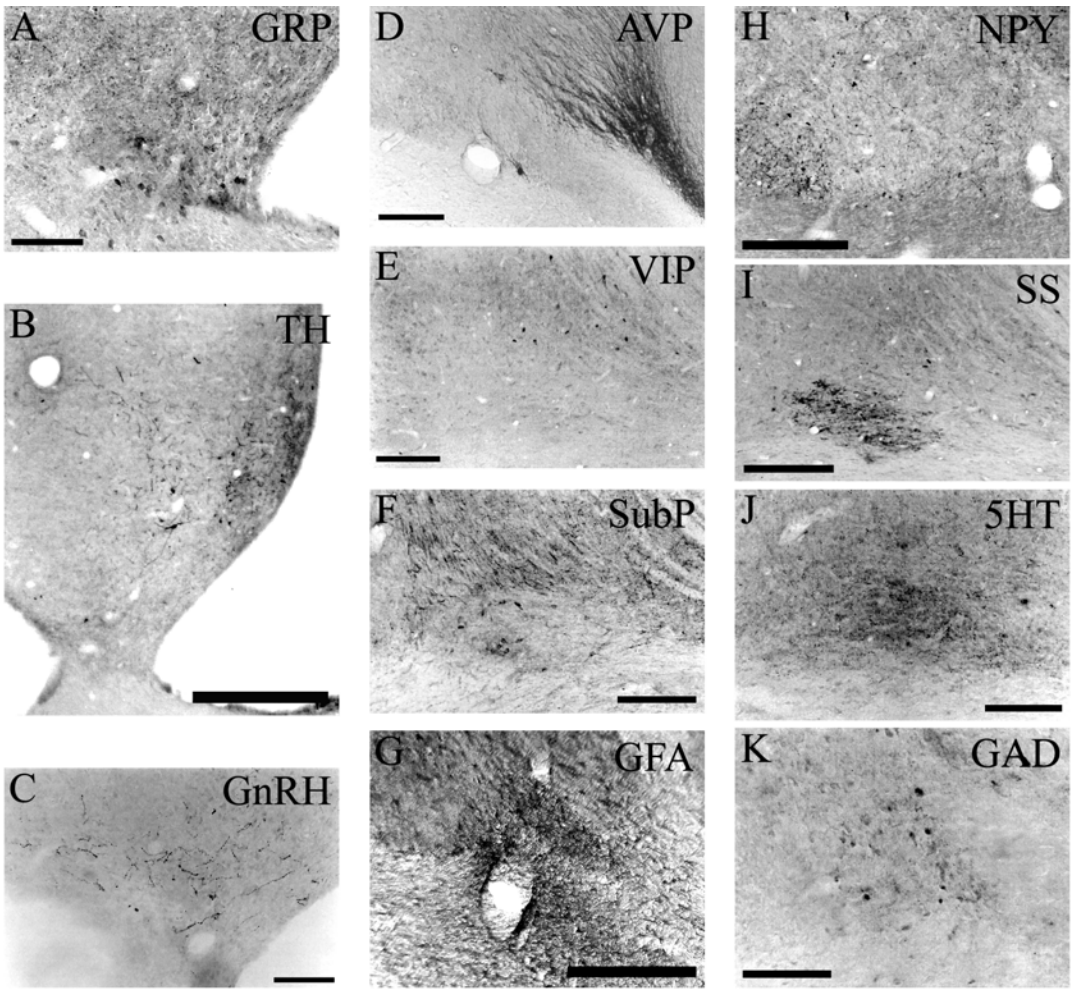

Fig. 21. Representative photomicrographs of immunohistochemical staining in the mSCN (A-C) and vSCN (D-K). Note the presence of TH fibers and cells (B) and GnRH fibers (C) in the mSCN. Cellular GAD distribution (K) in the vSCN follows the pattern of retinal input. For abbreviations, see list. Scale bar = 1 mm in B; 400 μm in D-I; 200 μm in A,C,J,K.

TABLE 6. Antigen distribution of the suprachiasmatic nuclei of the chick, sparrow and rat.

Antigen	Chicken				Sparrow		Rat	
	mSCN		vSCN		vSCN		SCN	
	fibers	cells	fibers	cells	fibers	cells	fibers	cells
AVP	+	++	dorsal	+	+	++	+++	+++
VIP	+	-	++	medial	+	medial	+++	+++
GRP	+	++	+	-	+++	++	++	++
5HT	+	-	+++	-	+++	-	+++	-
NPY	++	-	++	-	+	-	++	-
SubP	+	-	++	++	+	++	++	+
GFA		++		+++				+++
SS	+	-	+++	+++			++	+
GAD	++	-	+++	+++	+++	+++	+++	+++
TH	++	++	+	-			-	-
MT	+	+	-	-			-	-
GnRH	++	-	-	-			-	-

Strength of antigen signal: +++, strong; ++, moderate; +, sparse; -, none present. Cells left blank indicate no data is available in the literature. For abbreviations, see list.

nucleus (Fig. 20). TH-LI fibers and cells are found within mSCN, particularly in the medial portion (Figs. 20, 21B), while they surround, and only very occasionally enter vSCN (Fig. 20). In mSCN, there are sparse OT-LI fibers and cells (Fig. 20), as well as a moderate plexus of GnRH-LI fibers (Figs. 20, 21C). Neither OT-LI nor GnRH-LI is found within or proximal to the vSCN. The data are summarized in Table 6, and compared with data from previous studies.

Horizontal sections

Immunohistochemistry performed on off-horizontal sections that include both the mSCN and vSCN revealed a GFA-LI “bridge” of astrocytes that connects the two

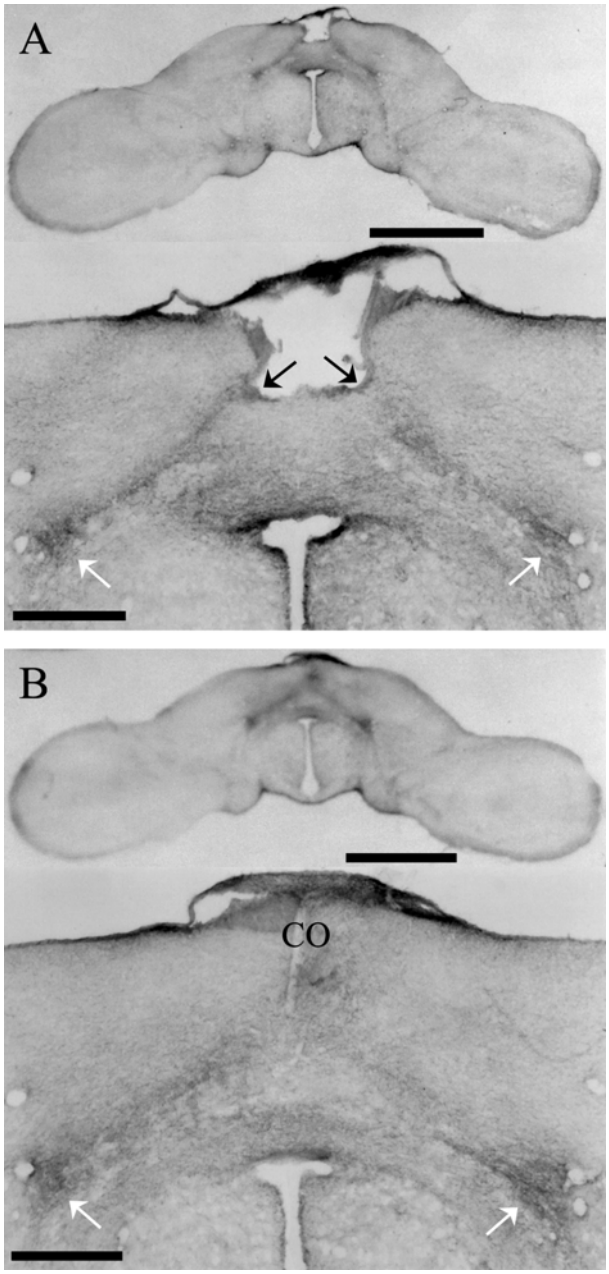

Fig. 22. The astrocytic bridge as demonstrated by immunohistochemical analysis with GFAP. **A** In a section cut on a horizontal plane containing both the mSCN (black arrows) and the vSCN (white arrows), the bridge is clearly visible extending between the two structures. **B** The section just inferior to A demonstrates that this bridge travels within the white matter ventral to the two structures. Scale bar = 17.8 mm in the upper panels of A and B; 4mm in the lower panels.

structures (Fig. 22). This astrocytic bridge is the only strongly stained GFA-LI structure in this region. The bridge appears to be a direct pathway that travels within (Fig. 22A) and slightly inferior to (Fig. 22B) the plane created by the two structures. We attempted to identify a neuronal connection that may be paired with this astrocytic bridge using antibodies against AVT, VIP, 5HT, NPY, SubP, SS, GAD and GABA. We were unable to identify any neuronal connection within this plane of section.

DISCUSSION

Our findings regarding retinal input to and antigen distribution of the anterior hypothalamus indicate that the chick vSCN is more similar to the mammalian SCN than is the mSCN. Previous studies, however, have indicated a role for both structures in the avian circadian system. We expand below upon our working model of the avian SCN, taking into consideration new findings regarding the mSCN and vSCN.

Physical properties of the avian suprachiasmatic nuclei

Based on location alone, the mSCN has been dubbed the avian homolog to the mammalian SCN. There is, however, significant dissimilarity worthy of mention: 1) it is smaller, 2) it is significantly shorter rostrocaudally, and 3) it is apposed to the preoptic recess of the third ventricle. Therefore, it is more similar in its position to the rostral portion of the rat SCN, called the preoptic suprachiasmatic nucleus by Palkovits and Brownstein (1988). Our findings here indicate that there is no retinal input to the mSCN. In the first paper of this series, we demonstrated using CTB tract tracing that

there are sparse fibers of passage and some retinal terminals in the mSCN and areas just dorsal to the mSCN (Chapter III). The lack of significant retinal input does not support the contention that the mSCN is the avian homolog of the mammalian SCN. The chemoarchitecture of the mSCN is also clearly dissimilar from that of the mammalian SCN. The mSCN contains cells and fibers that stain positively for TH, OT and GnRH, which do not populate the mammalian SCN (van den Pol and Tsujimoto, 1985). Concurrently, many of the antigens found within the mammalian SCN are not found in the mSCN or, if they are, are qualitatively different in their distribution. The exception to this is GRP, which we identified in the chick mSCN but not the vSCN. GRP-LI cells and fibers are found in the vSCN of the house sparrow (Cassone and Moore, 1987) and the mammalian SCN (Moore et al., 2002).

The position of the vSCN, on the other hand, is quite different than the mammalian SCN; it is more lateral and caudal. It is similar in its length, although it is larger in diameter and total volume than is the rat SCN (Moore et al., 2002); this is consistent with the fact that the entire chick brain is larger than that of the rat. The borders of the vSCN are defined by its retinal input, the terminals of which are found throughout the nucleus. This is also dissimilar from the mammalian SCN in that only a portion of the mammalian nucleus receives retinal input via the RHT. However, the location of that retinal input is variable among mammalian species studied thus far (Cassone et al., 1988b).

The chemoarchitecture of the vSCN is very similar to that of the mammalian SCN; it is well defined by a heterogeneous population of cells and fibers, present within

or bordering the nucleus, that react differentially to antibodies against AVP, VIP, 5HT, NPY, SubP, GFA, SS and GAD, all of which are present in the mammalian SCN. It does not react to antibodies generated against TH, OT and GnRH, antigens that are not present in the mammalian SCN. This chemoarchitectural similarity to the mammalian SCN is shared with the vSCN of the house sparrow (Table 6; Cassone and Moore, 1987). The chemoarchitectural similarity of the vSCN to the mammalian SCN is more striking than any similarities that exist between the mSCN and the mammalian SCN, indicating that the vSCN is a more likely homolog.

Of particular interest in this study is AVP-LI. AVP-LI fibers form a clear pathway between the vSCN and the hypothalamic paraventricular nucleus (PVN), a structure that communicates with the mammalian SCN via AVP fibers (Leak and Moore, 2001; Abrahamson and Moore, 2001). The fibers we report in the chick, however, do not arise from the vSCN, in which only a few sparse projection neurons are visible; instead, they appear to arise from a population of neurons in PVN itself, which contains a dense population of AVT-LI cells. This seems likely in light of our finding in Chapter III that CTB injections to the vSCN retrogradely labeled cells in PVN. These data explain a possible pathway of communication from PVN to the vSCN; however, they do not address the question of how the vSCN might return information to PVN. One may reasonably hypothesize that mSCN completes the circuit by sending efferents to PVN. First, abundant efferents from mSCN to PVN were identified by BDA iontophoresis and transport. Second, bilateral, bidirectional communication between the vSCN and the mSCN was demonstrated (Chapter III). Finally, as we have shown here, mSCN contains

a moderate number of cells positive for AVT. It is plausible, then, that there is a circuit between these two suprachiasmatic regions and the PVN.

Which came first…?

It is important to consider the developmental process that results in a heterogeneous population of cells in the SCN: do retinal terminals find the SCN based on antigenicity or does the appropriate antigen distribution develop after retinal innervation? Studies in anophthalmic mice are a useful means of addressing this query for rodents. The optic primordia of anophthalmic mice are resorbed during embryonic development and they are almost always born without eyes and optic nerves. This model system offers the rare ability to consider the SCN in an animal that, non-surgically, lacks retinal input. The SCN of these mice is cytoarchitecturally disrupted: one or both nuclei are frequently absent and, when both nuclei are present, they are asymmetric and vary in size (Laemle and Rusa, 1992). Two antigens in this model system have been studied—VIP and NPY. VIP-LI cells and fibers of the SCN, when present, are more diffuse than those in wildtype mice, and many ectopic sites of VIP immunoreactivity are present in the hypothalamus (Laemle and Rusa, 1992). It has been shown that when VIP is present in the SCN, it is expressed rhythmically (Laemle et al., 1995); however, this rhythmic expression is not sufficient to produce locomotor rhythms (Laemle and Ottenweller, 2001). Anophthalmic mice have three distinct behavioral phenotypes, ranging from rhythmic with a stable period, to rhythmic with an unstable period, to arrhythmic (Laemle and Ottenweller, 1998). The geniculohypothalamic tract

(GHT) in these mice has also been studied. Despite the lack of retinal innervation, the intergeniculate leaflet develops, but it is cytoarchitecturally disrupted. NPY terminal fields, an indicator of GHT input to the SCN, are formed, but they are dissimilar from the same input in eyed mice (Laemle et al., 1993).

VIP and NPY are therefore present in anophthalmic mice, but are disrupted in their distribution. These data suggest that that antigenicity is somewhat predetermined; however, the precise chemoarchitecture of the SCN is influenced by retinal input. There currently are no anophthalmic avian models available with which to carry out similar studies of the vSCN and mSCN; however, studies concerning the multiple light input pathways and their terminal formation in the context of antigen distribution development and cellular origin in the emerging hypothalamus would be very useful in the determination of the interactions that result in a functional SCN, particularly in the avian complex.

Developmental aspects of the molecular biology of circadian clocks may also provide a broader view of SCN formation. Several transcription factors and kinases are involved in a transcriptional-translational feedback loop that is central to a molecular model for the generation of circadian rhythms (Reppert and Weaver, 2002). Orthologs for these genes have been identified in chicks (Bailey et al., 2003, 2004) and have been identified in the mSCN of the Japanese quail (Yoshimura et al., 2001; Yasuo et al., 2003) and house sparrow (Brandstatter et al., 2001). In the house sparrow, *pPer2* expression has been demonstrated in both the mSCN and the vSCN (Brandstatter et al., 2001).

Astrocytes in the mammalian circadian system

Our immunohistochemical analysis presented some exciting data, indicating a function for astrocytes in the chick suprachiasmatic complex. However, the majority of study regarding astrocytes in the circadian system has been carried out in mammals, and so it is important to consider what is known about astrocytes in the rodent SCN. It was first suggested that astrocytes might play a role in the biological clock when it was demonstrated that GFA antibodies significantly label cells within the SCN of hamsters and rats (Morin et al., 1989). GFA expression in the rodent SCN is rhythmic (Lavialle and Serviere, 1993) and, when animals are enucleated, GFA expression in the SCN decreases (Lavialle et al., 2001). In fact, merely placing rats in constant darkness leads to a decrease in GFA expression, and reintroduction of animals to a light:dark cycle will restore GFA expression (Ikeda et al., 2003). Furthermore, administration of pituitary adenylate cyclase-activiating peptide (PACAP), an RHT neurotransmitter (Hannibal, 2002), to cultured astrocytes stimulates growth of their processes (Ikeda et al., 2003). These data strongly suggest a modulatory effect of light on astrocytes.

Many studies have indicated a functional role for astrocytes. Astrocytes associated with the RHT have been shown to modulate the concentration of glutamate, another RHT neurotransmitter (de Vries et al., 1993), in the extracellular fluid of the SCN (Lavialle and Serviere, 1995). Furthermore, release of glutamate and serotonin at retinal terminals in the SCN causes increased intracellular calcium concentration in both neurons and astrocytes, often triggering intercellular calcium waves via gap junctions between astrocytes (van den Pol et al., 1992). Fluorocitrate, which inhibits glial

metabolism, produces behavioral arrhythmicity when injected into the SCN (Prosser et al., 1994).

One may hypothesize, then, that astrocytes play a role in the generation of circadian rhythms. However, astrocytes do not confer rhythmicity upon neurons in a dispersed SCN culture (Welsh and Reppert, 1996). Within this culture, neurons overlay confluent astrocytes that exhibit connexin43 positive gap junctions. The neurons, however, are not gap-junctionally coupled to either astrocytes or to other neurons (Welsh and Reppert, 1996). These data suggest that the single-cell firing rates in SCN neurons are autonomous and not imposed by either astrocytes or by a subset of pacemaker neurons. It has also been demonstrated that blockade of gap junctional communication in the SCN may either phase delay or abolish rhythmic neuronal activity *in vitro* (Prosser et al., 1994); however, more recent studies have indicated that SCN neurons are indeed gap junctionally coupled (cf. Colwell, 2005) and, therefore, this arrhythmicity could be due to disruption of both neuronal and astrocytic communication. It is apparent that astrocytes play some role in the synchronization of rhythms in the mammalian SCN; however, this role is not well defined and is likely part of a network of interactions that cooperate to form a coordinated signal from the SCN.

The working model of the avian SCN and a potential role for astrocytes

In Chapter III, we introduced a working model of the avian suprachiasmatic complex. Our model (Fig. 23) states that there are three input pathways for light to the SCN: 1) RHT efferents primarily to the vSCN, with sparse input to the mSCN, 2) GHT

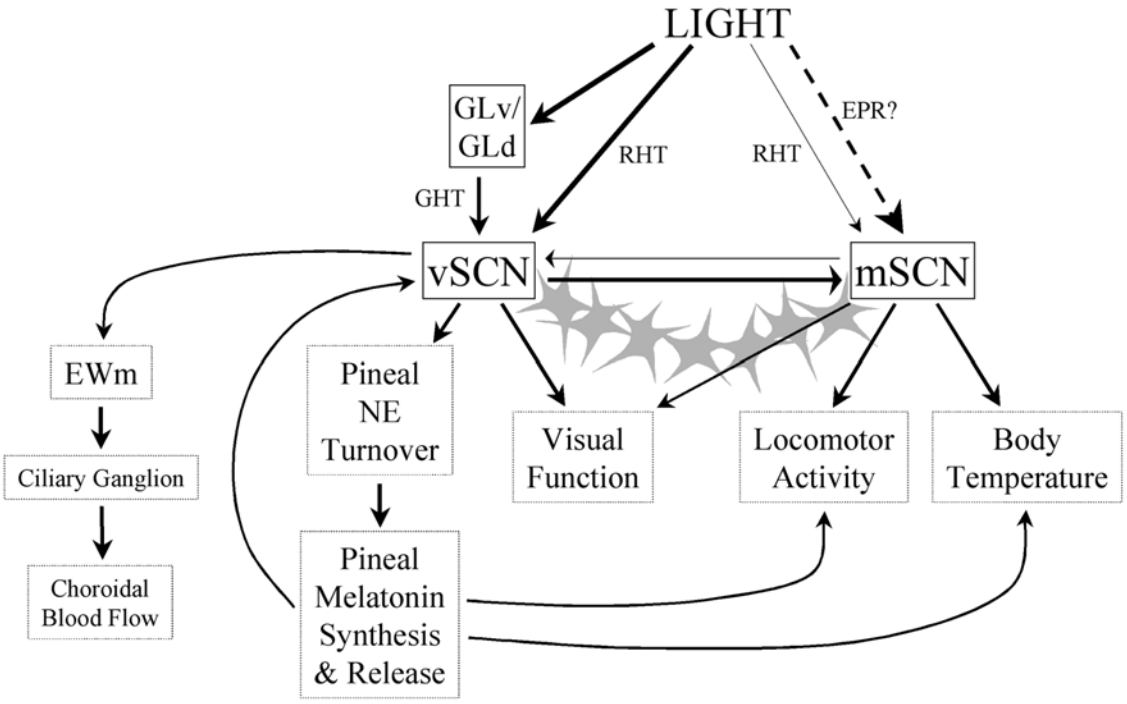

Fig. 23. An updated working model of the avian SCN. This model addresses input pathways of light to the avian SCN and summarizes what we hypothesize are the roles of the vSCN and mSCN in the circadian system. Solid lines represent connections supported by data in this document or in the literature. The dashed line represents a speculative multisynaptic pathway. New to this model is the addition of the astrocytic bridge, indicated by a chain of grey stars. For abbreviations, see list.

efferents to the vSCN and 3) encephalic photoreceptor input to the mSCN, which has been supported by indirect evidence (Yoshimura et al., 2001). We previously demonstrated that there is a bilateral and bidirectional neuronal connection between the mSCN and the vSCN (Chapter III), presumably allowing them to share light information and participate in multisynaptic pathways. In the current study, we identified a unique GFA-LI pathway between the mSCN and the vSCN, which we have named the astrocytic bridge. We were unable to identify a neuronal pathway within the same plane. These data suggest that the astrocytic bridge is a functional component of the suprachiasmatic complex.

Therefore, adding to our model, we hypothesize that the astrocytic bridge plays a modulatory role in the avian SCN, serving to modulate synaptic communication between the mSCN and vSCN and to synchronize neuronal signaling in these structures, as has been demonstrated in mammals. Astrocyte involvement in avian circadian structures is not a new concept: in the avian pineal gland, astrocytes coupled by gap junctions synchronize pineal cells (Berthoud et al., 2000). While avian suprachiasmatic astrocytes themselves have not been studied functionally, experiments in our laboratory have utilized astrocyte cultures from the chick diencephalon, which includes the suprachiasmatic region. These diencephalic astrocytes are gap junctionally coupled and they send signals via intercellular calcium waves (Peters et al., 2005), similar to the situation in mammals. These astrocytes also possess melatonin receptors, and their functional properties are affected by melatonin administration. First, melatonin increases resting intracellular calcium levels. Second, melatonin enhances the spread of

intercellular calcium waves. Third, melatonin administration decreases the degree of gap junctional coupling among diencephalic astrocytes (Peters et al., 2005). This third finding is counterintuitive, given that calcium wave spread is enhanced, and may be explained in one of three ways: 1) a functional switch results in the use of alternative mechanisms for calcium wave spread, 2) gap junctional efficiency is enhanced despite their lowered expression or 3) this is an *in vitro* phenomenon that will not hold true in *in vivo* studies. Given these data, it is likely that the astrocytic bridge is modulated by melatonin. This contention is supported by the finding that glucose metabolism in cultured diencephalic chick astrocytes may be entrained by melatonin cycles (Adachi et al., 2002). Given the current data, it is not possible to ascribe a specific function to the astrocytic bridge. Future studies involving suprachiasmatic astrocytes may provide further insight into their mechanism of action.

Both the mSCN and vSCN have been implicated in the literature as circadian pacemakers. Our model suggests that the mSCN drives locomotor activity and body temperature rhythms, based on lesion studies (Ebihara et al., 1987; Yoshimura et al., 2001). Meanwhile, the vSCN regulates choroidal blood flow via the medial nucleus of Edinger-Westphal (Gamlin et al., 1982; Fitzgerald et al., 1990; Reiner et al., 1990; Chapter III, Chapter V), visual function (Wu et al., 2000; McGoogan and Cassone, 1999; Chapter III) and pineal melatonin secretion via the sympathetic autonomic nervous system (Cassone et al., 1990). Pineal melatonin then has a variety of downstream effects, which likely includes modulation of the astrocytic bridge.

The question of homology

Homology exists when a property of two or more taxa is found in a common ancestor or when one is derived serially from the other (Northcutt, 1984). There is a paucity of information concerning the SCN over the full range of mammalian taxa; indeed, most circadian research has focused upon just three rodent species—the rat, *Rattus norvegicus*, the hamster, *Mesocricetus auratus*, and the mouse, *Mus musculus*. What information there is suggests that, by retinal input and antigen distribution alone, the vSCN is the homolog of the mammalian SCN; however, functional studies suggest a role for both structures. More information regarding the non-eutherian mammalian SCN is required before homology may be credited to any avian structure. Further study of the reptilian SCN may also provide invaluable information for tackling the question of homology. It is clear, however, that the mSCN and vSCN are involved in the circadian system, homologs or not.

CHAPTER V

DATA INDICATE THAT INTRAVITREAL INJECTION OF PSEUDORABIES VIRUS BARTHA RETROGRADELY INFECTS THE SUPRACHIASMATIC COMPLEX OF THE CHICK

INTRODUCTION

Many aspects of vertebrate ocular physiology are regulated by the parasympathetic autonomic nervous system, including pupilloconstriction, accommodation and choroidal blood flow (Marwitt et al., 1971; Erichsen and May, 2002; Ruskell, 1971). In mammals, preganglionic fibers from the nucleus of Edinger-Westphal (EW) travel with the oculomotor nerve and synapse in neurons of the ciliary ganglion, which send postganglionic fibers to the ciliary body and smooth muscles of the iris (Erichsen and May, 2002). Choroidal blood flow is regulated via a multisynaptic pathway involving the hypothalamic paraventricular nucleus, the superior salivatory nucleus and the pterygopalatine ganglion, from which postganglionic fibers to the choroid arise (cf. Smeraski et al., 2004). In birds, EW has two subdivisions (Cowan and Wenger, 1968; Narayanan and Narayanan, 1976). The medial aspect of EW is called EWm, while the lateral part is EWl. Preganglionic fibers from EWm synapse on choroid neurons in the ciliary ganglion, the postsynaptic fibers of which innervate blood vessels of the choroid (Reiner et al., 1983; Meriney and Pilar, 1987). Preganglionic fibers from EWl synapse on ciliary neurons in the ciliary ganglion and, similar to the situation in

mammals, postganglionic fibers innervate the ciliary body and iris (Martin and Pilar, 1963; Hess, 1965, 1966; Marwitt et al., 1971).

In previous chapters, a working model of the suprachiasmatic complex, involving two central structures, was developed. Data presented in this document and in the literature have indicated a role for both the visual suprachiasmatic nucleus (vSCN) and the medial suprachiasmatic nucleus (mSCN) in the avian circadian system. In the pigeon, the vSCN is involved in the regulation of choroidal blood flow. Horseradish peroxidase injections to EW retrogradely label cells in the contralateral vSCN and autoradiographic visualization of tritiated proline tract tracing from the vSCN identified a terminal field specifically in EWm (Gamlin et al., 1982). This terminal field corresponds to a substance P-like immunoreactive (SubP-LI) fiber plexus (Gamlin et al., 1982). The pigeon vSCN contains abundant SubP-LI cells (Gamlin et al., 1982) distributed similarly to those found in the chick (Chapter IV). Further, bilateral lesion of the vSCN eliminates the presence of the SubP-LI fiber plexus in EWm, suggesting that SubP is the neurotransmitter involved in this pathway (Gamlin et al., 1982). Studies involving stimulation of the vSCN (Reiner et al., 1990), as well as stimulation or lesion of EWm (Fitzgerald et al., 1990), clearly demonstrate their roles in the regulation of choroidal blood flow.

A similar regulatory pathway in mammals has been suggested by studies using Pseudorabies virus Bartha, an attenuated live viral strain capable of transsynaptically infecting CNS structures after peripheral application or injection into the CNS (Card et al., 1991). Intravitreal injection results in infection of a few retinorecipient structures,

including the SCN, intergeniculate leaflet, olivary pretectal nucleus and lateral terminal nucleus. This limited infection was initially attributed to restricted tropism to a subset of retinal ganglion cells, resulting in limited anterograde transport (Card et al., 1991). Genetic analysis, however, indicated this might not be the case (Brideau et al., 2000; Husak et al., 2000; Tomishima and Enquist, 2001). It was discovered that PRV Bartha infects structures by retrograde transport via autonomic circuits to the eye (Pickard et al., 2002). These data suggest that the SCN may modulate EW activity, similar to the situation in pigeons. However, because of the mammalian EW differs from birds both organizationally and functionally, SCN input to EW would play a modulatory role in pupilloconstriction and accommodation (Smeraski et al., 2004).

The purpose of this study was to combine the PRV tract tracing technique with an avian model to determine the course of retrograde infection to the suprachiasmatic complex through autonomic circuits, with specific emphasis on the timing of infection of the mSCN and the vSCN. In Chapter IV, vSCN efferents to EWm were identified and we hypothesized that the vSCN was involved in the regulation of choroidal blood flow, similar to pigeons. The data presented here support that hypothesis and suggest a future use for PRV tract tracing.

MATERIALS AND METHODS

Recombinant virus

A recombinant strain of PRV constructed to express EGFP, designated PRV-152, was used in this study. Homologous recombination of a plasmid possessing an EGFP

expression cassette cloned into the PRV gG gene and the PRV genome was used to produce this strain (Smith et al., 2000). Viruses were grown in pig kidney cells and stored at –80^{o}C. The final titer was 1 x 10^{8} pfu.

Intraocular injections

Fertilized eggs were obtained from Hy-Line Hatcheries (Bryan, TX) on embryonic day 9 and were kept in a humidified incubator at 37^{o}C for the duration of the experiment. Eggs were candled to locate the embryo and a small portion of the shell and outer shell membrane were removed above it. The hole in the shell was sealed with cellophane tape and the eggs were maintained in the incubator. On embryonic day 12, the tape was removed and two small holes were made in the chorioallantoic membrane. The embryo was secured with a fine hook and 2 μl PRV-152 was injected slowly into the vitreous chamber of one eye with a 10 μl Hamilton syringe. The syringe was left in place for at least one minute to prevent leakage. The hole in the shell was sealed and the egg was placed back into the incubator.

Tissue preparation and immunohistochemistry

Embryos (n=1 per timepoint) were removed from their shells and brains were taken at eight-hour time intervals, beginning at 48 hours post-injection until 96 hours post-injection. Brains were fixed at 4^{o}C in 4% paraformaldehyde in 0.1M phosphate buffer for sixteen hours and were then flash-frozen and stored at –80^{o}C in 2-methylbutane until use. Brains were sectioned frontally at 30 μm on a Lipshaw cryostat

(Pittsburgh, PA) and sections were collected in 10 mM phosphate buffered saline (PBS). Briefly, sections were incubated in 30% methanol and 0.75% hydrogen peroxide in PBS for 15 minutes, followed by a 15-minute incubation in 0.5% sodium borohydride in PBS to inhibit endogenous peroxidase activity. They were then blocked in PBS containing 0.3% Triton-X-100 and 1% normal goat serum (PBSGT) for one hour and then incubated in rabbit anti-PRV antibody (1:1000; Dr. J. Patrick Card, University of Pittsburgh) in PBSGT for 48 hours at 4^{o}C. Sections were incubated in biotinylated goat anti-rabbit secondary antibody (1:200; Vector Laboratories, Burlingame, CA) in PBSGT for two hours at room temperature followed by 90 minutes in avidin-biotin complex from a peroxidase standard kit (1:55; Vector Laboratories, Burlingame, CA) in PBSGT. Sections were incubated in 0.5% 3-3'-diaminobenzidine solution in 100 mM Tris buffer for five minutes after which 0.21% hydrogen peroxide was added to the solution. The color reaction was stopped once background coloration became evident. Sections were rinsed, mounted onto gelatin-coated slides and dried overnight. The slides were then rinsed in PBS and the color reaction was stabilized in 1% cobalt chloride solution. The slides were rinsed, dehydrated, cleared and coverslipped for analysis.

Microscopy and photography

An Olympus BH-2 light microscope (Melville, NY) with differential interference contrast optics was used to examine brain tissue. Photomicrographs were taken with an Olympus C-35AD-4 camera on Kodak Gold 200 film (Eastman Kodak Company, Rochester, NY). Prints were scanned at 300 DPI and opened in Adobe Photoshop 7.0.1

(Adobe Systems, Mountain View, CA), where they received minor brightness and contrast adjustments.

RESULTS

Many structures were infected within the time period in which samples were taken for analysis. A summary of the structures identified is available in Table 7. Structures reported in the results will be limited to those relevant to the central question of this study and are only reported at the time they were first identified. In no case was a structure infected at one time and not infected at all subsequent times. Initial label in each structure is relatively sparse, with the exception of EW and the vSCN, as described below. In general, signal strength in each infected structure intensifies over time. There are a few exceptions to this rule in these data, which may be directly attributed to the low sample size taken in this study. Further experiments with a larger sample size will need to be carried out for quantitative analysis to be meaningful. It is also important to note that all staining is visible bilaterally due to the strong interconnections of symmetrical structures, including EW.

Forty-eight hours post-injection, strong label was evident in EW (Fig. 24A). Retinorecipient structures infected at this time were the vSCN, which was moderately labeled (Fig. 24B), and the nucleus of the basal optic root (nBor; Fig. 24E). Several vSCN afferents were also labeled, including nBor, the ventral tegmental area (AVT), the external cellular layer (SCE) and the oculomotor nuclei and tract (OM). The only mSCN efferent infected was the vSCN; however, several structures that are both afferent

TABLE 7. Structures infected after intravitreal PRV Bartha injection

Structure	96h	88h	80h	72h	64h	48h
Telencephalon						
AA	+					
AId	+					
FPL	+	+				
INP	+	+				
nBSTL	+	+	+	+	+	
nBSTM	+	+	+	+		
PSV	+	+				
QF	+	+	+	+	+	+
Diencephalon						
Preoptic area						
MPO	+	+	+	+		
POM	+	+	+			
POP	+	+				
SOe	+	+				
Hypothalamus						
AM	+	+				
DMN	+	+	+	+		
IH	+	+	+	+		
IN	+	+	+			
LHy	+	+				
MM	+	+	+	+		
mSCN	+	+				
PVN	+	+	+	+	+	+
vSCN	+	+	+	+	+	+
Thalamus						
AL	+	+	+	+	+	
DLAlr	+	+	+			
GLd	+	+	+			
GLv	+	+	+	+		
ICT	+	+	+	+		
nCPa	+	+	+	+		
OV	+	+	+	+		
PVT	+	+	+	+	+	+
TT	+	+	+			
VLT	+	+	+	+		
Pretectum						
AP	+	+	+	+		
LM	+	+	+			
PPC	+	+	+			
pRot	+	+	+			
PTM	+	+	+			
SpL	+	+				
SpM	+					

TABLE 7 continued.

Structure	96h	88h	80h	72h	64h	48h
Mesencephalon						
AVT	+	+	+	+	+	+
EW	+	+	+	+	+	+
FLM	+	+	+	+	+	+
FRL	+	+	+	+		
FRM	+	+	+	+		
GCt	+	+	+	+	+	
ICo	+	+	+	+		
Imc	+	+	+			
IO	+	+	+	+		
Ipc	+	+				
LoC	+	+	+	+	+	
MLd	+	+	+	+		
nBor	+	+	+	+	+	+
OM	+	+	+	+	+	+
PPT	+	+	+	+	+	+
Ru	+	+	+	+	+	+
SAC	+	+	+	+	+	+
SCE	+	+	+	+	+	+
SCv	+	+	+	+	+	
SGC	+	+	+			
SGFS	+	+	+	+		
SGP	+	+	+	+	+	
TPc	+	+	+	+	+	+
TVM	+	+	+	+	+	+
Rhombencephalon						
CS	+	+	+	+		
Pap	+	+	+	+		
PL	+	+	+	+		

PRV infection of a structure as indicated by immunohistochemistry is indicated by a +. Absence of PRV immunoreactivity is indicated by a blank space. For abbreviations, see list.

to the vSCN and efferent from the mSCN were labeled, including the thalamic paraventricular nucleus (PVT; Fig. 24C), the hypothalamic paraventricular nucleus (PVN; Fig. 24D) and the central album layer of the optic tectum (SAC).

The brain collected 56 hours post-injection did not fix well, and therefore, no useful information could be obtained from these sections. Upon observing sections from 64 hours post-injection, it was evident that only a few more structures had been infected

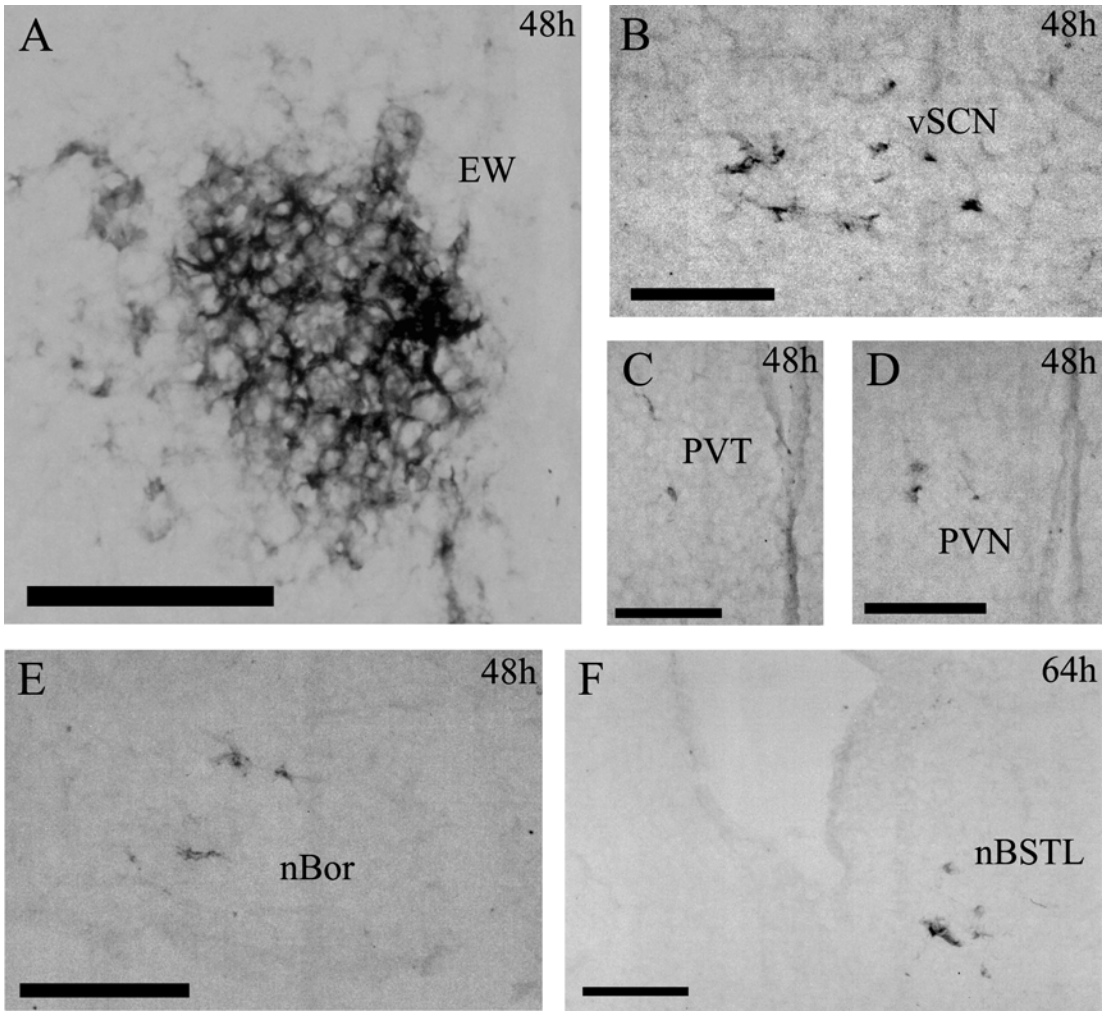

Fig. 24. PRV infection of structures 48 and 64 hours post-injection. **A** shows strong staining of EW, with **B** moderate staining of vSCN. Sparse staining is seen in all other structures. Scale bars: 400 μm.

in the intervening period of time. Two additional vSCN afferents, locus coeruleus (LoC) and the periventricular gray layer of the optic tectum (SGP), were infected. The lateral bed nucleus of the stria terminalis (nBSTL; Fig. 24F), an mSCN efferent, was labeled, as was the central gray (GCt), which is both a vSCN afferent and an mSCN efferent.

There was a large increase in the number of infected structures found 72 hours post-injection. Four retinorecipient structures were infected, including the ventrolateral thalamic nucleus (VLT; Fig. 25E), the ventrolateral geniculate nucleus (GLv; Fig. 25A), the superficial gray and fiber layer of the optic tectum (SGFS) and the pretectal area (AP). vSCN afferents infected included VLT, GLv and SGFS, as well as the intercalated nucleus (ICT), ansa lenticularis (AL) and the papillioform nucleus (Pap). Also infected were the mSCN efferent medial bed nucleus of the stria terminalis (nBSTM; Fig. 25D), dorsomedial nucleus (DMN; Fig. 25B) and medial mamillary nucleus (MM). Also infected were AP, the bed nucleus of the pallial commissure (nCPa) and the inferior hypothalamic nucleus (IH; Fig. 25B), which are both mSCN efferents and vSCN afferents.

Retinorecipient structures infected 80 hours post-injection included the rostrolateral part of the dorsolateral anterior nucleus (DLAlr; Fig. 26C), the mesencephalic lentiform nucleus (LM), the dorsolateral geniculate nucleus (GLd; Fig. 26D) and the perirotundal area (pRot; Fig. 26D), which is both a vSCN afferent and an mSCN efferent. vSCN afferents that were infected include LM and GLd, as well as the principal precommissural nucleus (PPC; Fig. 26D) and the central gray layer of the optic

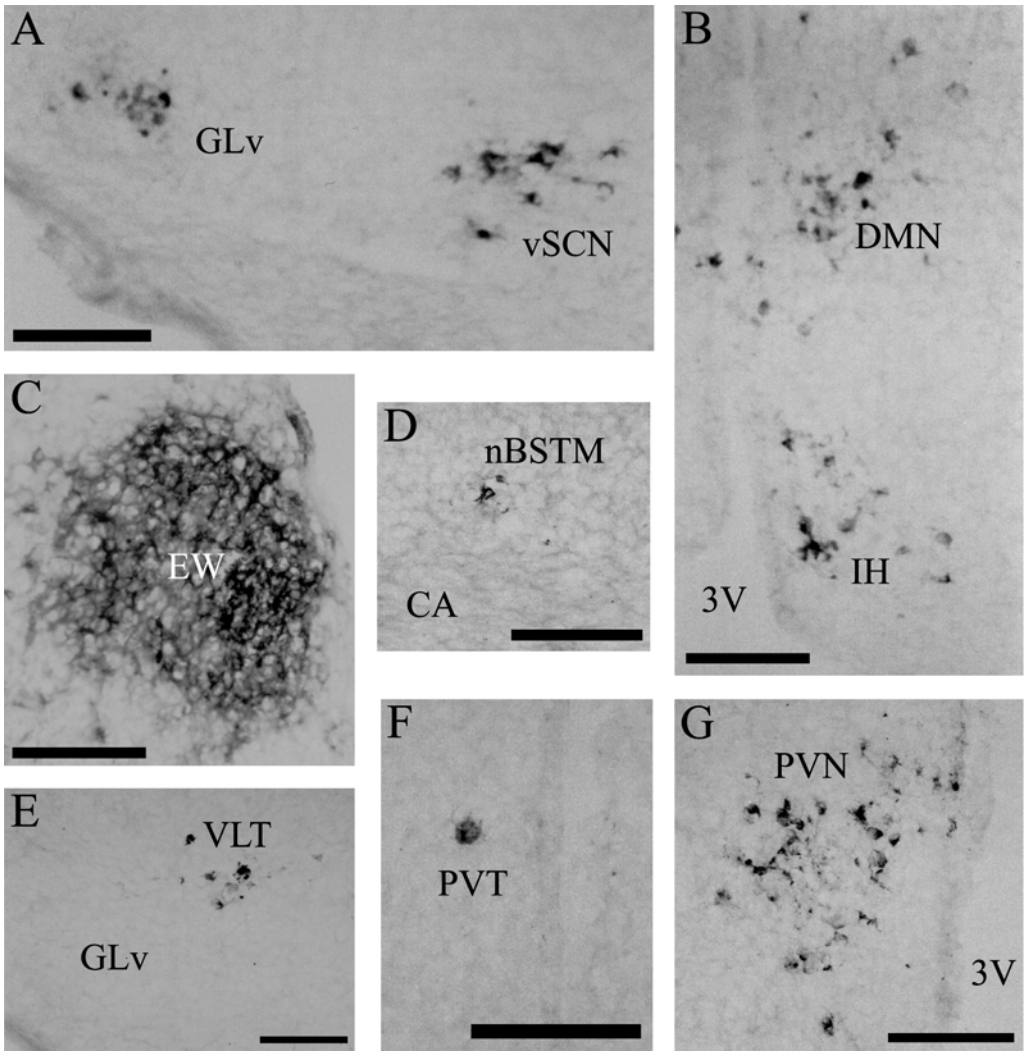

Fig. 25. PRV infection of structures 72 hours post-injection. **A** Note the stain in vSCN remains moderate, as should be expected based on the distribution of SubP cells in the adult vSCN. Glv infection is irregular. **C** EW infection has increased within the nucleus. **F** In this case, PVT staining is more sparse than before. This is likely due to variability in the progression of the infection in different birds. This effect would be minimized by a higher sample size. **G** PVN staining is abundant. Scale bars: 400 μm.

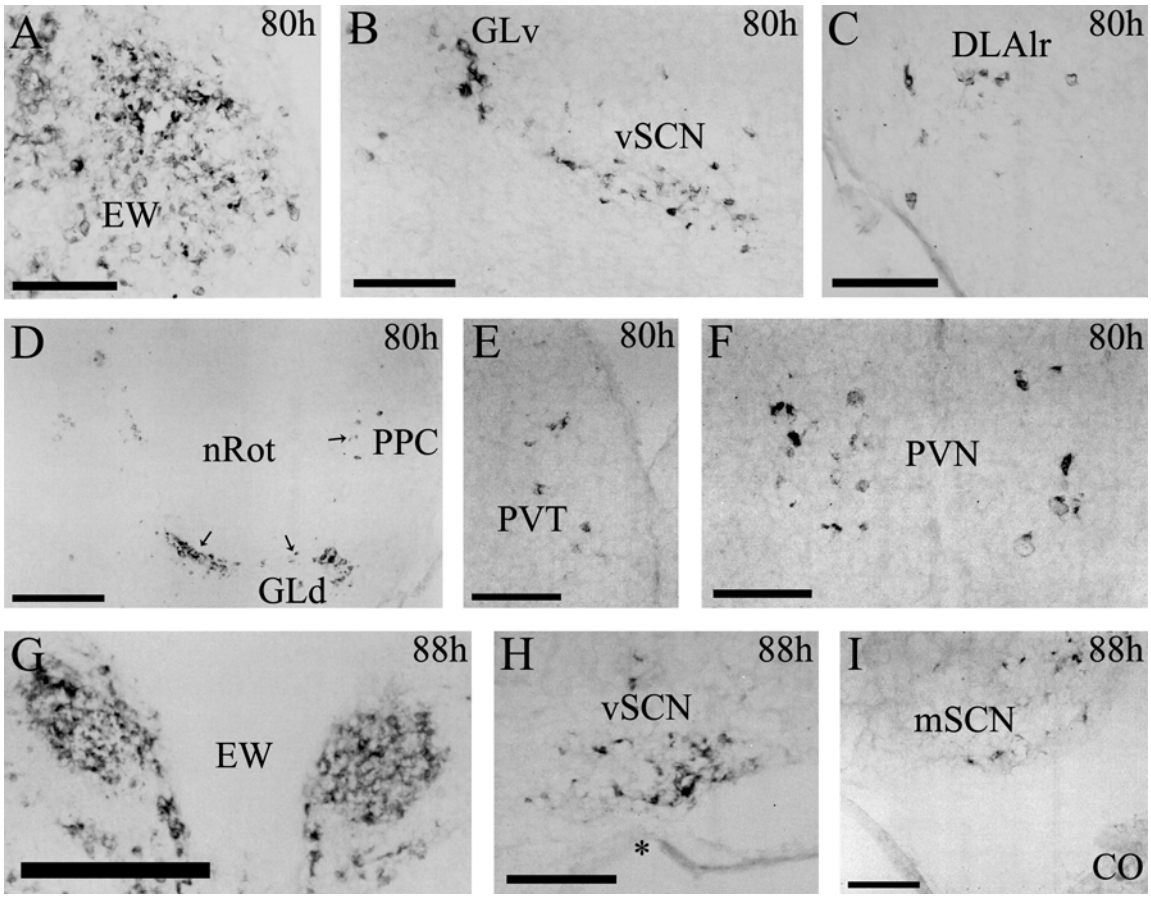

Fig. 26. PRV infection of structures 80 and 88 hours post-injection. **A** At 80h post-injection, neurons in EW are beginning to die and become necrotic, leading to a more punctate, less cellular appearance. **B** The moderate staining of vSCN remains steady. **D** Perirotundal staining is indicated by the black arrows. **E** PVT infection is again more prevalent, however, **F** PVN staining now appears less abundant than it was at 72h, again, likely due to differential progression of the virus. Shown here is bilateral staining, very common due to the amount of crosstalk between the structures involved. **G** Also showing bilateral staining is EW. The left nucleus is ipsilateral to the injection, and is degenerating faster than the nucleus on the right. **H** The vSCN remains constant in its infection state. An artifact of tissue mounting is indicated by the asterisk (*). **I** Staining is now visible in mSCN. Scale bars: A-C,E,F,H,I, 400mm; D,G, 1mm.

tectum (SGC). The infundibular nucleus (IN), an mSCN efferent, also stained positive for PRV.

Eighty-eight hours post-injection, fewer structures of interest were infected. The mSCN (Fig. 26I), a vSCN afferent, was labeled. Also labeled were the anterior hypothalamic nucleus (AM) and the lateral hypothalamic area (LHy), which are both mSCN efferents and vSCN afferents. Eight hours later, at 96 hours post-injection, most of the additional infected structures were found within the brainstem, and none of them are central to the discussion of the material.

DISCUSSION

The data presented here support the hypothesis that the chick vSCN is involved in regulation of choroidal blood flow. Further, the timing of infection indicates that the mSCN plays no direct role in parasympathetic regulation of ocular physiology. The findings here indicate a use for PRV tracing in developmental studies.

Infection of the vSCN occurred within 48 hours of injection, and reached its apparent maximal level by 72 hours post-injection. Subsequent infection of vSCN afferents, identified in Chapter III and enumerated above, supports much of that previously reported tract-tracing data. The rate of chick vSCN infection is much faster than the infection rate in the mammalian SCN: cells are first seen on the dorsolateral border of the SCN of hamsters at 48-72 hours post-injection and are not seen in the SCN proper until 72-96 hours post-injection (Smeraski et al., 2004; Pickard et al., 2002). This difference may be attributed to differences between model animals. In this preliminary

study, embryonic chicks were employed, whereas mammalian studies have used 12-20 week old rodents. In initial trials with PRV injection, we attempted to inject post-hatch chicks, as early as the day of hatching, but the virus was cleared from the nervous system without ever being visible. Therefore, for future studies utilizing tract-tracing methods in embryonic chicks, a quicker time course is required. Indeed, another group studying the embryonic chick retinohypothalamic tract using HRP conjugated wheat germ agglutinin injections took their first sample only six hours after injection (Shimizu et al., 1984). Interestingly, in the aforementioned study, the authors found that retinal terminals were not visible in the vSCN until embryonic day 15 (E15), and usually E16 (Shimizu et al., 1984). In the work presented here, a different pathway was exploited and the vSCN was identified at E14. Further, the already moderate label present in the vSCN 48 hours post-injection suggests that it may be visible even earlier. These data indicate that antigen distribution in the vSCN may develop in part before the development of retinal input. PRV tracing of the vSCN via EW in conjunction with other *in ovo* experiments could therefore be invaluable to future studies concerning the timeline of development of vSCN antigenicity and synaptic connections.

Infection of mSCN was not evident until 88 hours post-infection, suggesting that there is no direct neuronal connection between mSCN and EW, which is supported by the work presented in Chapter III. In that chapter, bilateral and bidirectional communication between vSCN and mSCN was also demonstrated. Many other structures efferent to mSCN were also infected prior to or concurrently with mSCN, as is outlined above. These structures in concert with the vSCN likely contributed to the

retrograde, transsynaptic pattern of infection that finally effected mSCN. Overall, these findings support the pigeon data showing that the vSCN functions in the suprachiasmatic role of modulating parasympathetic input to the eye.

As was found in mammals (Smeraski et al., 2004; Pickard et al., 2002), a subset of retinorecipient structures was infected, indicating that these structures may be worthy of study in future work regarding EW regulation. No absolute comparison to mammals may be made because the details of the mammalian SCN input to EW have not yet been established. However, it is clear that, if the suprachiasmatic regulation of EW is similar in birds and mammals, the ultimate effect of that regulation is likely different due to differences in parasympathetic wiring.

As a whole, EW in the pigeon is responsible for several aspects of ocular physiology (Marwitt et al., 1971). Taken separately, EWm is responsible for modulation of choroidal blood flow and EWl regulates pupilloconstriction and accommodation (cf. Gamlin and Reiner, 1991). In pigeons, the vSCN projects to EWm only, suggesting a role for the vSCN in regulation of choroidal blood flow (Fitzgerald et al., 1990). As is found in the pigeon, there are medial and lateral subdivisions of chick EW (Fujii, 1992), which have the same efferent connections (cf. Fujii and Lucaj, 1993). As was discussed previously, the projection from the pigeon vSCN to EWm appears to utilize the neurotransmitter SubP. As was reported in Chapter IV, SubP-LI neurons are present in the chick vSCN; however, the antigen distribution of EW has not been reported. Further, in Chapter III, it was shown that the vSCN sends efferents to EWm of the chick.

Despite the lack of data regarding chick EW antigen distribution, it is likely that the chick vSCN projects to EWm, similar to the pigeon.

The data presented, therefore, support out previously stated hypothesis (Chapter III) that the vSCN is involved in the regulation of choroidal blood flow via EWm and the ciliary ganglion, but offer no new information in this regard. Determining the distribution of SubP terminal fibers in EW would be a fairly simple way of supporting this hypothesis. With additional confirmation of this pathway in chick through tract tracing experiments that include injections to EW, one could reasonably expect the pigeon and chick pathways to be functionally homologous.

CHAPTER VI

CONCLUSIONS

SCN function and organization clearly differ between avian and mammalian species. Studies in mammals have indicated that the SCN is the primary pacemaker in the circadian system (cf. Moore et al., 2002). In contrast, birds have multiple central oscillators and pacemakers, which include the pineal gland, the retinae and a hypothalamic oscillator, presumed to be homologous to the mammalian SCN (cf. Cassone and Moore, 1987). The location of this avian hypothalamic oscillator has been the subject of debate for over twenty years. Two structures have been suggested in the literature—the mSCN and the vSCN. The data presented in this dissertation has been synthesized with data published by other groups into a working model of the avian SCN so that the debate may be taken in a new direction and allow more focused study of the avian suprachiasmatic nucleus.

The work presented here focused on one central question: where is the avian homolog to the mammalian SCN? This question was addressed using classic methods previously employed in mammalian species, which leads one to wonder, what is the advantage of taking this approach in birds? There are several developmental, organizational and functional properties of birds that make them a suitable model for circadian rhythms research. First and foremost, their visual sense is more similar to that of humans than the nocturnal rodents that are primarily studied in mammalian circadian literature. Most bird species are diurnal and rely upon cone-mediate color vision in light

conditions, as do humans, rather than relying upon rod-dominated vision, as do nocturnal rodents (Bowmaker et al., 1997). Second, whereas the desire to perform genetic studies once precluded the use of an avian model, techniques have been developed to allow such experimentation. Third, functionally the avian circadian system provides a rare ability to study multiple oscillatory structures individually and as a unit. Single structures may be lesioned or removed in order to assess the effect on the system as a whole. Further, the pineal and retinae may be easily maintained as either whole organ or dispersed cell cultures, allowing a multitude of *in vitro* studies to study specific clock functions unique to these pacemakers. While the vSCN has been successfully maintained in a slice culture (Juss et al., 1994), there have been no reported cultures of the mSCN. The further development of SCN culture systems remains an intriguing possibility. Finally, avian species provide us with a unique opportunity to conduct developmental studies by performing invasive procedures on embryos, an ability that was utilized in Chapter V. Intravitreal injection of pseudorabies virus Bartha in chicks at embryonic day 12 (E12) resulted in the retrograde label of the vSCN, via EWm, within 48 hours of injection. Previous studies failed to identify the embryonic vSCN until E15; however, by exploring a retrograde neuronal pathway, the vSCN was visible at E14. The strength of the staining in the vSCN indicates that it may be visible even earlier in development. This exciting finding demonstrates that a fundamental understanding of the avian circadian system may lead to valuable experiments that are not feasible in placental vertebrates.

The results reported in Chapter II indicate that both the vSCN and mSCN are involved in the avian circadian system. The vSCN displays both a daily and circadian

rhythm of 2DG uptake such that it is high during the day/subjective day, similar to the situation in the mammalian SCN (Schwartz and Gainer, 1977, Schwartz et al., 1980) and the sparrow vSCN (Cassone, 1988). The amplitude of this rhythm is significantly decreased when birds are placed into constant darkness (DD), suggesting that light may directly regulate the vSCN. Further, melatonin inhibits daytime uptake, which also occurs in the mammalian SCN (Cassone et al., 1988a) and the sparrow vSCN (Cassone and Brooks, 1991). This result indicates that melatonin interacts with the vSCN, a consideration that is supported by the discoveries that 2[^{125}I]iodomelatonin (IMEL), a melatonin agonist, binds strongly to the chick vSCN (Brooks and Cassone, 1992; Cassone et al., 1995; Rivkees et al., 1989) and that rhythmic melatonin administration to sparrows in DD entrains 2DG uptake in the vSCN (Lu and Cassone, 1993b). Interestingly, the mSCN displays a statistically significant circadian, but not daily, rhythm of 2DG uptake. It is possible that this finding is indicative of a unique role of the mSCN in the circadian system. Alternatively, given a larger sample size, the visible trend in daily mSCN 2DG uptake may be significant. Uptake is not rhythmic in the sparrow mSCN (Cassone, 1988), which is different from the situation in chicks. This finding suggests that there may be variability in the importance of these structures in different species of birds, similar to findings regarding the pineal and retinae.

Our results further indicate that the circadian system is involved in the regulation of visual function at many levels of sensory integration. All visual structures observed in the current study displayed rhythmic uptake of 2DG in LD conditions, while two—the optic tectum (TeO) and the nucleus of Edinger-Westphal (EW)—showed circadian

rhythmicity. Metabolic activity is also rhythmic in visual structures of the house sparrow (Lu and Cassone, 1993b). The observation that IMEL binding (Rivkees et al., 1989; Cassone and Brooks, 1991; Cassone et al., 1995) and melatonin receptor mRNA expression (Reppert et al., 1995) are prevalent in chick visual system structures supports a role for the circadian system in the regulation of vision.

Data in Chapter III demonstrate that both the mSCN and vSCN share common efferents and afferents with the mammalian SCN. Indeed, the two structures together are more similar in their pattern of connectivity than either structure individually. The mSCN efferents identified were more similar to those of the mammalian SCN than those of the vSCN. First, efferents to the septal lateral nucleus (SL) and the lateral bed nucleus of the stria terminalis (nBSTL) are closely apposed to the ventral portion of the lateral ventricle, where the lateral septal organ (LSO), a putative encephalic photoreceptor, is located (Vigh-Teichmann et al., 1980; Silver et al., 1988; Kuenzel, 1993; Li et al., 2004; Rathinam and Kuenzel, 2005). Efferents to the hypothalamic paraventricular nucleus (PVN) not only bear striking similarity to mammalian SCN efferents to that same nucleus, but the caudal portion of that nucleus is also in close proximity to another putative encephalic photoreceptor, the periventricular organ (PVO). Efferents to the hypothalamic dorsomedial nucleus (DMN) are also apposed to PVO. Further, there is strong efferent input from mSCN to the habenula, which is associated with pineal gland function, suggesting a possible pathway for suprachiasmatic regulation of pineal function. The vSCN has only one efferent connection in common with the mammalian SCN, and that is to the putative ventrolateral preoptic nucleus (VLPO)

homolog, which in mammals is responsible for sleep-wake regulation (Lu et al., 2000), and which was identified here on the basis of retinal input and GABA immunoreactivity. The vSCN also sends efferents to the medial part of the nucleus of Edinger-Westphal (EWm). While this efferent has not been described in mammals, indirect evidence obtained by means of retrograde pseudorabies virus transsynaptic tracing via autonomic circuits to the eye indicates a connection between EW and the SCN. Whether this connection is multisynaptic or direct is unknown (Pickard et al., 2002). A direct neuronal efferent from vSCN to EWm has been well described (Gamlin et al., 1982) and functionally demonstrated (Fitzgerald et al., 1990; Reiner et al., 1990) in pigeons, where it is involved in regulation of choroidal blood flow. Importantly, the efferent data suggest that the mSCN and vSCN communicate with one another bilaterally, bidirectionally and asymmetrically such that the mSCN receives more input from the vSCN than it sends back. This finding supports the contention that both structures are involved in the circadian system. Finally, both the vSCN and mSCN send efferents to the perirotundal area, which is homologous to the mammalian intergeniculate leaflet (IGL). The IGL is the only visually active efferent structure from the mammalian SCN. It is not, however, the only visual efferent of the mSCN or the vSCN.

Those efferents that are dissimilar from mammalian SCN efferents support the hypothesis that the circadian system is involved in the regulation of visual function. The mSCN sends efferents to a few structures associated with the tectofugal visual pathway, indicating a minor role in visual regulation. The vSCN, on the other hand, sends abundant efferents to structures of the tectofugal, thalamofugal and accessory optic

visual pathways. Functional data also support a role for the circadian system in visual regulation. Tectal visually evoked potential and electroretinogram (ERG) parameters are rhythmic in pigeons (Wu et al., 2000) and, in chicks, ERG parameters display circadian rhythmicity (McGoogan and Cassone, 1999).

The primary afferent to the mammalian SCN is the retinohypothalamic tract, which arises from retinal ganglion cells (RGCs) that are distributed throughout both retinae (Pickard, 1982). In contrast, the chick RHT is completely contralateral, terminating as a dense field in the vSCN and sending a sparse projection to the mSCN , which contains relatively few terminal fibers. The RGCs that give rise to the chick retinohypothalamic tract (RHT) are located within the dorsal region of the retinae, in stark contrast to the situation in mammals. This finding is interesting in light of some efferent data: vSCN efferents to the optic tectum, which is homologous to the mammalian superior colliculus, are localized in its ventral aspect. Because RGCs specifically from the dorsal retina project the ventral superficial gray and fiber layer of the optic tectum (SGFS), one may speculate that, as has been demonstrated in mammals (Morin et al., 2003), retinohypothalamic fibers bifurcate, sending light information to both the vSCN and SGFS. Evidence of retinopetal cells in the vSCN was also found in this study; however, the pigments in the retinae created too much background illumination under dark field to identify any terminal fibers after anterograde tracer injection into the vSCN, prohibiting verification of the projection. More study is required to validate this finding, although it is appealing to speculate that the vSCN plays a role in the modulation of its own input.

As was the case with efferents, the afferents of the mSCN and vSCN are more numerous than those of the mammalian SCN. The mSCN has several afferent structures in common with the mammalian SCN, including SL. nBSTL, DMN and the medial mammillary nucleus are also afferent to the mSCN and, while they are not mammalian SCN afferents, they are interesting because they represent putative pathways through which encephalic photoreceptors (EPRs) may send light information to the mSCN. The vSCN has several afferents in common with the mammalian SCN, including the ventrolateral geniculate nucleus (GLv), homologous to the mammalian lateral geniculate nucleus, which is the origin of the geniculohypothalamic tract (GHT) that terminates in the mammalian SCN (Card and Moore, 1982, 1989; Moore et al., 1984; Harrington et al., 1985; Moore and Speh, 1993; Moore and Card, 1994). This connection was confirmed by a CTB injection to the GLv, which labeled afferent fibers to the vSCN. Other visual structures in the pretectum are afferent to both the vSCN and the mammalian SCN, as is SGFS. As was found with its efferents, many vSCN afferents are visually active. These data indicate that the visual system may also modulate the circadian system. Both the vSCN and mSCN share afferents to several hypothalamic nuclei, including PVN, also a mammalian afferent, the caudal region of which is in close proximity to PVO. Finally, afferent data verified the existence of bilateral and bidirectional communication between the mSCN and vSCN. These pathways are asymmetrical in that the mSCN sends less information to vSCN than it receives. While the particulars of this association are dissimilar from the relationship between the mammalian SCN core and shell, in which the core sends efferents to the shell, while the

shell does not reciprocate (Abrahamson and Moore, 2001; Leak and Moore, 2001; Kriegsfeld et al., 2004), the overall design is reminiscent of the situation in rodents.

Together, the vSCN and mSCN are very similar in their synaptic connections to the mammalian SCN. Further, there is significant overlap in their interconnections, as has been shown with the core and shell of the mammalian SCN. It is important to note that, with the exception of a few of these connections, the efferents and afferents identified in these studies have not been confirmed by reciprocal injection into each structure. While it is possible to construct hypotheses from these findings, careful study is necessary in order to draw conclusions specific to each structure.

The data presented here, when taken into the context of what is known from the literature about the mSCN and vSCN, allowed the development of a working model of the avian suprachiasmatic nucleus (Fig. 27). According to this model, there are three inputs for light to the avian suprachiasmatic nucleus. The first is via the RHT to the vSCN, which has been identified in this document and many others, and, to a lesser degree, the mSCN, which has also been reported to receive retinal input in a variety of avian species. The second is the GHT, which was identified and confirmed here. Studies to verify the functional identity of this connection must be performed to substantiate this claim. The third input for light, and the most speculative portion of the model, is the transduction of light information via the EPRs to the mSCN. In the quail mSCN, *per2* expression is typically low at night. Birds whose eyes had been covered with opaque rubber caps were given a one-hour pulse of light in the middle of the night. This light pulse induced *per2* expression in the mSCN at a time when it would not

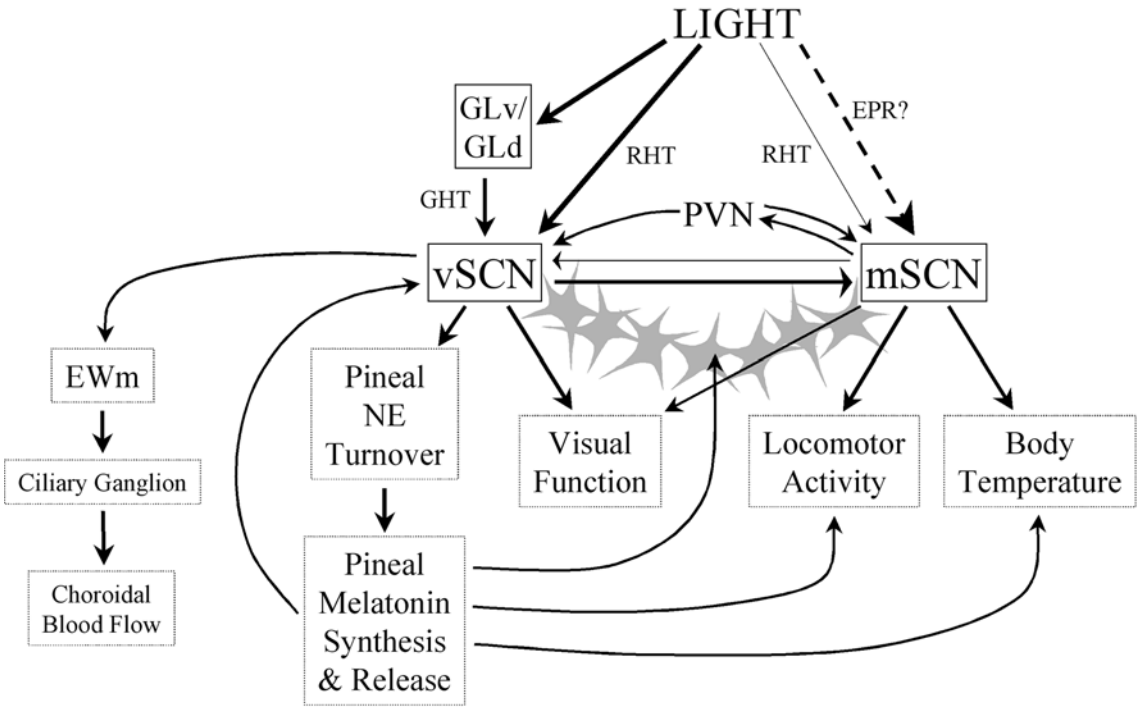

Fig. 27. A current working model of the avian SCN. This model addresses input pathways of light to the avian SCN and summarizes what we hypothesize are the roles of the vSCN and mSCN in the circadian system. Solid lines represent connections supported by data in this document or in the literature. The dashed line represents a speculative multisynaptic pathway. New to this model is the addition of the PVN and its various interconnections with vSCN and mSCN. For abbreviations, see list.

normally be present, indicating the activation of a light input pathway outside of the optic nerve and, thus, the RHT (Yoshimura et al., 2001). In order to verify this connection between EPRs and the mSCN, several experiments are necessary. First, injection of retrograde tracer to mSCN afferents in close proximity to putative EPRs may identify photoreceptor cells, identifying another afferent in this putative multisynaptic pathway. Second, double label of projections in this putative pathway for opsins would provide supporting evidence for a role in light transmission. Finally, by lesioning putative EPRs and repeating the experiments of Yoshimura et al. (2001), one could seek direct evidence of a link between them and the mSCN.

The central components to the working model of the avian SCN are the vSCN and the mSCN, which communicate bilaterally and bidirectionally (Chapter III). Previous studies have indicated a variety of functions for these structures. Based on lesioning data, I propose that the mSCN is responsible for the circadian regulation of body temperature and locomotor activity rhythms (Ebihara et al., 1987; Yoshimura et al., 2001). Data presented here indicate that the vSCN and mSCN both play a role in the regulation of visual system structures, with the vSCN being most influential. This hypothesis is supported by data from our laboratory, as described previously. I further hypothesize that the vSCN is involved in regulation of choroidal blood flow. This is based on a sparse efferent projection to EWm that indicates a connection similar to a demonatrated efferent in pigeons. The vSCN regulates EWm, which in turn affects choroidal blood flow via the parasympathetic ciliary ganglion (Gamlin et al., 1982; Fitzgerald et al., 1990; Reiner et al., 1990). Data in Chapter V support this hypothesis,

as well. The vSCN was infected within 48 hours of injection with pseudorabies virus Bartha, and was the most extensively infected structure, with the exception of the nucleus of Edinger-Westphal. The mSCN was not infected until 88 hours post-injection, indicating that it is not directly involved in the regulation of ocular physiology. Finally, it has been shown that lesions of the vSCN abolish norepinephrine turnover in the pineal gland, (Cassone et al., 1990) which affects melatonin biosynthesis. Pineal melatonin then has many downstream effects. As was described earlier, melatonin influences glucose metabolism in the vSCN. Melatonin also influences locomotor activity and body temperature rhythms, as was discussed in Chapter I.

Data in Chapter IV indicates that neither the vSCN nor the mSCN are organizationally identical to the mammalian SCN, although the vSCN is similar in many aspects. Cytoarchitectural studies revealed that the mSCN is smaller in diameter and rostrocaudally shorter than the mammalian SCN. Further, its location on the preoptic recess of the third ventricle corresponds only to a region of the mammalian SCN, called the preoptic suprachiasmatic nucleus (Palkovitz & Brownstein, 1988). Autoradiographic detection of tritiated proline indicated that there are no retinal terminals in the mSCN. Further, the mSCN is dissimilar from the mammalian SCN chemoarchitecturally. It contains small, tightly packed cells and fibers, many of which stain positive for antigens not found in the mammalian SCN. Those antigens that are common between the mammalian SCN and the mSCN are not organized within the borders of the mSCN. The exception to this finding is gastrin releasing peptide (GRP), which defines the mSCN well and is not found within the chick vSCN. In contrast, GRP is found in the vSCN of

the house sparrow and in the mammalian SCN, suggesting that perhaps GRP serves variable functions among species or that the mSCN and vSCN are somewhat different in their arrangement, as has been found between rodents and marsupials (Cassone et al., 1988b).

The chick vSCN is organizationally similar to the sparrow vSCN, and bears much more similarity to the mammalian SCN than does the mSCN. The chick vSCN is more lateral and caudal in the hypothalamus than the mSCN and the mammalian SCN. Rostrocaudally, the length of the vSCN is comparable to that of the mammalian SCN. However, the vSCN has a larger mean diameter and total volume than the rat SCN. This finding is consistent with the overall larger size of the chick brain. Retinohypothalamic tracing confirmed that the vSCN is defined by visual input, which fills the structure. Chemoarchitecturally, the vSCN contains a heterogeneous population of cells and fibers in or bordering the nucleus that stain for most antigens found in the mammalian SCN. Antigens absent in the mammalian SCN were also not found in the chick vSCN.

Based on chemoarchitectural data, as well as the efferent and afferent data obtained previously, one may hypothesize that the hypothalamic paraventricular nucleus (PVN) is part of a circuit with the vSCN and mSCN. PVN stands out because of a substantial vasopressin (AVP) immunoreactive fiber plexus that appears to connect it to the dorsal region of the vSCN. It has been shown in rodents that the SCN projects to PVN via AVP fibers (Leak and Moore, 2001; Abrahamson and Moore, 2001). In contrast, the projection observed in the chick appears to originate in PVN itself, as it contains a dense population of AVP immunoreactive cells, whereas the vSCN includes

only sparse AVP neurons insufficient for the formation of such a plexus. Interestingly, AVP immunoreactive cells are present in the mSCN. It is therefore likely that suprachiasmatic input to PVN arises from these cells in the mSCN, while the presence of AVP immunoreactive fibers in the mSCN and vSCN suggest that PVN efferents terminate in both of these structures. This hypothesis is supported by retrograde and anterograde tract tracing data from Chapter III and may be seen schematically in the working model of the avian SCN (Fig. 27). Injection of anterograde and retrograde tracers into the PVN as a part of overall verification of efferents and afferents identified in Chapter III would substantiate this hypothesis. Further, lesion of PVN or, more specifically, severing the fiber plexus between PVN and vSCN, would allow the observation of behavioral outputs and, thus, the collection of functional data that may indicate the purpose of this circuit.

Finally, we hypothesize that the astrocytic bridge, identified immunohistochemically on horizontal sections, plays a role in modulation of the suprachiasmatic nuclei. No neuronal connection was found within the same plane of section, suggesting that the astrocytic bridge is an active structure with a specific function. Most studies regarding suprachiasmatic astrocytes have been performed in rodent studies and they have indicated a possible role for astrocytes in the circadian system. In mammals, GFA is expressed rhythmically in the SCN (Lavialle and Serviere, 1993) and GFA expression may be inhibited by enucleation (Lavialle et al., 2001) or by placing a rodent in constant darkness (Ikeda et al., 2003). These data indicate that light modulates astrocyte morphology. Functionally, astrocytes send local signals within the

SCN in the form of intercellular calcium waves, presumably via gap junctions (van den Pol et al., 1992). In a dispersed SCN cell culture, it was found that astrocytes, and not neurons, are gap junctionally coupled (Welsh and Reppert, 1996). *In vivo*, inhibition of glial metabolism in the SCN leads to behavioral arrhythmicity, while *in vitro*, it has been demonstrated that blockade of gap junctional communication may either phase delay or abolish rhythmic neuronal activity (Prosser et al., 1994). It is important to note, however, that more recent studies have indicated that SCN neurons are indeed gap junctionally coupled (cf. Colwell, 2005) and, therefore, this arrhythmicity could be due to disruption of both neuronal and astrocytic communication. The body of work in rodent species has led researchers to the conclusion that SCN astrocytes play some role in the synchronization of rhythms in the mammalian SCN as a whole; however, this role is not well defined and is likely part of a complex system of interactions that result in the formation of a coordinated signal from the SCN.

The working model of the avian suprachiasmatic nucleus states (Fig. 27) that the astrocytic bridge plays a modulatory role in the suprachiasmatic complex. While astrocytes specifically located in the suprachiasmatic region have not been studied functionally, experiments in our laboratory have focused on astrocyte cultures from the chick diencephalon, which includes the suprachiasmatic region. It has been discovered that these diencephalic astrocytes are gap junctionally coupled and that they send signals via intercellular calcium waves (Peters et al., 2005), similar to the situation in mammals. These astrocytes have melatonin receptors, and are affected by melatonin administration. First, melatonin application to an astrocytic culture increases resting intracellular

calcium levels. Second, melatonin enhances the transmission of intercellular calcium waves by increasing the distance they spread. Third, melatonin administration results in decreased gap junctional coupling among diencephalic astrocytes (Peters et al., 2005). This finding is exactly the opposite of what one would expect to find, given the enhanced spread of calcium waves, and may be explained in one of three ways: 1) a functional switch occurs under melatonin administration that results in alternative mechanisms of calcium wave spread, 2) the waves are still spread via gap junctions and melatonin increases the efficiency with which the remaining gap junctions are capable of passing calcium or 3) this is an *in vitro* phenomenon that will not translate to *in vivo* studies. It is therefore likely that the astrocytic bridge is modulated by melatonin. This contention is supported by the identification of melatonin receptors on diencephalic astrocytes in culture (Peters et al., 2005). Further, data from our lab indicate that glucose metabolism in cultured diencephalic chick astrocytes may be entrained by melatonin cycles (Adachi et al., 2002, Peters et al, unpublished data). Melatonin administration cycles, however, fail to establish rhythms in clock gene expression (Peters et al., unpublished data). Clock genes, however, are entrained by environmental light cycles, indicating that diencephalic astrocytes have some photoreceptive capability. Light cycles are not capable of entraining glucose uptake (Peters et al., unpublished data), indicating differential regulation of diencephalic astrocyte function by at least melatonin and light. Given the current data, it is not possible to ascribe a particular function to the astrocytic bridge.

In order to address the role of the astrocytic bridge in avian suprachiasmatic complex, I suggest a multi-layered study utilizing a thick slice culture preparation. Using a cultured horizontal slice containing the mSCN, vSCN and astrocytic bridge, it would be possible to measure the electrophysiological properties of all three structures and to determine their interaction through a series of stimulation paradigms. Another technique that would be possible with such a preparation would be the study of gap junctional coupling within the astrocytic bridge itself. By loading dye into astrocytes in one portion of the structure and then stimulating those cells, it would be possible to compare the degree of coupling between astrocytes within the bridge to coupling elsewhere in the hypothalamus. The effects of melatonin on this coupling could be observed easily in such a preparation. *In vivo*, it would be interesting to determine whether lesion of either the vSCN or mSCN results in dissolution of the astrocytic bridge. Such studies would not only provide important information about astrocytes in the avian SCN, but the results could also have implications about the vertebrate circadian system in general.

As was discussed in Chapters III and IV, homology cannot yet be assigned to any one structure, or even to a group of structures. Having stated this, it is likely that homology does, in fact, exist. As has been indicated by others, it is unlikely that two systems with such similar components evolved in parallel from different ancestral precursors (cf. Menaker and Tosini, 1995). Although much is known about the rodent SCN, relatively little is known about the mammalian SCN as a whole and little will continue to be known until studies increase their focus on non-rodent species. It is

crucial to note that the studies that have been performed on non-eutherian species such as marsupials have indicated that the SCN is variable in its chemoarchitecture and the distribution of its retinal input, indicating variability within that taxon. As such, multiple avian models must also be studied in order to classify the avian SCN. Perhaps with a broader view of the vertebrate SCN, the differences that exist between birds and mammals would be no greater than the differences that exist within each taxon. There are new and interesting findings regarding the chick SCN in the work presented here. In combination with the data from the literature, a working model of the avian suprachiasmatic complex is now available from which to carefully design experiments, and the ability to expand that model to fit future data is limitless.

LITERATURE CITED

Abraham U, Albrecht U, Gwinner E, Brandstatter R. 2002. Spatial and temporal variation of passer Per2 gene expression in two distinct cell groups of the suprachiasmatic hypothalamus in the house sparrow (*Passer domesticus*). Eur J Neurosci 16:429-436.

Abrahamson EE, Moore RY. 2001. Suprachiasmatic nucleus in the mouse: retinal innervation, intrinsic organization and efferent projections. Brain Res 916:172-191.

Adachi A, Hasegawa M, Ebihara S. 1995. Measurement of circadian rhythms of ocular melatonin in the pigeon by *in vivo* microdialysis. NeuroReport 7:286-288.

Adachi A, Natesan AK, Whitfield-Rucker MG, Weigum SE, Cassone VM. 2002. Functional melatonin receptors and metabolic coupling in cultured chick astrocytes. Glia 39:268-278.

Aschoff J. 1981. Freerunning and entrained circadian rhythms. In: Aschoff J, editor. Handbook of Behavioral Neurobiology, volume 4: Biological Rhythms. New York: Plenum Press. p 81-93.

Bailey MJ, Cassone VM. 2004. Opsin photoisomerases in the chick retina and pineal gland: characterization, localization, and circadian regulation. Invest Ophthalmol Vis Sci 45:769-775.

Bailey MJ, Beremand PD, Hammer R, Bell-Pedersen D, Thomas TL, Cassone VM. 2003. Transcriptional profiling of the chick pineal gland, a photoreceptive circadian oscillator and pacemaker. Mol Endocrinol 17:2084-2095.

Bailey MJ, Beremand PD, Hammer R, Reidel E, Thomas TL, Cassone VM. 2004. Transcriptional profiling of circadian patterns of mRNA expression in the chick retina. J Biol Chem 279:52247-52254.

Bailey MJ, Chong NW, Xiong J, Cassone VM. 2002. Chickens' Cry2: molecular analysis of an avian cryptochrome in retinal and pineal photoreceptors. FEBS Lett 513:169-174.

Barrett RK, Takahashi JS. 1995. Temperature compensation and temperature entrainment of the chick pineal cell circadian clock. J Neurosci 15:5681-5692.

Berthoud VM, Hall DH, Strahsburger E, Beyer EC, Saez JC. 2000. Gap junctions in the chicken pineal gland. Brain Res 861:257-270.

Binkley S, Hryshchyshyn M, Reilly K. 1979. N-acetyltransferase activity responds to environmental lighting in the eye as well as in the pineal gland. Nature 281:479-481

Binkley S, Kluth E, Menaker M. 1971. Pineal function in sparrows: circadian rhythms in body temperature. Science 15:311-314.

Binkley S, Riebman JB, Reilly KB. 1978. The pineal gland: a biological clock *in vitro*. Science 202:1198-1120.

Bons N. 1976. Retinohypothalamic pathway in the duck (*Anas platyrhynchos*). Cell Tissue Res 168:343-360.

Bowmaker JK, Heath LA, Wilkie SE, Hunt DM. 1997. Visual pigments and oil droplets from six classes of photoreceptor in the retinas of birds. Vision Res 37:2183-2194.

Brandstatter R, Abraham U, Albrecht U. 2001. Initial demonstration of rhythmic *Per* gene expression in the hypothalamus of a non-mammalian vertebrate, the house sparrow. Neuroreport 12:1167-1170.

Brideau AD, Banfield BW, Enquist LW. 1998. The Us9 gene product of pseudorabies virus, an alphaherpesvirus, is a phosphorylated tail-anchored type II membrane protein. J Virol 72:4560-4570.

Brooks DS, Cassone VM. 1992. Daily and circadian regulation of 2-[125]iodomelatonin binding in the chick brain. Endocrinology 131:1297-1304.

Calaza KC, Gardino PF. 2000. Evidence of muscarinic acetylcholine receptors in the retinal centrifugal system of the chick. Braz J Med Biol Res 33:1075-1082.

Cantwell EL, Cassone VM. 2002. Daily and circadian fluctuation in 2-deoxy[(14)C]-glucose uptake in circadian and visual system structures of the chick brain: effects of exogenous melatonin. Brain Res Bull 57:603-611.

Card JP, Moore RY. 1982. Ventral lateral geniculate nucleus efferents to the rat suprachiasmatic nucleus exhibit avian pancreatic polypeptide-like immunoreactivity. J Comp Neurol 206:390-396.

Card JP, Moore RY. 1989. Organization of lateral geniculate-hypothalamic connections in the rat. J Comp Neurol 284:135-147.

Card JP, Whealy ME, Robbins AK, Moore RY, Enquist LW. 1991. Two alpha herpesvirus strains are transported differentially in the rodent visual system. Neuron 6:957-969.

Cassone VM. 1988. Circadian variation of [14C]2-deoxyglucose uptake within the suprachiasmatic nucleus of the house sparrow, *Passer domesticus*. Brain Res 459:178-82.

Cassone VM. 1990. Melatonin: time in a bottle. Oxf Rev Reprod Biol 12:319-367.

Cassone VM. 1991. Melatonin and suprachiasmatic nucleus function. In: Klein DC, Moore RY, Reppert SM, editors. Suprachiasmatic Nucleus: The Mind's Clock. New York, NY: Oxford University Press. p 309-323.

Cassone VM. 1992. The pineal gland influence rat circadian activity rhythms in constant light. J Biol Rhythms 7:27-40.

Cassone VM. 1998. Melatonin's role in vertebrate circadian rhythms. Chronobiol Int 15:457-473.

Cassone VM, Brooks DS. 1991. Sites of melatonin action in the brain of the house sparrow, *Passer domesticus*. J Exp Zool 260:302-309.

Cassone VM, Menaker M. 1994. Is the avian circadian system a neuroendocrine loop? J Exp Zool 232:539-549.

Cassone VM, Moore RY. 1987. Retinohypothalamic projection and suprachiasmatic nucleus of the house sparrow, *Passer domesticus*. J Comp Neurol 266:171-182.

Cassone VM, Natesan AK. 1997. Time and time again: the phylogeny of melatonin as a transducer of biological time. J Biol Rhythms 12:489-497.

Cassone VM, Brooks DS, Kelm TA. 1995. Comparative distribution of 2[125]Iodomelatonin binding in the brains of diurnal birds—outgroup analysis with turtles. Brain Behav Evol 45:241-256.

Cassone VM, Forsyth AM, Woodlee GL. 1990. Hypothalamic regulation of circadian noradrenergic input to the chick pineal gland. J Comp Physiol A 167:187-192.

Cassone VM, Roberts MH, Moore RY. 1988a. Effects of melatonin on 2-deoxy-[1-14C]glucose uptake within rat suprachiasmatic nucleus. Am J Physiol 255:R332-337.

Cassone VM, Speh JC, Card JP, Moore RY. 1988b. Comparative anatomy of the mammalian hypothalamic suprachiasmatic nucleus. J Biol Rhythms 3:71-91.

Chabot CC, Menaker M. 1992a. Effects of physiological cycles of infused melatonin on circadian rhythmicity in pigeons. J Comp Physiol A 170:615-622.

Chabot CC, Menaker M. 1992b. Circadian feeding and locomotor rhythms in pigeons and house sparrows. J Biol Rhythms 7:287-299.

Chabot CC, Menaker M. 1994. Feeding rhythms in constant light and constant darkness: the role of the eyes and the effect of melatonin infusion. J Comp Physiol A 175:75-82.

Chen S, Aston-Jones G. 1995. Evidence that cholera toxin B subunit (CTb) can be avidly taken up and transported by fibers of passage. Brain Res 674:107-111.

Chen Y, Naito J. 1999. Morphological classification of ganglion cells in the central retina of chicks. J Vet Med Sci 61:537-542.

Chou TC, Bjorkum AA, Baus SE, Lu J, Scammell TE, Saper CB. 2002. Afferents to the ventrolateral preoptic nucleus. J Neurosci 22:977-990.

Colwell CS. 2000. Rhythmic coupling among cells in the suprachiasmatic nucleus. J Neurobiol 43:379-388.

Colwell CS. 2005. Bridging the gap: coupling single-cell oscillators in the suprachiasmatic nucleus. Nat Neurosci 8:10-12.

Cooper ML, Pickard GE, Silver R. 1983. Retinohypothalamic pathway in the dove demonstrated by anterograde HRP. Brain Res Bull 10:715-718.

Cowan WM, Wenger E. 1968. Degeneration in the nucleus of origin of the preganglionic fibers to the chick ciliary ganglion following early removal of the optic vesicle. J Exp Zool 168:105-124.

Crosby EL, Showers MJL. 1969. Comparative anatomy of the preoptic and hypothalamic areas. In: Haymaker W, Anderson E, Nauta WJH, editors. The Hypothalamus. Springfield, IL: ChC Thomas. p 61-135.

Dai J, Swaab DF, Van der Vliet J, Buijs RM. 1998. Postmortem tracing reveals the organization of hypothalamic projections of the suprachiasmatic nucleus in the human brain. J Comp Neurol 400:87-102.

de Vries MJ, Nunes Cardozo B, van der Want J, de Wolf A, Meijer JH. 1993. Glutamate immunoreactivity in terminals of the retinohypothalamic tract of the brown Norwegian rat. Brain Res 612:231-237.

Deguchi T. 1979. A circadian oscillator in cultured cells of chicken pineal gland. Nature 282:94-96.

Drucker-Colin R, Aguilar-Roblero R, Garcia-Hernandez F, Fernandez-Cancino F , Bermudez-Rattoni F. 1984. Fetal suprachiasmatic nucleus transplants: diurnal rhythm recovery of lesioned rats. Brain Res 311:353-357.

Dunlap JC. 1999. Molecular bases for circadian clocks. Cell 96:271-290.

Ebihara S, Kawamura H. 1981. The role of the pineal organ and the suprachiasmatic nucleus in the control of circadian locomotor rhythms in the Java sparrow, *Padda oryzivora*. J Comp Physiol 141:207-214.

Ebihara S, Oshima I, Yamada H, Goto M, Sato K. 1987. Circadian organization in the pigeon. In: Hiroshige T, Honma K, editors. Comparative Aspects of Circadian Clocks. Sapporo, Japan: Hokkaido University Press. p 88-94.

Ebihara S, Uchiyama K and Oshima I. 1984. Circadian organization in the pigeon, *Columba livia*: the role of the pineal organ and the eye. J Comp Physiol 154:59-69.

Ehrlich D, Mark R. 1984. An atlas of the primary visual projections in the brain of the chick *Gallus gallus*. J Comp Neurol 223:592-610.

Ehrlich D, Zappia JV, Saleh CN. 1988. Development of the supraoptic decussation in the chick (*Gallus gallus*). Anat Embryol (Berl) 177:361-370.

Engelage J, Bischof H. 1993. The organization of the tectofugal pathway in birds: a comparative review. In: Zeigler HP, Bischof H, editors. Vision, Brain, and Behavior in Birds. Cambridge, MA: The MIT Press. p 25-46.

Erichsen JR, May PJ. 2002. The pupillary and ciliary components of the cat Edinger-Westphal nucleus: a transsynaptic transport investigation. Vis Neurosci 19:15-29.

Fitzgerald MEC, Vana BA, Reiner A. 1990. Control of choroidal blood flow by the nucleus of Edinger-Westphal in pigeons: a laser Doppler study. Invest Ophthalmol Vis Sci 31:2483-2492.

Fujii JT. 1992. Repetitive firing properties in subpopulations of the chick Edinger Westphal nucleus. J Comp Neurol 316:279-286.

Fujii JT, Lucaj Z. 1993. Calcium-binding proteins in the chick Edinger Westphal nucleus. Brain Res 605:200-206.

Gamlin PD, Cohen DH. 1988. Retinal projections to the pretectum in the pigeon (*Columba livia*). J Comp Neurol 269:1-17.

Gamlin PD, Reiner A. 1991. The Edinger-Westphal nucleus: sources of input influencing accommodation, pupilloconstriction, and choroidal blood flow. J Comp Neurol 306:425-438.

Gamlin PD, Reiner A, Karten HJ. 1982. Substance P-containing neurons of the avian suprachiasmatic nucleus project directly to the nucleus of Edinger-Westphal. Proc Natl Acad Sci USA 79:3891-3895.

Gardino PF, Schmal AR, Calaza KC. 2004. Identification of neurons with acetilcholinesterase and NADPH-diaphorase activities in the centrifugal visual system of the chick. J Chem Neuroanat 27:267-273.

Gaston S. 1971. The influence of the pineal organ on the circadian activity rhythm in birds. In: Menaker M, editor. Biochronometry. Washington DC: National Academy of Science. p 541-548.

Gaston S, Menaker M. 1968. Pineal function: the biological clock in sparrows? Science 160:1125-1127.

Green DJ, Gillette R. 1982. Circadian rhythm of firing rate recorded from single cells in the rat suprachiasmatic nucleus brain slice. Brain Res 245:198-200.

Groos G, Hendriks J. 1982. Circadian rhythms in electrical discharge of rat suprachiasmatic neurons recorded *in vitro*. Neurosci Lett 34:283-288.

Güntürkün O, Miceli D, Watanabe M. 1993. Anatomy of the avian thalamofugal pathway. In: Zeigler HP, Bischof H, editors. Vision, Brain, and Behavior in Birds. Cambridge, MA: The MIT Press. p 25-46.

Gwinner E. 1978. Effects of pinealectomy on circadian locomotor activity rhythms in European starlings, *Sturnus vulgaris*. J Comp Physiol A 126:123-129.

Gwinner E. 1989. Melatonin and the circadian system of birds: model of internal resonance. In: Hiroshige T, Homan K, editors. Circadian Clocks and Ecology. Sapporo, Japan: Hokkaido University Press. p 127-145.

Gwinner E, Benzinger I. 1978. Synchronization of a circadian rhythm in pinealectomized European starlings by daily injections of melatonin. J Comp Physiol A 127:209-213.

Hamm HE, Menaker M. 1980. Retinal rhythms in chicks: circadian variation in melatonin and serotonin N-acetyltransferase activity. Proc Natl Acad Sci USA 77:4998-5002.

Hannibal J. 2002. Pituitary adenlate cyclase-activating peptide in the rat central nervous system: an immunohistochemical and *in situ* hybridization study. J Comp Neurol 453:389-417.

Harrington ME, Nance DM, Rusak B. 1985. Neuropeptide Y immunoreactivity in the hamster geniculo-suprachiasmatic tract. Brain Res Bull 15:465-472.

Hartwig HG. 1974. Electron microscopic evidence for a retinohypothalamic projection to the suprachiasmatic nucleus of *Passer domesticus*. Cell Tissue Res 153:89-99.

Hastings MH, Herzog ED. 2004. Clock genes, oscillators, and cellular networks in the suprachiasmatic nuclei. J Biol Rhythms 19:400-413.

Heigl S, Gwinner E. 1995. Synchronization of circadian rhythms of house sparrows by oral melatonin: effects of changing period. J Biol Rhythms 10:225-233.

Hess A. 1965. Developmental changes in the structure of the synapse on the myelinated cell bodies of the chicken ciliary ganglion. J Cell Biol 25:1-19.

Hess A. 1966. The fine structure of the striated muscle fibers and their nerve terminals in the avian iris: morphological “twitch-slow” fibers. Anat Rec 154:356-357.

Husak PJ, Kuo T, Enquist LW. 2000. Pseudorabies virus membrane proteins gI and gE facilitate anterograde spread of infection in projection-specific neurons in the rat. J Virol 74:10975-10983.

Ikeda T, Iijima N, Munekawa K, Ishihara A, Ibata Y, Tanaka M. 2003. Functional retinal input stimulates expression of astroglial elements in the suprachiasmatic nucleus of postnatal developing rat. Neurosci Res 47:39-45.

Inouye ST, Kawamura H. 1979. Persistence of circadian rhythmicity in a mammalian hypothalamic “island” containing the suprachiasmatic nucleus. Proc Natl Acad Sci USA 76:5962-5966.

Juss TS, Davies IR, Follett BK, Mason R. 1994. Circadian rhythm in neuronal discharge activity in the quail lateral hypothalamic retinorecipient nucleus (LHRN) recording *in vitro*. J Physiol 485:132.

Kalsbeek A, Teclemariam-Mesbah R, Pevet P. 1993. Efferent projections of the suprachiasmatic nucleus in the golden hamster (*Mesocricetus auratus*). J Comp Neurol 332:293-314.

Kasal CA, Menaker M, Perez-Polo JR. 1979. Circadian clock in culture: N-acetyltransferase activity of chick pineal glands oscillates *in vitro*. Science 203:656-658.

King VM, Follett BK. 1997. c-fos expression in the putative avian suprachiasmatic nucleus. J Comp Physiol A 180:541-551.

Klein DC, Coon SL, Roseboom PH, Weller JL, Bernard M, Gastel JA, Zatz M, Iuvone PM, Rodriguez IR, Begay V, Falcon J, Cahill GM, Cassone VM, Baler R. 1997. The melatonin rhythm-generating enzyme: molecular regulation of serotonin N-acetyltransferase in the pineal gland. Recent Prog Horm Res 52:307-357.

Klein DC, Moore RY. 1979. Pineal N-acetyltransferase and hydroxyindole-O-methyltransferase: control by the retinohypothalamic tract and the suprachiasmatic nucleus. Brain Res 174:245-262.

Korf HW, von Gall C, Stehle J. 2003. The circadian system and melatonin: lessons from rats and mice. Chronobiol Int 20:697-710.

Kriegsfeld LJ, Leak RK, Yackulic CB, LeSauter J, Silver R. 2004. Organization of suprachiasmatic nucleus projections in Syrian hamsters (*Mesocricetus auratus*): an anterograde and retrograde analysis. J Comp Neurol 468:361-379.

Kuenzel WJ. 1993. The search for deep encephalic photoreceptors within the avian brain, using gonadal development as a primary indicator. Poult Sci 72:959-967.

Kuenzel WJ, Masson M. 1988. A Stereotaxic Atlas of the Brain of the Chick (*Gallus domesticus*). Baltimore, MD: The Johns Hopkins University Press.

Kuenzel WJ, van Tienhoven A. 1982. Nomenclature and location of avian hypothalamic nuclei and associated circumventricular organs. J Comp Neurol 206:293-313.

Laemle LK, Fugaro C, Bentley T. 1993. The geniculohypothalamic pathway in a congenitally anophthalmic mouse. Brain Res 618:352-357.

Laemle LK, Ottenweller JE. 1998. Daily patterns of running wheel activity in male anophthalmic mice. Physiol Behav 64:165-171.

Laemle LK, Ottenweller JE. 2001. The relationship between circadian rhythmicity and vasoactive intestinal polypeptide in the suprachiasmatic nucleus of congenitally anophthalmic mice. Brain Res 917:105-111.

Laemle LK, Ottenweller JE, Fugaro C. 1995. Diurnal variations in vasoactive intestinal polypeptide-like immunoreactivity in the suprachiasmatic nucleus of congenitally anophthalmic mice. Brain Res 688:203-208.

Laemle LK, Rusa R. 1992. VIP-like immunoreactivity in the suprachiasmatic nuclei of a mutant anophthalmic mouse. Brain Res 589:124-128.

Lavialle M, Begue A, Papillon C, Vilaplana J. 2001. Modifications of retinal afferent activity induce changes in astroglial plasticity in the hamster circadian clock. Glia 34:88-100.

Lavialle M, Serviere J. 1993. Circadian fluctuations in GFAP distribution in the Syrian hamster suprachiasmatic nucleus. Neuroreport 4:1243-1246.

Lavialle M, Serviere J. 1995. Developmental study in the circadian clock of the golden hamster: a putative role of astrocytes. Brain Res Dev Brain Res 86:275-282.

Leak RK, Moore RY. 2001. Topographic organization of suprachiasmatic nucleus projection neurons. J Comp Neurol 433:312-334.

Lehman MN, Silver R, Gladstone WR, Kahn RM, Gibson M, Bittman EL. 1987. Circadian rhythmicity restored by neural transplant. Immunocytochemical characterization of the graft and its integration with the host brain. J Neurosci 6:1626-1638.

LeSauter J, Silver R. 1999. Localization of a suprachiasmatic nucleus subregion regulating locomotor rhythmicity. J Neurosci 19:5574-5585.

Li H, Ferrari MB, Kuenzel WJ. 2004. Light-induced reduction of cytoplasmic free calcium in neurons proposed to be encephalic photoreceptors in chick brain. Brain Res Dev Brain Res 153:153-161.

Long MA, Jutras MJ, Connors BW, Burwell RD. 2005. Electrical synapses coordinate activity in the suprachiasmatic nucleus. Nat Neurosci 8:61-66.

Lu J, Cassone VM. 1993a. Pineal regulation of circadian rhythms of 2-deoxy[^{14}C]glucose uptake and 2[^{125}I]iodomelatonin binding in the visual system of the house sparrow, *Passer domesticus*. J Comp Physiol A 173: 765-774.

Lu J, Cassone VM. 1993b. Daily melatonin administration synchronizes circadian patterns of brain metabolism and behavior in pinealectomized house sparrows, *Passer domesticus*. J Comp Physiol A 173:775-782.

Lu J, Greco MA, Shiromani P, Saper CB. 2000. Effect of lesions of the ventrolateral preoptic nucleus on NREM and REM sleep. J Neurosci 20:3830-3842.

Lu J, Shiromani P, Saper CB. 1999. Retinal input to the sleep-active ventrolateral preoptic nucleus in the rat. Neuroscience 93:209-214.

Martin AR, Pilar G. 1963. Dual mode of synaptic transmission in the avian ciliary ganglion. J Physiol 168:443-463.

Marwitt R, Pilar G, Weakly JN. 1971. Characterization of two ganglion cell populations in avian ciliary ganglion. Brain Res 25:317-334.

McGoogan JM, Cassone VM. 1999. Circadian regulation of chick eletroretinogram: effects of pinealectomy and exogenous melatonin. Am J Physiol 277:R1418-1427.

Meier RE. 1973. Autoradiographic evidence for a direct retinohypothalamic projection in the avian brain. Brain Res 53:417-421.

Menaker M. 1968. Extraretinal light perception in the sparrow. Proc Natl Acad Sci USA 59:414-421.

Menaker M. 1982. In search of principles of vertebrate circadian organization. In: Aschoff J, Daan S, Groos GA, editors. Vertebrate Circadian Systems: Structure and Physiology. Berlin: Springer. p 1-12.

Menaker M, Tosini G. 1995. The evolution of vertebrate circadian systems. In: Honma K, Honma S, editors. Proceedings of the Sixth Sapporo Symposium on Biological Rhythms. Sapporo, Japan: Hokkaido University Press. p 39-52.

Menaker M, Underwood H. 1976. Extraretinal photoreception in birds. Photophysiology 23:299-306.

Meriney SD, Pilar G. 1987. Cholinergic innervation of the smooth muslce cells in the choroid coat of the chick eye and its development. J Neurosci 7:3827-3839.

Mey J, Johann V. 2001. Dendrite development and target innervation of displaced retinal ganglion cells of the chick (*Gallus gallus*). Int J Devl Neurosci 19:517-531.

Mikkelson JD, Vrang N. 1994. A direct pretectosuprachiasmatic projection in the rat. Neuroscience 62:497-505.

Moga MM, Moore RY. 1997. Organization of neural inputs to the suprachiasmatic nucleus in the rat. J Comp Neurol 389:508-534.

Montagnese CM, Szekely AD, Adam A, Csillag A. 2004. Efferent connections of septal nuclei of the domestic chick (*Gallus domesticus*): an anterograde pathway tracing study with a bearing on functional circuits. J Comp Neurol 469:437-456.

Moore RY. 1973. Retinohypothalamic projection in mammals: a comparative study. Brain Res 49:403-409.

Moore RY. 1979. The retinohypothalamic tract, suprachiasmatic hypothalamic nucleus and central neural mechanisms of circadian rhythm regulation. In: Suda M, Hayashi O, Hakagawa H, editors. Biological Rhythms and Their Central Mechanism. Amsterdam: Elsevier/North Holland Press. p 343-354.

Moore RY. 1982. Organization and function of a central nervous system circadian oscillator: The suprachiasmatic hypothalamic nucleus. Fed Proc 42:2783-2789.

Moore RY, Card JP. 1994. Intergeniculate leaflet: an anatomically and functionally distinct subdivision of the lateral geniculate complex. J Comp Neurol 344:403-430.

Moore RY, Eichler VB. 1972. Loss of a circadian adrenal corticosterone rhythm following suprachiasmatic lesions in the rat. Brain Res 42:201-206.

Moore RY, Klein DC. 1974. Visual pathways and the central neural control of a circadian rhythm in pineal serotonin N-acetyltransferase activity. Brain Res 10:17-33.

Moore RY, Lenn NJ. 1972. A retinohypothalamic projection in the rat. J Comp Neurol 146:1-14.

Moore RY, Speh JC. 1993. GABA is the principal neurotransmitter of the circadian system. Neurosci Lett 150:112-116.

Moore RY, Gustafson EL, Card JP. 1984. Identical immunoreactivity of afferents to the rat suprachiasmatic nucleus with antisera against avian pancreatic polypeptide, molluscan cardioexcitatory peptide and neuropeptide Y. Cell Tissue Res 236:41-46.

Moore RY, Hilaris AE, Jones BE. 1978. Serotonin neurons of the midbrain raphe: ascending projections. J Comp Neurol 180:417-438.

Moore RY, Karapas F, Lenn NJ. 1971. A retinohypothalamic projection in the rat. Anat Rec 169:382-383.

Moore RY, Speh JC, Leak RK. 2002. Suprachiasmatic nucleus organization. Cell Tissue Res 309:89-98.

Morin LP, Blanchard JH, Provencio I. 2003. Retinal ganglion cell projections to the hamster suprachiasmatic nucleus, intergeniculate leaflet, and visual midbrain: bifurcation and melanopsin immunoreactivity. J Comp Neurol 465:401-416.

Morin LP, Goodless-Sanchez N, Smale L, Moore RY. 1994. Projections of the suprachiasmatic nuclei, subparaventricular zone and retrochiasmatic area in the golden hamster. Neuroscience 61:391-410.

Morin LP, Johnson RF, Moore RY. 1989. Two brain nuclei controlling circadian rhythms are identified by GFAP immunoreactivity in hamsters and rats. Neurosci Lett 99:55-60.

Nalbach H, Wolf-Oberhollenzer F, Remy M. 1993. Exploring the image. In: Zeigler HP, Bischof H, editors. Vision, Brain, and Behavior in Birds. Cambridge, MA: The MIT Press. p 25-46.

Narayanan CH, Narayanan Y. 1976. An experimental inquiry into the central source of preganglionic fibers to the chick ciliary ganglion. J Comp Neurol 166:101-110.

Natesan AJ, Geetha L, Zatz M. 2002. Rhythm and soul in the avian pineal. Cell Tissue Res 309:35-45.

Newman GC, Hospod FE, Patlak CS, Moore RY. 1992. Analysis of *in vitro* glucose utilization in a circadian pacemaker model. J Neurosci 12:2015-2021.

Norgren RB, Silver R. 1989. Retinohypothalamic projections and the suprachiasmatic nucleus in birds. Brain Behav Evol 34:73-83.

Norgren RB, Silver R. 1990. Distribution of vasoactive intestinal peptide-like and neurophysin-like immunoreactive neurons and acetylcholinesterase staining in the ring dove hypothalamus with emphasis on the question of an avian suprachiasmatic nucleus. Cell Tissue Res 259:331-339.

Northcutt RG. 1984. Evolution of the vertebrate central nervous system: patterns and processes. Amer Zool 24:701-716.

Nyce J, Binkley S. 1977. Extraretinal photoreception in chickens: entrainment of the circadian locomotor activity rhythm. Photochem Photobiol 25:529-531.

Oertel WH, Tappaz ML, Berod A, Mugnaini E. 1982. Two-color immunohistochemistry for dopamine and GABA neurons in rat substantia nigra and zona incerta. Brain Res Bull 9:463-474.

Oliver J, Bouillé C, Herbuté S, Baylé JD. 1978. Retrograde transport from the preoptic-anterior hypothalamic region to retinal ganglion cells in quail. Neurosci Lett 9: 291-295.

Oshima I, Yamada H, Goto M, Sato K, Ebihara S. 1989. Pineal and retinal melatonin is involved in the control of circadian locomotor and body temperature rhythms in the pigeon. J Comp Physiol A 166:217-226.

Palkovits M, Brownstein MJ. 1988. Maps and Guide to Microdissection of the Rat Brain. New York: Elsevier. pp 110-115.

Pang SF, Chow PH, Wong TM, Tso EC. 1983. Diurnal variations of melatonin and N-acetylserotonin in the tissues of quails (*Coturnix sp*.), pigeons (*Columba livia*), and chickens (*Gallus domesticus*). Gen Comp Endocrinol 51:1-7.

Peters JL, Cassone, VM, Zoran MJ. 2005. Melatonin modulates intercellular communication among cultured chick astrocytes. Brain Res 1031:10-19.

Pickard GE. 1982. The afferent connections of the suprachiasmatic nucleus of the golden hamster with emphasis on the retinohypothalamic projection. J Comp Neurol 211:65-83.

Pickard GE, Smeraski CA, Tomlinson CC, Banfield BW, Kaufman J, Silcos CL, Enquist LW, Sollars PJ. 2002. Intravitreal injection of the attenuated pseudorabies virus PRV Bartha results in infection of the hamster suprachiasmatic nucleus only by retrograde transsynaptic transport via autonomic circuits. J Neurosci 22:2701-2710.

Pittendrigh CS. 1960. Circadian rhythms and the circadian organization of living systems. Cold Spring Harb Symp Quant Biol 25:159-182.

Pittendrigh CS. 1993. Temporal organization: reflections of a Darwinian clock-watcher. Annu Rev Physiol 55:16-54.

Prosser RA, Edgar DM, Heller HC, Miller JD. 1994. A possible glial role in the mammalian circadian clock. Brain Res 643:296-301.

Ralph MR, Foster RG, Davis FC, Menaker M. 1990. Transplanted suprachiasmatic nucleus determines circadian period. Science 247:975-978.

Rathinam T, Kuenzel WJ. 2005. Attenuation of gonadal response to photostimulation following ablation of neurons in the lateral septal organ of chicks. Brain Res Bull 64:455-461.

Rea MA. 1989. Light increases Fos-related protein immunoreactivity in the rat suprachiasmatic nuclei. Brain Res Bull 23:577-581.

Reiner A, Fitzgerald MED, Gamlin PDR. 1990. Central neural circuits controlling choroidal blood flow: a laser-Doppler study. Invest Ophthalmol Vis Sci Suppl 31:38.

Reiner A, Karten JH, Gamlin PDR, Erichsen JT. 1983. Parasympathetic ocular control: functional subdivisions and circuitry of the avian nucleus of Edinger-Westphal. Trends Neurosci 6:140-145.

Reiner A, Perkel DJ, Bruce LL, Butler AB, Csillag A, Kuenzel W, Medina L, Paxinos G, Shimizu T, Striedter G, Wild M, Ball GF, Durand S, Gunturkun O, Lee DW, Mello CV, Powers A, White SA, Hough G, Kubikova L, Smulders TV, Wada K, Dugas-Ford J, Husband S, Yamamoto K, Yu J, Siang C, Jarvis ED. 2004. Revised nomenclature for avian telencephalon and some related brainstem nuclei. J Comp Neurol 473:377-414.

Reppert SM, Sagar SM. 1983. Characteristics of the day-night variations of retinal melatonin content in the chick. Invest Ophthalmol Vis Sci 24:294-300.

Reppert SM, Weaver DR. 2002. Coordination of circadian timing in mammals. Nature 418:935-941.

Reppert SM, Weaver DR, Cassone VM, Godson C, Kolakowski Jr. LF. 1995. Melatonin receptors are for the birds: molecular analysis of two receptor subtypes differentially expressed in chick brain. Neuron 15:1003-1015.

Rivkees SA, Cassone VM, Weaver DR, Reppert SM. 1989. Melatonin receptors in chick brain: characterization and localization. Endocrinology 125:363-368.

Rogers SW. 1999. Allosaurus, crocodiles, and birds: evolutionary clues from spiral computed tomography of an endocast. Anat Rec 257:162-173.

Rosenwasser AM, Trubowitsch G, Adler NT. 1985. Circadian rhythm in metabolic activity of suprachiasmatic, supraoptic and raphe nuclei. Neurosci Lett 58:183-187.

Rusak B, Zucker I. 1979. Neural regulation of circadian rhythms. Physiol Rev 59:449-526.

Ruskell GL. 1971. Facial parasympathetic innervation of the choroidal blood vessels in monkeys. Exp Eye Res 12: 166-172.

Sawaki Y, Nihonmatsu I, Kawamura H. 1984. Transplantation of the neonatal suprachiasmatic nuclei into rats with complete bilateral suprachiasmatic lesions. Neurosci Res 1:67-72.

Schwartz WJ. 1990. Different *in vivo* metabolic activities of suprachiasmatic nuclei of Turkish and golden hamsters. Am J Physiol 259:R1083-1085.

Schwartz WJ, Davidsen LC, Smith CB. 1980. *In vivo* metabolic activity of a putative circadian oscillator, the rat suprachiasmatic nucleus. J Comp Neurol 189:157-167.

Schwartz WJ, Gainer H. 1977. Suprachiasmatic nucleus: use of 14C-labeled deoxyglucose uptake as a functional marker. Science 197:1089-1091.

Sherin JE, Elmquist JK, Torrealba F, Saper CB. 1998. Innervation of histaminergic tuberomammillary neurons by GABAergic and galaninergic neurons in the ventrolateral preoptic nucleus of the rat. J Neurosci 15:4705-4721.

Shibata S, Oomura Y, Kita H, Hattori H. 1982. Circadian rhythmic changes of neuronal activity in the suprachiasmatic nucleus of the rat hypothalamic slice. Brain Res 247:154-158.

Shimizu I, Yoshimoto M, Kojima T, Okadao N. 1984. Development of retinohypothalamic projections in the chick embryo. Neurosci Lett 50:43-47.

Shimizu T, Cox K, Harvey JK, Britto LRG. 1994. Cholera toxin mapping of retinal projections in pigeons (*Columba livia*), with emphasis on retinohypothalamic connections. Vis Neurosci 11: 441-446.

Silver R, Witkovsky P, Horvath P, Alones V, Barnstable CJ, Lehman MN. 1988. Coexpression of opsin- and VIP-like-immunoreactivity in CSF-contacting neurons of the avian brain. Cell Tissue Res 253:189-198.

Simpson SM, Follett BK. 1981. Pineal and hypothalamic pacemakers: their role in regulating circadian rhythmicity in the Japanese quail. J Comp Physiol A 144:381-389.

Siuciak JA, Drause DN, Dubocovich ML. 1991. Quantitative pharmacological analysis of 2-^{125}I-iodomelatonin binding sites in discrete areas of the chicken brain. J Neurosci 11:2855-2864.

Skene DJ, Vivien-Roels B, Pevet P. 1991. Day and nighttime concentrations of 5-methoxytryptophol and melatonin in the retina and pineal gland from different classes of vertebrates. Gen Comp Endocrinol 84:405-411.

Smeraski CA, Sollars PJ, Ogilvie MD, Enquist LW, Pickard GE. 2004. Suprachiasmatic nucleus input to autonomic circuits identified by retrograde transsynaptic transport of pseudorabies virus from the eye. J Comp Neurol 471:298-313.

Smith BN, Banfield VW, Smeraski CA, Wilcox CL, Dudek FE, Enquist LW, Pickard GE. 2000. Pseudorabies virus expressing enhanced green fluorescent protein: a tool for *in vitro* electrophysiological analysis of transsynaptically labeled neurons in identified central nervous system circuits. Proc Natl Acad Sci 97:9264-9269.

Steele CT, Zivkovic BD, Siopes T, Underwood H. 2003. Ocular clock are tightly coupled and act as pacemaker in the circadian system of Japanese quail. Am J Physiol 284:R208-218.

Stehle J. 1990. Melatonin binding sites in brain of the 2-day-old chicken: an autoradiographic localisation. J Neural Transm Gen Sect 81:83-89.

Stephan FK, Berkley KJ, Moss RL. 1981. Efferent connections of the rat suprachiasmatic nucleus. Neuroscience 6:2625-2641.

Stephan FK, Zucker I. 1972. Circadian rhythms in drinking behavior and locomotor activity of rats are eliminated by hypothalamic lesions. Proc Natl Acad Sci USA 69:1583-1586.

Takahashi JS, Menaker M. 1979. Physiology of avian circadian pacemakers. Fed Proc 38:2583-2588.

Takahashi JS, Menaker M. 1982. Role of the suprachiasmatic nucleus in the circadian system of the house sparrow. J Neurosci 2:815-828.

Tei H, Okamura H, Shigeyoshi Y, Fukuhara C, Ozawa R, Irose M, Sakaki Y. 1997. Circadian oscillation of a mammalian homologue of the *Drosophila period* gene. Nature 389:512-516.

Tombol T, Eyre M, Zayats N, Nmeth A. 2003. The ramifications and terminals of optic fibres in layers 2 and 3 of the avian optic tectum: a Golgi and light and electron microscopic anterograde tracer study. Cells Tissues Organs 175:202-222.

Tomishima MJ, Enquist LW. 2001. A conserved α-herpesvirus protein necessary for axonal localization of viral membrane proteins. J Cell Biol 154:741-752.

Uchiyama H. 1989. Centrifugal pathways to the retina: influence of the optic tectum. Vis Neurosci 3:183-206.

Underwood H, Goldman BD. 1987. Vertebrate circadian and photoperiodic systems: role of the pineal gland and melatonin. J Biol Rhythms 2:279-315.

Underwood H, Siopes T. 1984. Circadian organization in Japanese quail. J Exp Zool 232:557-566.

van den Pol AN. 1980. The hypothalamic suprachiasmatic nucleus of rat: intrinsic anatomy. J Comp Neurol 191:661-702.

van den Pol AN, Finkbeiner SM, Cornell-Bell AH. 1992. Calcium excitability and oscillations in suprachiasmatic nucleus neurons and glia *in vitro*. J Neurosci 12:2648-2664.

van den Pol AN, Tsujimoto KL. 1985. Neurotransmitters of the hypothalamic suprachiasmatic nucleus: immunocytochemical analysis of 25 neuronal antigens. Neuroscience 15:1049-1086.

van Tienhoven A, Jühász LW. 1962. The chicken telencephalon, diencephalon and mesencephalon in stereotaxic coordinates. J Comp Neurol 118:185-198.

Vannucci S, Hawkins R. 1983. Substrates of energy metabolism of the pituitary and pineal glands. J Neurochem 41:1718-1725.

Veenman CL, Reiner A, Honig MG. 1992. Biotinylated dextran amine as an anterograde tracer for single- and double-labeling studies. J Neurosci Methods 41:239-254.

Vigh-Teichmann I, Rohlich P, Vigh B, Aros B. 1980. Comparison of pineal complex, retina and cerebrospinal fluid contacting neurons by immunocytochemical antirhodopsin reaction. Z Mikrosk Anat Forsch 94:623-640.

Wallman J, Letelier J. 1993. Eye movements, head movements, and gaze stabilization in birds. In: Zeigler HP, Bischof H, editors. Vision, Brain, and Behavior in Birds. Cambridge, MA: The MIT Press. p 25-46.

Watanabe M. 1987. Synaptic organization of the nucleus dorsolateralis anterior thalami in the Japanese quail (*Coturnix coturnix japonica*). Brain Res 401:279-291.

Watts AG. 1991. The efferent projections of the suprachiasmatic nucleus: anatomical insights into the control of circadian rhythms. In: Klein DC, Moore RY, Reppert SM, editors. Suprachiasmatic Nucleus: The Mind's Clock. New York: Oxford University Press. p 77-106.

Watts AG, Swanson LW. 1987. Efferent projections of the suprachiasmatic nucleus: II. studies using retrograde transport of fluorescent dyes and simultaneous peptide immunohistochemistry in the rat. J Comp Neurol 258:230-252.

Watts AG, Swanson LW, Sanchez-Watts G. 1987. Efferent projections of the suprachiasmatic nucleus: I. studies using anterograde transport of *Phaseolus vulgaris* leucoagglutinin in the rat. J Comp Neurol 258:204-229.

Welsh DK, Reppert SM. 1996. Gap junctions couple astrocytes but not neurons in dissociated cultures of rat suprachiasmatic nucleus. Brain Res 706:30-36.

Wu CC, Russell RM, Karten HJ. 1999. The transport rate of cholera toxin B subunit in the retinofugal pathways of the chick. Neuroscience 92:665-676.

Wu CC, Russell RM, Nguyen RT, Karten HJ. 2003. Tracing developing pathways in the brain: a comparison of carbocyanine dyes and cholera toxin B subunit. Neuroscience 117:831-845.

Wu WQ, McGoogan JM, Cassone VM. 2000. Circadian regulation of visually evoked potentials in the domestic pigeon, *Columba livia*. J Biol Rhythms 15:317-328.

Yamazaki S, Numano R, Abe M, Hida A, Takahashi R, Ueda M, Block GD, Sakaki Y, Menaker M, Tei H. 2000. Resetting central and peripheral circadian oscillators in transgenic rats. Science 288:682-685.

Yasuo S, Watanabe M, Okabayashi N, Ebihara S, Yoshimura T. 2003. Circadian clock genes and photoperiodism: comprehensive analysis of clock gene expression in the mediobasal hypothalamus, the suprachiasmatic nucleus, and the pineal gland of Japanese Quail under various light schedules. Endocrinology 144:3742-3748.

Yoshimura T, Suzuki Y, Makino E, Suzuki T, Kuroiwa A, Matsuda Y, Namikawa T, Ebihara S. 2000. Molecular analysis of avian circadian clock genes. Mol Brain Res 78:207-215.

Yoshimura T, Yasuo S, Suzuki Y, Makino E, Yokota Y, Ebihara S. 2001. Identification of the suprachiasmatic nucleus in birds. Am J Physiol 280:R1185-1189.

Zatz M, Mullen DA, Moskal JR. 1988. Photoendocrine transduction in cultured chick pineal cells: effects of light, dark, and potassium on the melatonin rhythm. Brain Res 438:199-215.

Zeller K, Duelli R, Vogel J, Schröck H, Kuschinsky W. 1995. Autoradiographic analysis of the regional distribution of Glut3 glucose transporters in the rat brain. Brain Res 698:175-179.

Zimmerman NH, Menaker M. 1979. The pineal gland: a pacemaker within the circadian system of the house sparrow. Proc Natl Acad Sci USA 76:999-1003.

VITA

Elizabeth Layne Cantwell
Department of Biology
Texas A&M University
College Station, TX 77843-3258
Phone: (979) 458-4119

EDUCATION

1996	B.A. Biology, University of Virginia, Charlottesville, VA
2005	Ph.D. Zoology, Texas A&M University, College Station, TX

RESEARCH EXPERIENCE

June 1995-June 1996	Undergraduate Research Assistant in the lab of Michael Menaker, Ph.D., University of Virginia
Aug. 1996-Aug. 2005	Graduate Researcher in the lab of Vincent M. Cassone, Ph.D., Texas A&M University

TEACHING EXPERIENCE

Courses Taught:

Fall 1996	Introductory Biology Lab
Sept. 1997-May 2001	Human Anatomy and Physiology Lab
Sept. 2000-May 2002	Honors Human Anatomy and Physiology Lab
Sept. 2002-May 2003	Special Topics in Human Anatomy & Physiology
Sept. 2003-present	Human Anatomy & Physiology

MEMBERSHIPS

January 1996-present	Society for Research on Biological Rhythms
March 1998-present	Society for Neuroscience

PUBLICATIONS

Cantwell EL, Cassone VM. 2002. Daily and circadian fluctuation in 2-deoxy[^{14}C]glucose uptake in circadian and visual system structures of the chick brain: effects of exogenous melatonin. Brain Res Bull 57:603-11.

Cantwell EL, Cassone VM. 2005. The Chicken Suprachiasmatic Nuclei I. Efferent and Afferent Connections. (in preparation)

Cantwell EL, Cassone VM. 2005. The Chicken Suprachiasmatic Nuclei II. Autoradiographic and Immunohistochemical Analysis. (in preparation)